



UNIVERSITEIT VAN PRETORIA
UNIVERSITY OF PRETORIA
YUNIBESITHI YA PRETORIA

In-Situ Subsurface Density Estimations using a Seismic Technique

By

Christoffel Johannes Stephanus Fourie

Submitted in partial fulfillment of the requirements for the degree Philosophiae Doctor
(PhD) in Exploration Geophysics in the Faculty of Natural and Agricultural Sciences,
University of Pretoria

Pretoria

September 2007



I, C.J.S. Fourie hereby declare that this thesis "In-Situ Subsurface Density Estimations using a Seismic Technique", which I hereby submit for the degree PHd (Exploration Geophysics) at the University of Pretoria, is my own work and has not previously been submitted by me for a degree at this or any other tertiary institution - Regulation 57.4(e)

November 2007

ABSTRACT

A new geophysical method was developed to satisfy a need for in-situ density measurements. Various situations, such as a gravity dam wall requires that density measurements should be done without damage to the structure. The sample volume should also not be that large in order to be sensitive enough for variations.

This method measures the in-situ density of the weathered layer and other man made structures, using seismic waves in three directions. The seismic waves utilized are P-waves and S-waves. It is however surface waves that are treated like body waves because they do not separate at this shallow depth.

These waves are very sensitive to the attenuation factor, which is in turn sensitive to certain physical properties of the propagation medium. This factor is utilised when the multi layer problem is encountered. The maximum depth of exploration is 2-5m and depends solely on the seismic skin depth.

This method utilises a large base plate. The source is a large sledge hammer and shots are done at each side of the base plate. Different dominant frequencies are identified and used to calculate the densities of the layers associated with that specific frequency. The velocities of the subsurface are determined by small seismic refraction surveys.

The method will find application mainly in the civil and engineering geology fields. The main application will be to determine subsurface densities and small movement elasticity modulli for engineers to aid in obtaining adequate design parameters.

Case studies on three different geologic environments are presented. The results indicate that this method will be useful, although certain modifications are recommended to make this method even faster and more user friendly.

CONTENTS	PAGE
CHAPTER 1 – <u>Review of existing density determinations</u>	
1.1. Introduction	1
1.2. Previous Work	3
1.2.1. Geophysics Related Work	3
1.2.2. Engineering Geology Related Work	8
CHAPTER 2 – <u>Theoretical Study</u>	
2.1. Introduction	11
2.2. P-wave model	12
2.2.1. Determination of the mass M_{0p}	12
2.2.2. Determination of the volume V_{0p}	15
2.2.3. Determination of the density	21
2.3. S-wave model	22
2.3.1. Determination of the mass M_{0s}	22
2.3.2. Determination of the volume V_{0s}	24
2.3.3. Determination of the density	29
2.4. The multi layered situation	30
2.4.1 Introduction	30
2.4.2. Multilayer mathematical approach	30
2.4.3. Depth of penetration and layer thickness	32
CHAPTER 3 – <u>Development of dedicated Software</u>	
3.1. Introduction	34
3.2. Development of dedicated software to process the density sounding data	35
3.2.1 Using the software	35

CHAPTER 4 – Equipment and experimental work

4.1. Introduction	43
4.2. Development of trail equipment	43
4.3. First field test at Leeuwfontein	46
4.4. Discussion of Leeuwfontein experiment and results	52
4.5. Second field test at Donkerhoek	53
4.6. Discussion of Donkerhoek experiment and results	59
4.7. Third field test at Country View	60
4.8. Fieldwork at Country View	62
4.9. Discussion of Country View experiment and results	67

CHAPTER 5 – Conclusions and Recommendations

5.1. Conclusions and Recommendations	68
5.2 Acknowledgements	70

REFERENCES	72
-------------------	-----------

APPENDIX I – Refereed papers published from this work

APPENDIX II – Laboratory results

FIGURES

CHAPTER 1 – Review of existing density determinations

1.1. Relationship between P-wave velocity and density (After Griffiths and King, 1969).	5
1.2. Determining density by replacement with sand of known density (After Design of small dams, 1965).	9

CHAPTER 2 – Theoretical Study

2.1. Schematic representation of the problem (After Fourie, 2005).	11
2.2. Representation of the problem by using a weight on a spring (After Fourie, 2005).	12
2.3. Determination of the excited mass (After Fourie, 2005).	14
2.4. Influence of the seismic wave underneath the base plate.	15
2.5. An example of a Harmonic oscillator that decays exponentially with time.	17
2.6. Schematic representation of the S-wave model as a mass between two springs (After Fourie, 2005).	22
2.7. Determination of the excited mass (After Fourie, 2005).	24
2.8. Area of influence underneath the base plate.	25
2.9. Schematic diagram of the layering in a weathered layer.	31

CHAPTER 3 – Development of dedicated Software

3.1. The main menu when the software package Seisrho is executed	36
3.2. Data import screen of the Seisrho package	37
3.3. Pick frequencies and calculate mass on the main menu	38
3.4. Main mass calculation interface	39
3.5. Main menu to filter the segy data	40
3.6. Window to filter the segy trace data. The lower and higher frequencies can be selected by the arrow buttons.	40
3.7. Main menu of density and volume calculation	41
3.8. Main window to obtain the volume and density	42
3.9. Main menu to create summary interpretation file	42

CHAPTER 4 – Equipment and experimental work

4.1. Large square 50Kg steel base plate of 1.23m by 1.23m	43
4.2. Mounting of Springheather 3-component geophone on	44

base plate, with sand sacks to provide the weight.	
4.3. Ears - α seismograph system used which is developed by the CGS	45
4.4. Seismic source was a sledge hammer. A shot was done at all four sides of the plate.	45
4.5. The 2528CB Silverton 1:50 000 sheet. It depict the geology of the immediate area just north of Pretoria. The Leeuwfontein area is indicated inside the square.	47
4.6. The topographic information of Leeuwfontein overlain on the geology. The quarry site and fieldwork position is indicated with a cross.	48
4.7. The quarry site where the first tests were carried out. The thickness of the Syenites is much more than the penetration of the technique: - simulating a single layer situation.	49
4.8. Hand held core drilling used for sampling. Water with cutting oil is used to ease the drilling process.	49
4.9. Example of a frequency spectrum of the traces that were used to determine the corner frequencies used to calculate the masses.	50
4.10. Plot to obtain the excited mass M_0 from sounding 1. The gradient is $1/k$.	51
4.11. The geology of the Donkerhoek area is indicated in the square	53
4.12. Clay weathering product of the Silverton shales at Donkerhoek	54
4.13. 50Kg weight that was constructed to replace sand sacks	55
4.14. Bison seismograph that replaced the ears- α seismograph	55
4.15. Geophones that replaced the single Springheather 3-D geophone used in the first experiment.	56
4.16. DCP test performed at each sounding position	56
4.17. Plot to obtain excited mass M_0 from sounding 1. The gradient is $1/k$ for the Z-component (P-wave) and $1/2k$ for the X and Y components (S-wave),	58
4.18. Geometrics strataview seismograph with 24-channels that replaced the Bison Geopro seismograph, mainly because it is a	60

floating point system.

4.19. Enlarged portion of the 2528CC Verwoerdburg 1: 50 000 sheet indicating Country View.	61
4.20. Weathering profile of the Halfway House Granites at Country View	61
4.21. Site at Country View Estates	62

TABLES

CHAPTER 1 – Review of existing density determinations

Table 1: P-wave velocities for certain rock types (after Griffith and King, 1969)	6
---	---

CHAPTER 4 – Equipment and experimental work

Table 4.1: Physical property values of the Leeuwfontein Syenites as determined by the physical property laboratory of the CGS.	50
Table 4.2: Results for both soundings performed at Leeuwfontein	52
Table 4.3: Final results from Leeuwfontein soundings.	52
Table 4.4: Seismic wave velocity values of Silverton shale clays as determined by small seismic refraction surveys.	57
Table 4.5: Final results from Donkerhoek soundings.	59
Table 4.6: Summarised results from Country View	63
Table 4.6: Summarised results from Country View	64
Table 4.6: Summarised results from Country View	65
Table 4.6: Summarised results from Country View	66



List of Symbols

SYMBOL	EXPLANATION	SYMBOL	EXPLANATION
F_p	P - wave force	F_s	S - wave force
k_p	P - wave spring constant	k_s	S - wave spring constant
x_p	P - wave displacement	x_s	S - wave displacement
M_{0p}	Excited Groundmass	M_{0s}	Excited Groundmass
\ddot{x}_p	P-wave acceleration	\ddot{x}_s	S-wave acceleration
ω_{0p}	P-wave Initial Angular Frequency	ω_{0s}	S-wave Initial Angular Frequency
Δm	Additional mass	ω_{1s}	Angular Frequency of the S - wave
ω_{1p}	Angular Frequency of the P - wave	h_s	Depth below base plate
A	Area of influence	V_{0s}	Volume of excited mass by S - wave
L	Length of base plate	b_s	Damping factor of the S - wave
h_p	Depth below base plate	v_s	Velocity of the S - wave
α	Influence angle	ϵ_s	S – wave attenuation
V_{0p}	Volume of excited mass by P - wave	Q_s	S – wave quality factor
b_p	Damping factor of the P-wave	A_{0s}	Initial S - wave amplitude
v_p	Velocity of the P-wave	$A_s(\epsilon)$	Decayed S - wave amplitude
ϵ_p	P – wave attenuation	E_s	S - wave energy
Q_p	P – wave quality factor	δ_s	S – wave logarithmic decrement
A_{0p}	Initial P - wave amplitude	f_s	S – wave frequency
$A_p(\epsilon)$	Decayed P - wave amplitude	λ_s	S - Wave length
E_p	P - wave energy	E_{ks}	S - wave kinetic energy
δ_p	P – wave logarithmic decrement	ρ_{0s}	Horizontal density
f_p	P – wave frequency		
λ_p	P-Wave length		
E_{kp}	P - wave kinetic energy		
ρ_{0p}	Vertical density		



SYMBOL	EXPLANATION	SYMBOL	EXPLANATION
F_p	P - wave force	F_s	S - wave force
k_p	P - wave spring constant	k_s	S - wave spring constant
x_p	P - wave displacement	x_s	S - wave displacement
M_{0p}	Excited Groundmass	M_{0s}	Excited Groundmass
\ddot{x}_p	P-wave acceleration	\ddot{x}_s	S-wave acceleration
ω_{0p}	P-wave Initial Angular Frequency	ω_{0s}	S-wave Initial Angular Frequency
Δm	Additional mass	ω_{1s}	Angular Frequency of the S - wave
ω_{1p}	Angular Frequency of the P - wave	h_s	Depth below base plate
A	Area of influence	V_{0s}	Volume of excited mass by S - wave
L	Length of base plate	b_s	Damping factor of the S - wave
h_p	Depth below base plate	v_s	Velocity of the S - wave
α	Influence angle	ε_s	S – wave attenuation
V_{0p}	Volume of excited mass by P - wave	Q_s	S – wave quality factor
b_p	Damping factor of the P-wave	A_{0s}	Initial S - wave amplitude
v_p	Velocity of the P-wave	$A_s(\varepsilon)$	Decayed S - wave amplitude
ε_p	P – wave attenuation	E_s	S - wave energy
Q_p	P – wave quality factor	δ_s	S – wave logarithmic decrement
A_{0p}	Initial P - wave amplitude	f_s	S – wave frequency
$A_p(\varepsilon)$	Decayed P - wave amplitude	λ_s	S - Wave length
E_p	P - wave energy	E_{ks}	S - wave kinetic energy
δ_p	P – wave logarithmic decrement	ρ_{0s}	Horizontal density
f_p	P – wave frequency		
λ_p	P-Wave length		
E_{kp}	P - wave kinetic energy		
ρ_{0p}	Vertical density		

CHAPTER 1

Review of existing density determinations

1.1 Introduction

Modern developments in geophysics, geology and engineering have resulted in increasingly sophisticated techniques of analysis of problems in soil mechanics. The reasons for this are threefold:

- Better and more sophisticated technology are more readily available.
- The need to determine parameters more accurately.
- The need to decrease the cost of development projects.

These improved methods have also highlighted the problems inherent to conventional sampling and laboratory testing procedures. Frequently, these testing procedures cannot supply suitable accurate parameters for either sophisticated techniques of analysis (such as finite element analysis) or even for modern design calculations.

Various authors have shown that the action of 'sampling' causes significant disturbance due to mechanical deformation and to the inevitable difference in stress history between a sampled element of subsurface and a similar element in the field (Davis and Poulos, 1966). This confirms the need to sample physical properties in-situ (for example density and small movement elasticity modulus), in particular for the construction and engineering industry.

Although tests like the Dynamic Cone Penetrometer Test and the consolidation test can give an indication of density variations in the subsurface, accurate in-situ density determinations could up to now, only be determined down to a shallow depth by using the neutron based Troxler equipment. Variations in the moisture content can however influence these determinations. If accurate density and other subsurface

parameters are needed from greater depths, an undisturbed sample is needed.

Physical properties derived from field geophysical techniques tend to be much larger than those obtained from conventional laboratory testing, for example stiffnesses derived from field seismics (Clayton C.R.I. and Heyman G., 2001). A laser interferometry system was developed to evaluate the sensitivity and accuracy of displacement transducers (Heyman G., Clayton C.R.I., and Reed G.T., 1997) in order to investigate the extent of the linear-elastic range of geomaterials in triaxial stress space.

This argument has led in the past to the belief that geophysical measurements are useful in design problems associated with large events like earthquakes where large movements occur, but could not be used in engineering calculations of small ground movements around foundations and structures. This now raises the question: Is it worth while to develop and apply any geophysical techniques for engineering applications?

It was argued (Auld, 1977) that seismic methods are dynamic, giving negligible time for plastic or creep strains to occur and that the strains that it induces are very small. It was only recently acknowledged that stresses and strains around tunnels are actually very small and allow geophysical techniques the capability to yield these parameters (Jardin et. al, 1986).

It has been shown that the results of the very-small-strain stiffness measured in the laboratory by making use of a Fabry-Perot laser interferometer under high pressure (Clayton C.R.I. and Heyman G., 2001) were comparable with geophysical data from the same sites where the samples were taken. The movements during the seismic experiments were measured using displacement transducers.

This proves that the use of geophysical techniques is suitable in deriving in-situ engineering parameters and that the developments of such geophysical techniques are necessary and advisable.

1.2 Previous Work

1.2.1 Geophysics Related work

In order to emphasize the importance of accurate in-situ measurements on all the physical properties (including densities) vital to engineers, this section will concentrate on important issues from existing literature. The Seismic Refraction method can be used to determine the densities of the subsurface (Griffiths and King, 1969, Darracott, 1976). The densities are obtained indirectly by measuring the velocities of the P-waves and S-waves.

For a P-wave or pressure wave the particle movement is in the same direction as the wave propagation (longitudinal wave). In the case of a S-wave or shear wave the particle movement is perpendicular to the wave propagation (transverse wave). The basic equations describing these velocities are:

$$V_p = \sqrt{\frac{k + \frac{4}{3}G}{\rho}} \quad 1.$$

And

$$V_s = \sqrt{\frac{G}{\rho}} \quad 2.$$

Where k is the elastic (Bulk) or incompressibility modulus, G is the shear or rigidity modulus and ρ is the density.

In a solid with a larger density, the elastic modulus (k) and the shear modulus (G) are larger because it is harder to compress and it is thus more difficult to deform the medium, resulting in larger velocities. It can thus be shown from the above equations, that larger densities are associated with higher velocities. By using the seismic refraction method, the density is measured in-situ. The density value is

however only an indication of the real value due to the large sampling volume, which is directly proportional to the size of the seismic spread (6,12,24 channel and geophone spacing).

Engineers routinely use the ratio of V_p/V_s to get an indication of the density and “hardness” of the subsurface, and generally the following hold true (Darracott, 1976):

- High V_p and a V_p/V_s ratio of approximately $\sqrt{3}$ indicates unweathered bedrock.
- Low V_p and a V_p/V_s ratio of approximately $\sqrt{3}$ indicates sandy or gravel fill.
- Low V_p and a high V_p/V_s ratio indicate clayey material, usually above the water table.
- V_p velocity about 1500 m/s, high V_p/V_s ratio may indicate soft clay material, below the water table.

It is impossible to distinguish between minor layers inside the weathered layer if the velocity contrasts are small. For most rocks there is an empirical relationship between the V_p and the rock quality, namely the higher the velocity the better the rock quality (Brown and Robertshaw, 1953). They determined the empirical relationship between Young’s modulus (E) and V_p :

$$E = 111.15V_p^{2.34} \quad 3.$$

Where the unit for E is in Pa.

Poisson’s ratios can be obtained from seismic velocities (Brown and Robertshaw, 1953). Poisson’s ratio is the ratio of transverse contraction strain to longitudinal extension strain in the direction of the stretching force. Tensile deformation is considered positive and compressive deformation is considered negative. The definition of Poisson’s ratio contains a minus sign so that the majority of materials have a positive ratio.

$$\nu = \frac{-\epsilon_{trans}}{\epsilon_{longitudinal}} \quad 4.$$

Where ϵ and ν are the symbols for deformation and Poisson's ratio. This relationship can be used to obtain:

$$\frac{V_p}{V_s} = \frac{1-\nu}{\frac{1}{2}-\nu} \quad 5.$$

If the subsurface is compacted, it is found that the elastic modulus k and G increase more rapidly than does the density, which makes the determination of the density difficult (Griffiths and King, 1969). An empirical relationship obtained from experimental results between velocity and density is shown in Figure 1.1,

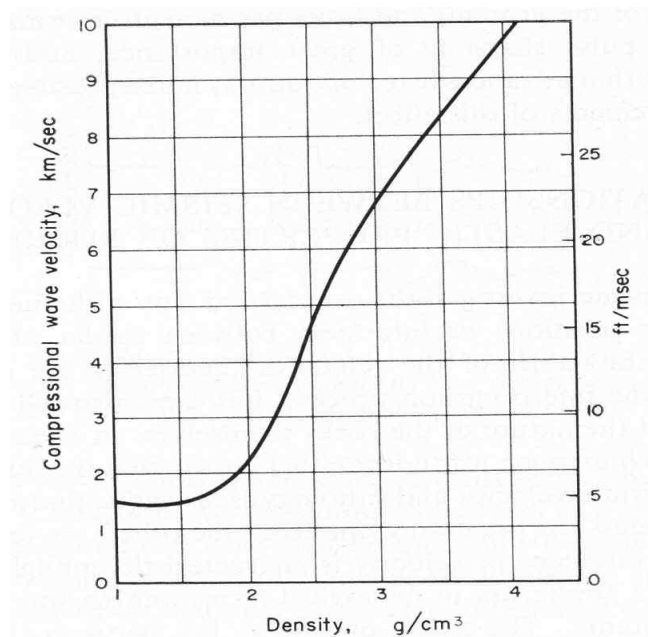


Figure 1.1: Relationship between P-wave velocity and density (after Griffiths and King, 1969)

Data from a particular rock type may fit the form of the graph well, but other variables (mineral composition, cementation, degree of fissuring) should be taken

into account if the velocity and hence density of the material is estimated. This means that if, on the contrary, the velocity has been measured, and an estimate of these other variables is needed then the velocity is to be used to make an accurate estimate of density (Griffiths and King, 1969).

It is difficult to assign a specific velocity and a density to a rock type, but it is possible to quote a range of velocities which would cover a certain lithology. Table 1 is an example:

Lithology	P-wave velocity (km/s)	Density (g/cm ³)
Clastic rocks, unconsolidated	0.3-1.8	1.5-2.2
Clastic rocks, consolidated and cemented	1.5-3.7	2.0-2.6
Clastic rocks in orogenic belts	3.1-6.2	2.5-2.8
Metamorphic rocks	4.6-6.2	2.7-3.0
Limestone	3.1-6.2	2.4-2.7
Igneous rocks	4.6-4.2	2.4-3.0

Table1: P-wave velocities for certain rock types (after Griffith and King, 1969).

Table 1 shows the general trend of increasing velocity with increasing density (i. e. decreasing porosity). It also shows the extend to which rock types can be separated on the basis of seismic velocity. The large areas of overlap indicate the insensitivity of the seismic velocity to small variations in density.

Materials of exceptionally low velocity are usually encountered near the surface (weathered layer) and are of considerable importance to the civil engineer. Properties such as its elasticity (especially the small movement elasticity modulus), plasticity, strength and density are the most important. Young's modulus can only be determined if the velocity, density and Poisson's ratio are known.

The seismic cone test (Heymann, 2003) is used to measure the in situ S and P waves of the soil. The largest advantage of this test is that it allows for the measurement of the void ratio on undisturbed material at in situ stress conditions.

Heymann (2003) used the seismic cone test on a gold tailings dam and compared it with an undisturbed sample from the day wall (outside wall) of the same dam, indicating that the void ratio of the day wall is smaller. According to Heymann (2003) the small strain stiffness and Poisson's ratio can also be calculated from the velocity measurements where small movements occur.

Shear waves provide a direct way of determining the dynamic shear modulus of the ground independent of Poisson's ratio (Abbiss, 1981). In this study two shear wave methods have been applied to determine in situ properties as a function of depth on three clay sites. The first method was shear wave refraction and the second measured the velocity of Rayleigh waves generated by vibrators. In addition pressure wave velocities were measured enabling the dynamic Poisson's ratio to be calculated.

Shear wave methods have the advantage that the shear modulus is directly related to the shear wave velocity (Equation 2, Abbiss, 1981). This is not necessarily the case for the p-wave velocity where the modulus may depend to a large extent on Poisson's ratio.

The modulus of chalk at Munford was compared from a seismic survey and a large tank test (Abbiss, 1979). A steel tank of 18.3m in diameter and approximately 20m high was filled with water to produce a pressure of 179kNm^{-2} . Displacements under the tank were measured in vertical shafts, by means of very accurate displacement transducers. In this way strains were measured at various levels down to 16.3m below the tank, nearly to the water table.

It was found that the dynamic Young's moduli calculated from a seismic refraction survey of the chalk are proportional to the moduli determined from the full scale tank loading test. It corresponds with the finite element analyses of the full scale tank loading test. The moduli showed a linear increase with depth.

The main problem of a shear wave refraction survey is to identify the s-wave arrivals between the p-waves. The best way to remedy the situation is to use a source that is rich in s-waves in the direction of the survey (Abbiss, 1981). The signal to noise ratio can also be improved by stacking the signal. By reversing the connections of the S-wave geophone so that it is out of sequence with the polarity reversals of the source will assist in the stacking of S-wave but will zero the p-wave (Abbiss, 1981).

The density and thickness of the overburden (Depth to bedrock) can also be determined by the gravity method. Techniques and algorithms calculating the depth to basement (Thanassoulas, C. and Tsokas G.N., 1985) of which one was developed by Tsuboi (1983) exist. The smallest thickness (for a single layer) 500m was achieved by Thanassoulas,C. and Tsokas G.N. This indicates that the method is not sensitive enough to distinguish between very thin layers inside a weathered layered profile.

1.2.2 Engineering Geology Related Work

A large variety of field and laboratory tests have been developed and used, of which the “density-in-place” tests are applicable to this study. This test measures the in-place density in a foundation, a borrow area, or a compacted embankment by excavating holes. This is done by weighing the material that is excavated and the volume of the hole is determined by filling it with calibrated sand (Design of small dams, 1965). To obtain a dry density of the sample a water content determination of the excavated material is performed.

Air-dry uniform sand passing through the no. 16 sieve and retained by the no. 30 sieve has been found to be satisfactory. Clean blow sand or dune sand is the most suitable (Design of small dams, 1965). When large test holes are used in gravel soils, coarse sand having rounded particles is recommended. It should pass through the no. 4 sieve but should be retained by the no. 8 sieve. The sand is calibrated by pouring it into a container of known volume of approximately the size

and shape of the type of excavation to be used, weighing it and calculating its unit weight.

At the test location, all loose soil is removed from the area and a work platform is used to support the edges of the excavation (Figure 1.2). This protects the area that is being measured from the weight of the operator, which may deform and change the dimensions of the hole (Design of small dams, 1965). Care must thus be taken not to stand too close to the hole. Although this method gives a good indication of the density, it is not as accurate as an in-situ measurement.



Figure 1.2: Determining density by replacement with sand of known density (After Design of small dams, 1965).

It is sometimes necessary to obtain densities for deeper foundations, which usually penetrate different layers of the subsurface. The following simple method has been used successfully to obtain in-place density in stages of depth in foundations and borrow areas (Design of small dams, 1965):

A platform and auger are used. The platform is set up in such a way that the operator is 1m away from the hole, to prevent damage and compression of the soil around the hole. The auger is used to drill the hole and the soil is saved. The process is repeated until the second layer is reached. The depth of the hole is measured up to the first interface and the removed soil is weighed. The diameter of the hole is known (auger diameter) and the volume can be calculated. These parameters combined with the weight of the soil, enable the calculation of the density of the removed soil. This process is repeated for every layer encountered.

The density or specific gravity of undisturbed samples can also be measured in the laboratory. The no. 4 fraction of the soil is commonly tested by the flask method (Design of small dams, 1965). A 500ml long-necked flask is calibrated for volume at several temperatures. One hundred grams of oven dried soil is washed into the flask with distilled water. A vacuum is applied to the mixture to get rid of all air and the temperature of the mixture is recorded. The weight of the flask with the mixture is then measured. The volume of the 100g soil is calculated and the specific gravity is then computed.

To determine the specific gravity of gravel and cobbles, the material remains immersed in water for 24 hours and is then blotted with a towel. This is the surface-dry condition. It is then weighed and its water displacement is measured.

CHAPTER 2
Theoretical study

2.1 Introduction

In order to obtain the density of the subsurface, without disturbance or damage, it is essential that we must be able to obtain the mass (M_0) and the volume (V_0) of the sample area (Figure 2.1). The challenge lies herein to be able to obtain M_0 and V_0 from indirect sources of measurement, since the direct approaches like drilling is deemed undesirable in some cases.

The method that is proposed tries to measure the mass and the volume of the sample to be investigated through the use of seismic waves, a bearing plate on the surface, a three component geophone and weights to be added to the bearing plate.

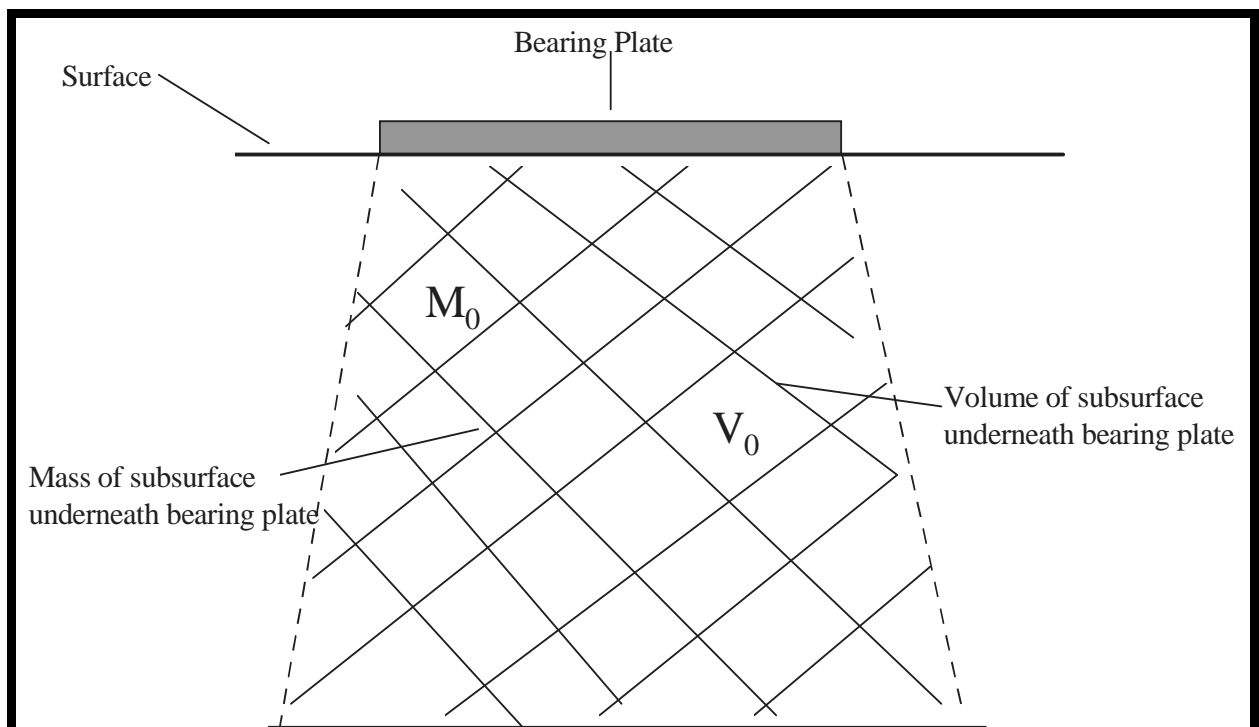


Figure 2.1: Schematic representation of the problem.

In order to try and derive a mathematical model, we make the assumption that we can represent the system by using a very simple model; a mass on a spring that is equal to the mass of the subsurface underneath the bearing plate. The other end of the spring is tied to an edifice (Figure 2.2).

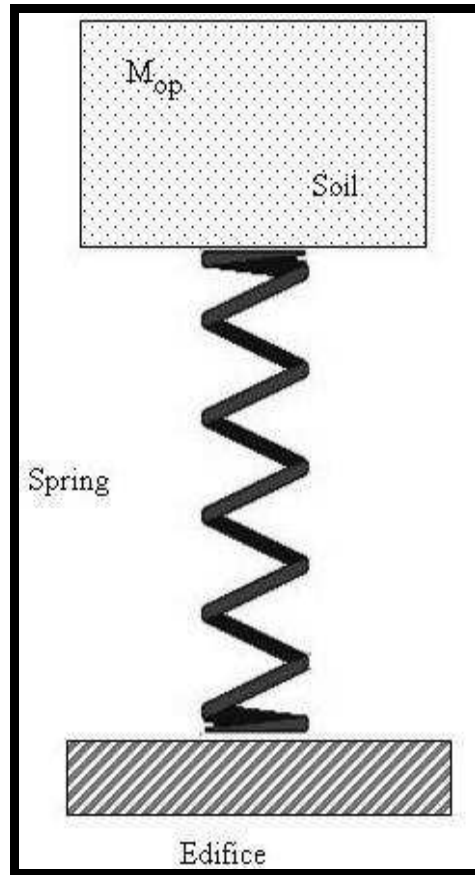


Figure 2.2: Representation of the problem by using a weight on a spring.

2.2 P-wave model

2.2.1 Determination of the mass M_{op}

From the above assumption we can write the following relation from Hooke's law:

$$F_p = -k_p x_p \quad 1$$

Where k_p is the spring constant and x_p is the displacement.

From Newton II:

$$M_{0p}\ddot{x}_p + k_p x_p = 0 \quad 2$$

We have further that $k_p = \omega_{0p}^2 M_{0p}$ and that the wave function for displacement is

$$x_p = x_{0p} \sin(\omega_{0p}t + \phi) \quad 3$$

To obtain the mass M_{0p} we have to plot the frequency of the vibration versus the increased mass ($M_{0p} + \Delta m$). From equation 2 we have:

$$\ddot{x}_p + \frac{k_p}{M_{0p}} x_p = 0 \quad 4$$

And

$$\omega_{0p}^2 = \frac{k_p}{M_{0p}} \quad 5$$

Thus

$$k_p = \omega_{p0}^2 M_{0p} \quad 6$$

If we add a mass Δm to the mass M_{0p} and k_p stays the same, the angular frequency changes to ω_{1p}^2 . Equation 6 then changes to:

$$k_p = \omega_{1p}^2 (M_{0p} + \Delta m) \quad 7$$

And because:

$$\frac{1}{\omega_{0p}^2} = \frac{1}{k_p} M_{0p} \quad 8$$

it implies that

$$\frac{1}{\omega_{1p}^2} = \frac{1}{k_p} (M_{0p} + \Delta m) \quad 9$$

Equation 9 is a straight line and we also have two unknowns, k_p and M_{0p} . If we rewrite equation 9 a bit we obtain:

$$\frac{1}{\omega_{1p}^2} = \frac{M_{0p}}{k_p} + \frac{\Delta m}{k_p} \quad 10$$

Since M_{0p}/k_p is an unknown, it is also a constant, say y_p .

$$\frac{1}{\omega_{1p}^2} = y_p + \frac{\Delta m}{k_p} \quad 11$$

or

$$\frac{1}{\omega_{1p}^2} = \frac{1}{k_p} \Delta m + y_p \quad 12$$

If we now plot Δm against $1/\omega_{1p}^2$, the slope of the line will be $1/k_p$. M_{0p} can be obtained from y_p or by the extension of the line. Where the line intersects with the Δm axis, the absolute value of M_{0p} can be read off. These values are accurate since the line is straight (Figure.2.3).

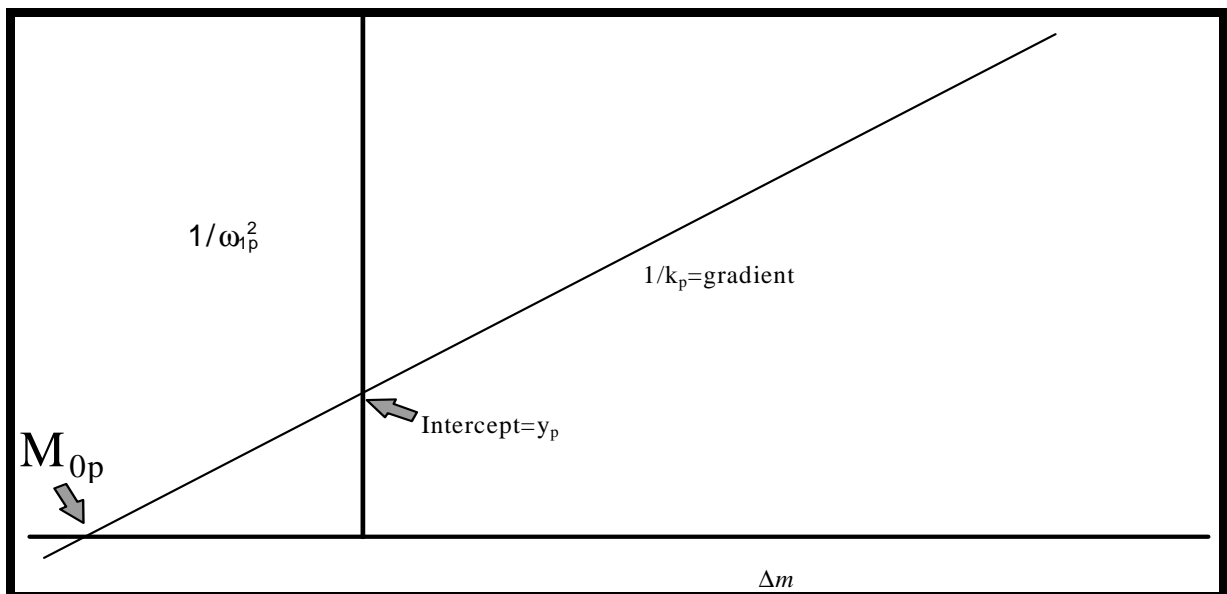


Figure 2.3: Determination of the excited mass.

2.2.2 Determination of the volume V_{op} .

If we assume that we are going to use a square base plate with side L , and that the diffusion angle from the plate is α , then the resulting area underneath the plate (Figure. 2.4) is the following:

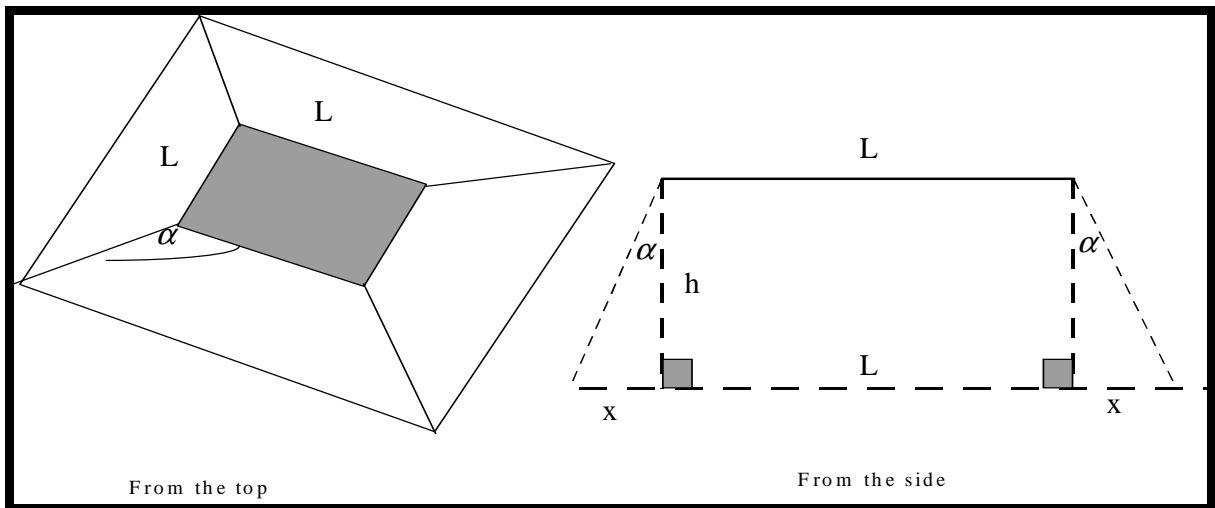


Figure 2.4: Influence of the excited wave underneath the base plate.

The new length is $L + 2x$ and since $\tan\alpha = x/h$ the new area is:

$$A = (L + 2h_p \tan \alpha)^2 \quad 13$$

The volume of the vibrating column $V_{op} = A \times h_p$. The height of the vibrating volume is unknown. The objective is to express the height of the volume in terms of elements that we can measure, like the wavelength or the velocity of seismic waves.

During the excitation of the ground mass, the movement experiences attenuation. The differential equation that expresses the system is as follows:

$$F_p + b_p v_p = -k_p x_p \quad 14$$

Where b_p is the attenuation coefficient and v_p is the velocity of the medium.

If we assume that the attenuation factor is dependant on the velocity of the ground movement and that x_p is the differential movement of a differential volume under the plate, then:

$$m_{0p} \frac{d^2 x_p}{dt^2} + b_p \frac{dx_p}{dt} + k_p x_p = 0 \quad 15$$

$$\frac{d^2 x_p}{dt^2} + \frac{b_p}{m_{0p}} \frac{dx_p}{dt} + \frac{k_p}{m_{0p}} x_p = 0 \quad 16$$

and

$$\frac{d^2 x_p}{dt^2} + \frac{b_p}{m_{0p} \omega_{0p}} \omega_{0p} \frac{dx_p}{dt} + \omega_{0p}^2 x_p = 0 \quad 17$$

$$\frac{d^2 x_p}{dt^2} + 2\varepsilon_p \omega_{0p} \frac{dx_p}{dt} + \omega_{0p}^2 x_p = 0 \quad 18$$

Where

$$\varepsilon_p = \frac{1}{2} \frac{b_p}{m_{0p} \omega_{0p}} \quad 19$$

If we assume that the damping is not much, a solution to this differential equation is:

$$A(\varepsilon)_p = A_{0p} e^{-\varepsilon \omega_{0p} t} \quad 20$$

This is a harmonic oscillation that decays exponentially with time (Figure 2.5):

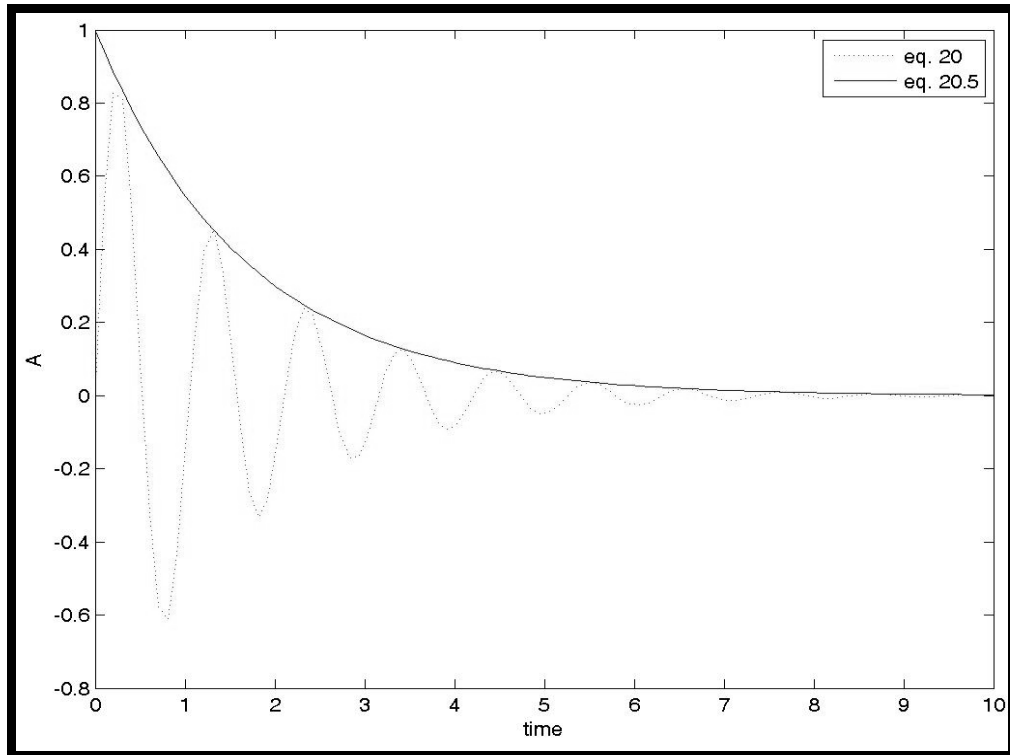


Figure 2.5: An example of a Harmonic oscillator that decays exponentially with time.

We can express ε_p in terms of the quality factor Q_p :

$$\varepsilon_p = \frac{1}{2Q_p} \quad 21$$

Thus equation 20 changes to:

$$A(\varepsilon)_p = A_{0p} e^{-\omega_{0p}t/2Q_p} \quad 22$$

Where Q_p (quality factor) is defined in terms of the fractional loss of energy per cycle of oscillation. In other words:

$$\frac{1}{Q_p} = \frac{-\Delta E_p}{2\pi E_p} \quad 23$$

The quality factor can also be expressed in terms of the logarithmic decrement:

$$Q_p = \frac{\pi}{\delta_p} \quad 24$$

If we now substitute equation 24 and the fact that $t = x/v$ and $\omega = 2\pi f$ into equation 22 we get:

$$A(\varepsilon)_p = A_{0p} e^{-\left(\frac{f_p \pi}{Q_p V_p}\right) x_p} \quad 25$$

This transforms to

$$A(\varepsilon)_p = A_{0p} e^{-\frac{\psi_p x_p}{\lambda_p}} \quad 26$$

where $f_p/V_p = 1/\lambda_p$ and $\pi/Q_p = \psi_p$. Equation 26 expresses the decrease in amplitude of a wave due to attenuation as a function of distance travelled. ψ_p is an attenuation constant that is frequency dependant. High frequency waves will attenuate more quickly. If we now want to express the decrease in amplitude as a function of depth h_p , we get

$$A(\varepsilon)_p = A_{0p} e^{-\frac{\psi_p h_p}{\lambda_p}} \quad 27$$

The depths that would be investigated will be quite small, and in the order of 3-10m. We can thus assume that the velocity at a depth h_p of the seismic wave is V_p . If we assume that there is no frequency dispersion at these shallow depths ($\omega_p = \omega_{0p}$), and ω_{0p} is on the ground at ($h_p = 0$), we can express the volume as:

$$V_p = A_{0p} \omega_{0p} e^{-\frac{\psi_p h_p}{\lambda_p}} \quad 28$$

The kinetic energy of the column will be equal to the energy of the source. If we now attempt to calculate the kinetic energy of the vibrating column, we get:

$$E_{kp} = \frac{1}{2} m_{0p} v_p^2 \quad 29$$

If we now examine the kinetic energy of a small volume at a depth h_p , and that $m_p = \rho_p * V_p$ and that Volume (V_p) = $A_p * h_p$ we get

$$dE_{kp} = \frac{1}{2} \rho_p A V_p^2 dh_p \quad 30$$

And if we substitute equations 13 and 29 into equation 30,

$$dE_{kp} = \frac{1}{2} \rho_p (A_{0p} \omega_p)^2 (L + 2h_p \tan \alpha)^2 e^{-2\frac{\psi_p h_p}{h_p}} dh_p \quad 31$$

$$dE_{kp} = \frac{1}{2} \rho_p (A_{0p} \omega_{0p})^2 (L^2 + 4h_p L \tan \alpha + 4h_p^2 \tan^2 \alpha) e^{-2\frac{\psi_p h_p}{\lambda_p}} dh_p \quad 32$$

If we now integrate equation 32 to find the total kinetic energy of the vibrating column, we would also be able to find the total volume that has been energised. So

$$E_{kp} = \frac{1}{2} \rho_p (A_{0p} \omega_{0p})^2 \int_0^{h_p} (L^2 + 4h_p L \tan \alpha + 4h_p^2 \tan^2 \alpha) e^{-2\frac{\psi_p h_p}{\lambda_p}} dh_p \quad 33$$

In order to solve this integral, it should be divided into three separate equations:

$$E_{kp1} = \frac{1}{2} \rho_p (A_{0p} \omega_{0p})^2 \int_0^{h_p} (L^2) e^{-2\frac{\psi_p h_p}{\lambda_p}} dh_p \quad 34a$$

$$E_{kp2} = \frac{1}{2} \rho_p (A_0 \omega_{0p})^2 \int_0^{h_p} (4L \tan \alpha) h_p e^{-2 \frac{\psi_p h_p}{\lambda_p}} dh_p \quad 34b$$

$$E_{kp3} = \frac{1}{2} \rho_p (A_0 \omega_{0p})^2 \int_0^{h_p} (4 \tan^2 \alpha) h_p^2 e^{-2 \frac{\psi_p h_p}{\lambda_p}} dh_p \quad 34c$$

The solution of equation 34a is

$$E_{kp1} = \frac{1}{2} \rho_p (A_0 \omega_{0p})^2 e^{-2 \frac{\psi_p h_p}{\lambda_p}} \left[-L^2 \frac{\lambda_p}{2\psi_p} \right] \quad 35$$

The part in brackets of the equation represents the volume. Since volume can't be negative, we must use the absolute value and the volume contribution of the first part of the integral is:

$$V_{1p} = L^2 \frac{\lambda_p}{2\psi_p} \quad 36$$

The solution of equation 34b is:

$$E_{kp2} = \frac{1}{2} \rho_p (A_0 \omega_{0p})^2 e^{-2 \frac{\psi_p h_p}{\lambda_p}} \left[-2L \frac{h_p \lambda_p \psi_p}{\psi_p^2} - L \frac{\lambda_p^2}{\psi_p^2} \right] \tan \alpha \quad 37$$

The volume in brackets if we substitute $h_p = \lambda_p / 2\psi_p$ reduces to:

$$V_{2p} = 2L \left(\frac{\lambda_p}{\psi_p} \right)^2 \tan \alpha \quad 38$$

The solution of equation 34c is:

$$E_{kp3} = \frac{1}{2} \rho_p (A_{0p} \omega_{0p})^2 e^{-2\frac{\psi_p h_p}{\lambda_p}} \left[-\frac{h_p^2 \lambda_p}{2\psi_p^2} - \frac{\lambda_p^2 h_p}{2\psi_p^2} - \frac{\lambda_p^3}{4\psi_p^3} \right] 4 \tan^2 \alpha \quad 39$$

The volume in brackets if we substitute $h_p = \lambda_p/2\psi_p$ reduces to:

$$V_{3p} = \frac{5}{2} \left(\frac{\lambda_p}{\psi_p} \right)^3 \tan^2 \alpha \quad 40$$

The total volume $V_{0p} = V_{1p} + V_{2p} + V_{3p}$. This implies that

$$V_{0p} = \frac{L^2 \lambda_p}{2\psi_p} + 2L \left(\frac{\lambda_p}{\psi_p} \right)^2 \tan \alpha + \frac{5}{2} \left(\frac{\lambda_p}{\psi_p} \right)^3 \tan^2 \alpha \quad 41$$

2.2.3 Determination of the density

In order to obtain the density of the vibrating volume it is then logical that we should divide M_0 by equation 41:

$$\rho_{0p} = \frac{M_{0p}}{\frac{L^2 \lambda_p}{2\psi_p} + 2L \left(\frac{\lambda_p}{\psi_p} \right)^2 \tan \alpha + \frac{5}{2} \left(\frac{\lambda_p}{\psi_p} \right)^3 \tan^2 \alpha} \quad 42$$

If the diffusion angle of the waves from the edges of the square edifice $\alpha \approx 0$, as we expected, equation 42 reduces to:

$$\rho_{0p} = \frac{M_{0p}}{\left(\frac{L^2 \lambda_p}{2\psi_p} \right)} \quad 43$$

To obtain λ_p , we have to obtain the velocity of the medium. This can be achieved by doing a small seismic refraction survey, employing a geophone spacing of 0.5m. It is also

necessary to use the frequency f_p of the vibrating volume V_{op} . This can be obtained from the linear plot in Figure 2.3. The angular frequency ω_p of the vibrating volume V_{op} can be found where the line intercepts with the Y-axis.

The attenuation constant ψ_p can be estimated by calculating the damping factor Q_p from the seismic trace.

2.3 S-wave model

2.3.1 Determination of the mass M_{os} .

In order to try and derive a mathematical model for the s-wave situation, we also assume a very simple mass on a spring model. Since the mass on the spring that oscillates in the s-wave (lateral) direction has host rock on both sides, it can be visualised in Figure 2.6.

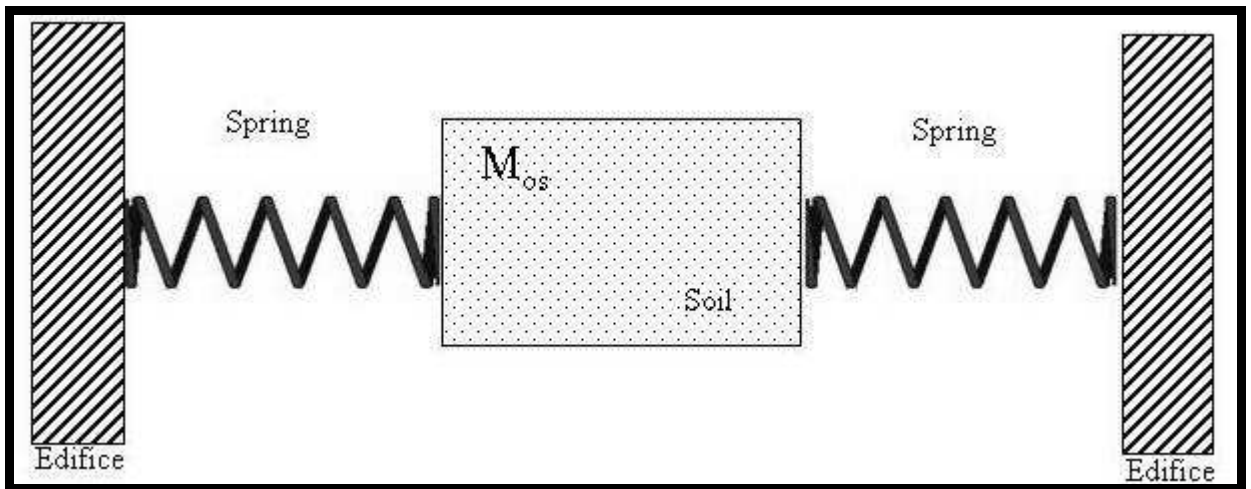


Figure 2.6: Schematic representation of the S-wave model as a mass between two springs.

If we make the assumption that the lateral dimension of the volume we sample is so small that the values of the spring constants are the same, we will be able to write:

$$F_s + k_s x_s = -k_s x_s \quad 44$$

Thus from Newton II:

$$M_{0s}\ddot{x}_s + 2k_s x_s = 0 \quad 45$$

$$\ddot{x}_s + \frac{2k_s}{M_{0s}} x_s = 0 \quad 46$$

Thus

$$\omega_{0s}^2 = \frac{2k_s}{M_{0s}} \quad 47$$

If we add a mass Δm to the mass M_{0s} and k_s stays the same, the angular frequency changes to ω_{1s} . Equation 47 can then be written as:

$$2k_s = \omega_{1s}^2 (M_{0s} + \Delta m) \quad 48$$

And

$$\frac{1}{\omega_{1s}^2} = \frac{1}{2k_s} (M_{0s} + \Delta m) \quad 49$$

Similarly to equation 9, equation 49 is a straight line with two unknowns, k_s and M_{0s} . We can thus transform equation 49 into:

$$\frac{1}{\omega_{1s}^2} = \frac{M_{0s}}{2k_s} + \frac{\Delta m}{2k_s} \quad 50$$

Similarly, since $M_{0s}/2k_s$ is an unknown, it is also constant, say y_s .

$$\frac{1}{\omega_{1s}^2} = y_s + \frac{\Delta m}{2k_s} \quad 51$$

$$\frac{1}{\omega_{1s}^2} = \frac{1}{2k_s} \Delta m + y_s$$

If we now plot Δm against $1/\omega_{1s}^2$, the slope of the line will be $1/k_s$. M_{0H} can be obtained from y or by the extension of the line. Where the line intersects with the Δm axis, the absolute value of M_{0s} can be read off. These values are accurate since the line is straight (Figure.2.7).

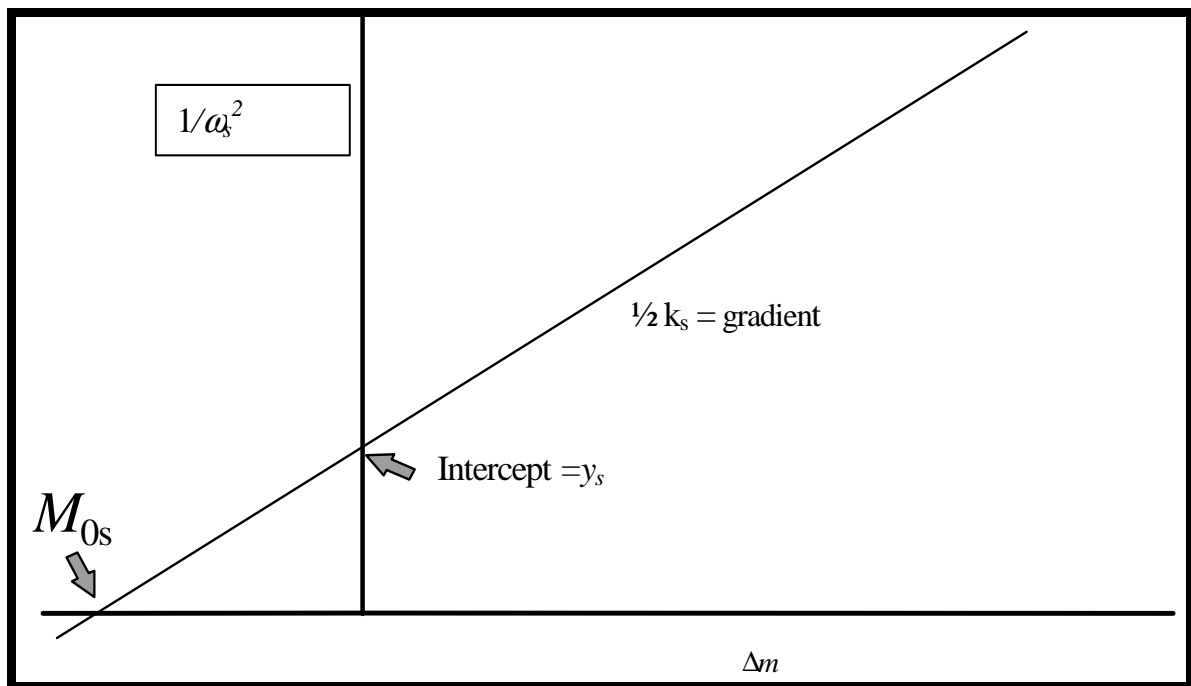


Figure 2.7: Determination of the excited mass by the Shear wave.

2.3.2 Determination of the volume V_{0s} .

Similarly, if we assume that we are going to use a rectangular base plate with dimensions L , and if the diffusion angle from the plate is α , then the resulting area underneath the plate (Figure. 2.8) is the following:

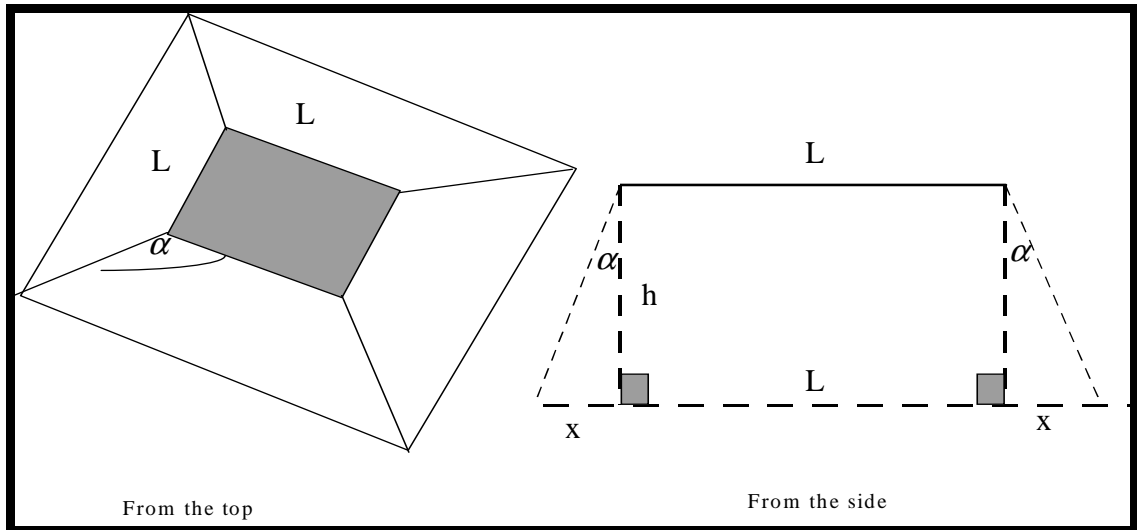


Figure 2.8: Area of influence under the base plate

The new length is $L + 2x$ and since $\tan\alpha = x/h$ the new area is:

$$A = (L + 2h_s \tan \alpha)^2 \quad 53$$

The volume of the vibrating column $V_{0s} = A \times h_s$. The height of the vibrating volume is unknown. The objective is to express the height of the volume in terms of elements that we can measure, like the wavelength or the velocity of seismic waves.

During the excitation of the ground mass, the movement experiences attenuation. The differential equation that expresses the system is as follows:

$$F_s + b_s V_s + k_s x_s = -k_s x_s \quad 54$$

Where b_s is the attenuation coefficient and V_s is the velocity of the medium.

If we assume that the attenuation factor is dependant on the velocity of the ground movement and that x_s is the differential movement of a differential volume under the plate, then:

$$m_{0s} \frac{d^2 x_s}{dt^2} + b_s \frac{dx_s}{dt} + 2k_s = 0 \quad 55$$

And if we substitute $2k_s = \kappa_s$

$$\frac{d^2 x_s}{dt^2} + \frac{b_s}{m_{0s}} \frac{dx_s}{dt} + \frac{\kappa_s}{m_{0s}} = 0 \quad 56$$

And

$$\frac{d^2 x_s}{dt^2} + \frac{b_s}{m_{0s} \omega_{0s}} \omega_{0s} \frac{dx_s}{dt} + \omega_{0s}^2 x_s = 0 \quad 57$$

$$\frac{d^2 x_s}{dt^2} + 2\varepsilon_s \omega_{0s} \frac{dx_s}{dt} + \omega_{0s}^2 x_s = 0 \quad 58$$

where $\varepsilon_s = \frac{1}{2} \frac{b_s}{m_s \omega_{0s}}$.

As previously, the solution to this differential equation is:

$$A_s(\varepsilon) = A_0 e^{-\varepsilon \omega_{0s} t} \quad 59$$

This is a harmonic oscillation that decays exponentially with time. We can express ε in terms of the quality factor Q_s :

$$\varepsilon_s = \frac{1}{2Q_s} \quad 60$$

Thus equation 59 changes to:

$$A_s(\varepsilon) = A_{0s} e^{-\omega_0 t / 2Q_s} \quad 61$$

Q is defined in terms of the fractional loss of energy per cycle of oscillation. In other words:

$$\frac{1}{Q_s} = \frac{-\Delta E_s}{2\pi E_s} \quad 62$$

The quality factor can also be expressed in terms of the logarithmic decrement:

$$Q_s = \frac{\pi}{\delta_s} \quad 63$$

If we now substitute equation 62 and the fact that $t=x/v$ and $\omega=2\pi f$ into equation 61 we get:

$$A_s(\varepsilon) = A_{0s} e^{-\left(\frac{f_s \pi}{Q_s V_s}\right) x_s} \quad 64$$

This transforms to

$$A_s(\varepsilon) = A_{0s} e^{-\frac{\psi_s x_s}{\lambda_s}} \quad 65$$

Where $f_s/V_s = 1/\lambda_s$ and $\pi/Q_s = \psi_s$. Equation 65 expresses the decrease in amplitude of a wave due to attenuation as a function of distance travelled. ψ_s is an attenuation constant that is frequency dependant. High frequency waves will attenuate more quickly. If we now want to express the decrease in amplitude as a function of depth h_s , we get

$$A_s(\varepsilon) = A_{0s} e^{-\frac{\psi_s h_s}{\lambda_s}} \quad 66$$

The depths that would be investigated will be quite small, and in the order of 3-10m. We can thus assume that the velocity at a depth h of the seismic wave is V_s . If we assume

that there is no frequency dispersion at these shallow depths ($\omega_{hs} = \omega_0$, and ω_0 is on the ground at $h = 0$), we can write:

$$V_s = A_{0s} \omega_{0s} e^{-\frac{\psi_s h_s}{\lambda_s}} \quad 67$$

The kinetic energy of the column will be equal to the energy of the source. If we now attempt to calculate the kinetic energy of the vibrating column, we get:

$$E_{ks} = \frac{1}{2} m_s V_s^2 \quad 68$$

If we now look at the kinetic energy of a small volume at a depth h_s , and that $m_s = \rho_s V_s$ and that Volume (V_s) = $A * h_s$ we get

$$dE_{ks} = \frac{1}{2} \rho_s A V_s^2 dh_s \quad 69$$

And if we substitute equations 13 and 29

$$dE_{ks} = \frac{1}{2} \rho_s (A_{0s} \omega_{0s})^2 (L + 2h_s \tan \alpha)^2 e^{-2\frac{\psi_s h_s}{\lambda_s}} dh_s \quad 70$$

$$dE_{ks} = \frac{1}{2} \rho_s (A_{0s} \omega_{0H})^2 (L^2 + 4h_s L \tan \alpha + 4h_s^2 \tan^2 \alpha) e^{-\frac{2\psi_s h_s}{\lambda_s}} dh_s \quad 71$$

If we now integrate equation 71 to find the total kinetic energy of the vibrating column, we would also be able to find the total volume that has been energised. So

$$E_{ks} = \frac{1}{2} \rho_s (A_{0s} \omega_{0s})^2 \int_0^{h_s} (L^2 + 4h_s L \tan \alpha + 4h_s^2 \tan^2 \alpha) e^{-\frac{2\psi_s h_s}{\lambda_s}} dh_s \quad 72$$

In order to solve this integral, it should be divided into three separate equations:

$$E_{ks1} = \frac{1}{2} \rho_s (A_{0s} \omega_{0s})^2 \int_0^{h_s} (L^2) e^{-2 \frac{\psi_s h_s}{\lambda_s}} dh_s \quad 73a$$

$$E_{ks2} = \frac{1}{2} \rho_s (A_{0s} \omega_{0s})^2 \int_0^{h_s} (4L \tan \alpha) h_s e^{-2 \frac{\psi_s h_s}{\lambda_s}} dh_s \quad 73b$$

$$E_{ks3} = \frac{1}{2} \rho_s (A_{0s} \omega_{0s})^2 \int_0^{h_s} (4 \tan^2 \alpha) h_s^2 e^{-2 \frac{\psi_s h_s}{\lambda_s}} dh_s \quad 73c$$

The solutions of equation 73a, 73b and 73c are the same as for the Z-component.

The total volume $V_{0s} = V_{1s} + V_{2s} + V_{3s}$. This implies that:

$$V_{0s} = \frac{L^2 \lambda_s}{2 \psi_s} + 2L \left(\frac{\lambda_s}{\psi_s} \right)^2 \tan \alpha + \frac{5}{2} \left(\frac{\lambda_s}{\psi_s} \right)^3 \tan^2 \alpha \quad 74$$

2.3.3 Determination of the density

In order to obtain the density of the vibrating volume it is then logical that we should divide M_s by equation 74:

$$\rho_{0s} = \frac{M_{0s}}{\frac{L^2 \lambda_s}{2 \psi_s} + 2L \left(\frac{\lambda_s}{\psi_s} \right)^2 \tan \alpha + \frac{5}{2} \left(\frac{\lambda_s}{\psi_s} \right)^3 \tan^2 \alpha} \quad 75$$

If the diffusion angle of the waves from the edges of the square edifice $\alpha \cong 0$, as we expected, equation 75 reduces to:



$$\rho_{0s} = \frac{M_{0s}}{\left(\frac{L^2 \lambda_s}{2\psi_s} \right)} \quad 76$$

To obtain λ_s , we have to obtain the velocity of the medium. This can be achieved by doing a small seismic refraction survey, employing a geophone spacing of 0.5m. It is also necessary to use the frequency f_s of the vibrating volume V_s . This can be obtained from the linear plot in Figure 2.6. The angular frequency ω_{0H} of the vibrating volume V_{0s} can be found where the line intercepts with the Y-axis.

The attenuation constant ψ_s can be estimated by calculating the damping factor Q_s from the seismic trace.

2.4 The multi layered situation

2.4.1 Introduction

In almost all of the cases, a single layer only scenario will not be encountered. Since this technique will almost always be used as an engineering application, the weathered layer will mostly be investigated. The weathered layer is in exceptional cases only single layer. It is usually at least two layers and then the bedrock. At the surface, it usually consists of a lower density soil cover, and then of higher density clays or semi weathered soils (Figure 2.9).

2.4.2 Multilayer mathematical approach

During a density sounding the aim is to obtain the densities of the individual layers. The objective is also the same with other geophysical methods, like the D.C. Resistivity method. The total resistivity at the surface is obtained by summing the individual layer resistivities which are in series (Telford et al., 1986).

$$R_t = \sum_{n=1}^n R_n = R_1 + R_2 + R_3 + \dots + R_n$$

77

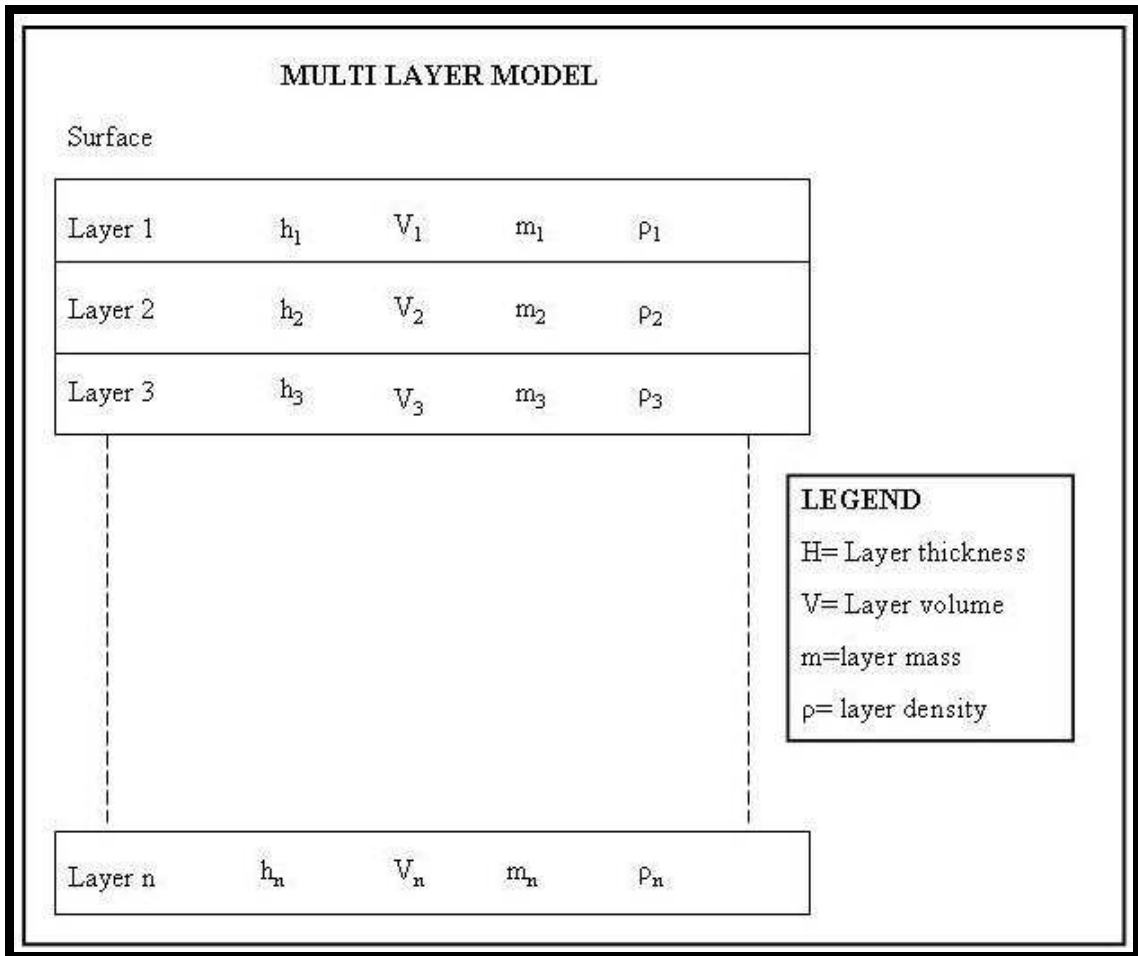


Figure 2.9: Schematic diagram of the layering in a weathered layer.

Unfortunately, the densities of the different layers cannot be added together to get a total density, but the masses and the volumes of the different layers can be added. So,

$$\rho_t \neq \sum_{n=1}^n \rho_n \neq \rho_1 + \rho_2 + \rho_3 + \dots + \rho_n \tag{78}$$

but

$$m_t = \sum_{n=1}^n m_n = m_1 + m_2 + m_3 + \dots + m_n \tag{79}$$

and

$$V_t = \sum_{n=1}^n V_n = V_1 + V_2 + V_3 + \dots + V_n \quad 80$$

This translates back to layer thicknesses:

$$h_t = \sum_{n=1}^n h_n = h_1 + h_2 + h_3 + \dots + h_n \quad 81$$

By obtaining different masses and different volumes separately, it is possible to obtain the densities for the different layering.

2.4.3 Depth of penetration and layer thickness

It has been shown that the penetration into and the return of high frequencies from the earth is affected and limited by attenuation and energy losses due to reverberation and transmission losses. Changes in frequency content also occurs (Waters, 1981). To a first approximation the loss of amplitude follows an exponential law:

$$A(z) = A_0 e^{-\alpha z} \quad 82$$

where α is the attenuation constant.

By following the same reasoning as in equations 14 to 28 and 54 to 67, the attenuation constant α can be written as:

$$\alpha = \frac{\pi \times f}{Q \times V} \quad 83$$

Where f is the frequency, V is the velocity and Q is the quality factor.

The $1/Q$ factor that is embedded into equation 83 is called the Specific dissipation constant (Griffiths and King, (1969), Waters, (1981), Kibble, (1985) and Sears et. al,

(1987)). It is a measure of how vibrational energy is dissipated.

It is thus true that α depends on the following factors:

- It is frequency dependant. Higher frequency results in higher attenuation.
- High velocity, and thus high density, results in a slower attenuation

This means that for layers in the weathered layer, the following scenarios may occur:

- If the velocity and the density of the layer are low, higher frequencies will be attenuated quickly and will be removed from the signal.
- If the velocity and the density of the layer are higher, the higher frequencies will be preserved.
- The lower density layers are usually near the surface. It thus filter out the higher frequencies (earth is acting as a low pass filter), and lower frequencies are associated with deeper layering.

CHAPTER 3

Development of dedicated software

3.1 Introduction

After the theoretical development of the method was completed, data had to be collected in the field to test and evaluate the theory. Dedicated software to process the density sounding data did not exist. The approach was to first test the method on a homogeneous single layer situation of mafic rocks. This was mainly to test the validity of the method, but also because it would be easier to process the single layer data by using different software.

The data of the first two soundings at Leeuwfontein (Figure 4.5) was processed by using Seisan™. This commercial software package is developed to process earthquake seismic data. Seisan™ can calculate a Power-frequency spectrum of the trace, which forms the heart of the density sounding data processing. The data obtained from these single layer soundings proved to be encouraging and a single layer only situation was surveyed on a weathering profile.

Previous knowledge of the geology at Donkerhoek (Figure 4.11) was the main decision for the second field test. A detailed geophysical study was done at Donkerhoek to obtain the best position for the Core Library buildings (Crail et al, 1993). It showed the areas where the weathering profile was more than 3m thick. This is theoretically thick enough to represent a single layer case.

Changes were also made to the equipment for easier handling. This forced the development of test software in Matlab™ and Scilab. The software developed in Matlab™ proved to be a little easier to use than Sisan™. The processing of the data was limited to computers that have a copy of Matlab™. Dedicated software had to be developed for this method, using programming software capable of producing executables.

3.2 Development of dedicated software to process the density sounding data

The software to process this data was developed in Visual Basic because it was:

- Easy to develop, as basic is a fairly easy programming language
- Easy to make changes
- Cheap, as the visual basic package is not that expensive
- Possible to create files that would install and run on any computer with windows, even if visual basic is not installed.
- Created Data files are in files that are compatible with Excel, which makes it easy to access.
- The determination of the frequency is the most important aspect, while processing this data. The most important calculation that this program must perform, is to determine the power spectrum of the seismic trace. The determination of the excited mass, the small movement elasticity modulus and the depth of investigation depend on the accurate determination of the frequency. Various methods were develop to make the Graphical User Interface (GUI) around this more user friendly.

3.2.1 Using the software

The developed processing software is called Seisrho. The “New Project” tag is selected when the processing of a new sounding is started. The “Open project” tag is selected when one works on a previously created or existing project. If the “New Project” tag is selected it activates the rest of the tags. A directory called “rawdata” and a directory called “segdata” are created during this process.

Sounding data is gathered using a seismograph. At this stage two seismographs are supported: - the 24 - channel Bison 8026 and the 24 - channel Geometrics Strataview. The data is transferred from the seismographs to the computer using

Mirror – III in the case if the Bison seismograph and Laplink for the Geometrics seismograph. The process is quite simple. Download or Laplink the raw seismograph data of the density sounding into the created directory called “rawdata”.

The data in the specific seismograph format is then imported into the Seisrho package using the “Import Data” tag under the “File” menu (Figure 3.1). A single file can be imported, while the option for all data files to be imported also exists. (Figure 3.2). The program default is to look for the seismograph data in the directory “rawdata”. The data is then imported and in the process it is converted into SEG Y format, which is the industry standard for seismic related data. During the import and conversion of the data, the data is stored in the created directory called “seg ydata”.

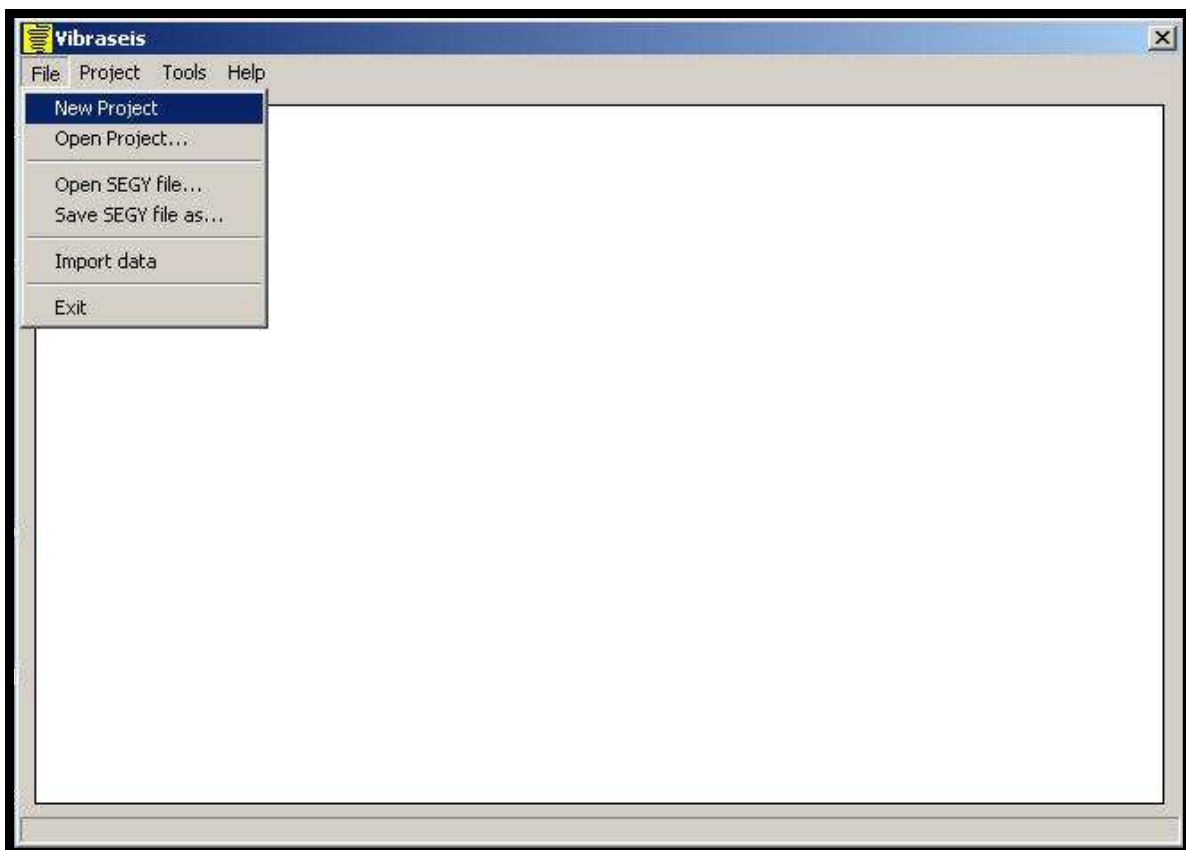


Figure 3.1: The main menu when the software package Seisrho is executed.

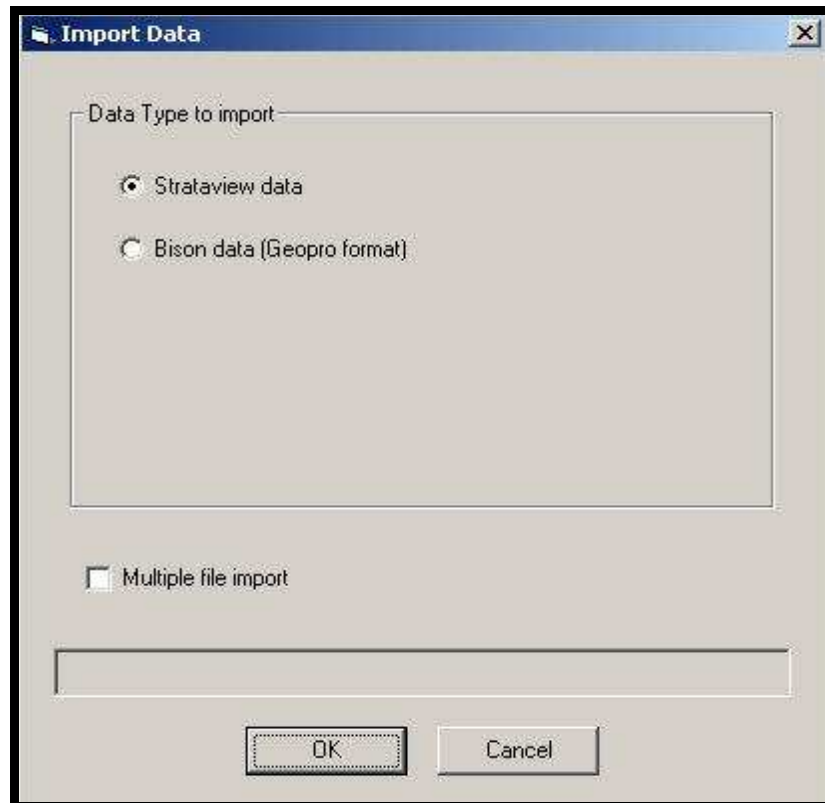


Figure 3.2: Data import screen of the Seisrho package

The data in the “seggydata” directory is the data to be used for further for the processing. Inside this directory, subdirectories called “layer1” up to “layer n” (depending on the chosen number of layers) will be created. All the relevant processing information for each layer will be stored inside the specific directory. This will also include files that contain all the filtering and Q-factor information, which is used to calculate the density of each layer.

The first step during the processing of the density sounding is to obtain the excited ground masses of the different layers present. This option can be selected from the main menu as “Pick Frequencies and Calculate Mass (Figure 3.3). This is done for all three components, X, Y and Z. The method on how the excited ground masses are calculated is explained in Fourie and Cole (CGS report 2004-0095) and involves a plot of $1/\omega^2$ vs added mass to obtain a straight line. The excited ground mass is the position where this line intersects the Y-axis.

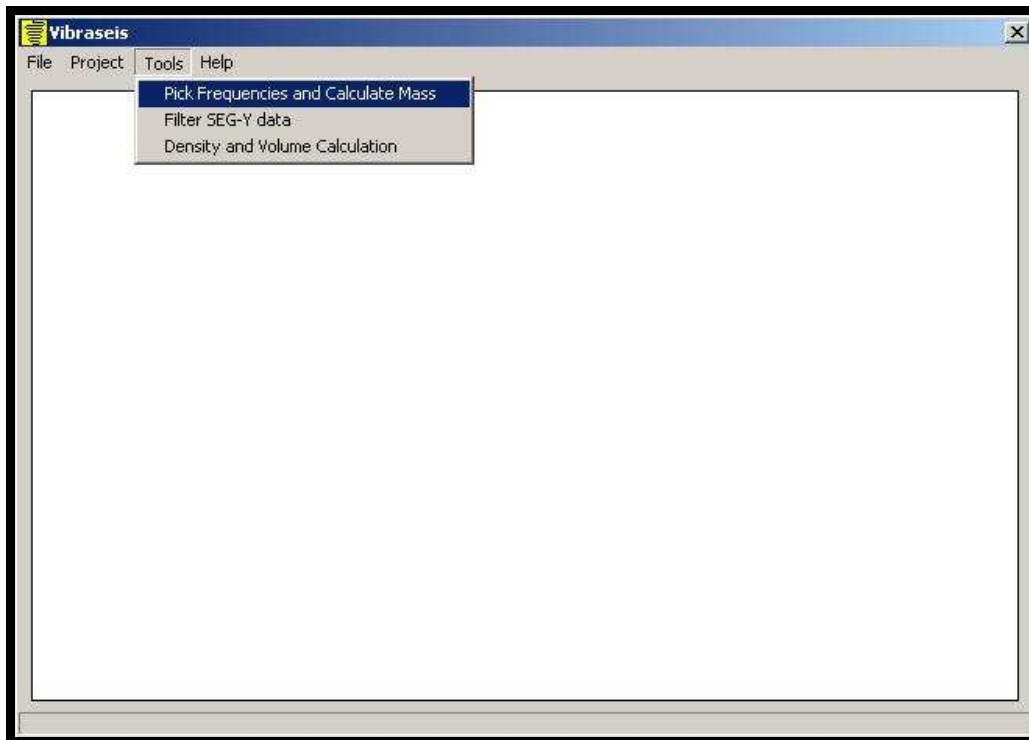



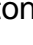
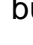


Figure 3.3: Pick frequencies and calculate mass on the main menu

All three components can be chosen for analysis by selecting the “X”, “Y” or “Z” option. The excited ground mass of more than one layer can be determined by using this interface. Figure 3.4 shows the main interface for mass calculation. An extra layer is added by clicking on the F button. A layer can be removed if the  button is selected. The display of the power spectrum in the top window can be customised by selecting the frequency window under the “Power Spectrum” option. Dominant frequencies are then selected by the  or  buttons and by moving the cursor towards the main peaks and press the mouse button to select the frequency. The next and previous shot records can be selected by pressing the  or  buttons.

This chosen frequency is then used to automatically calculate a mass. The bottom window displays the line that is fitted through the data. A direct estimation of the mass and k-value is given on a continuous basis.

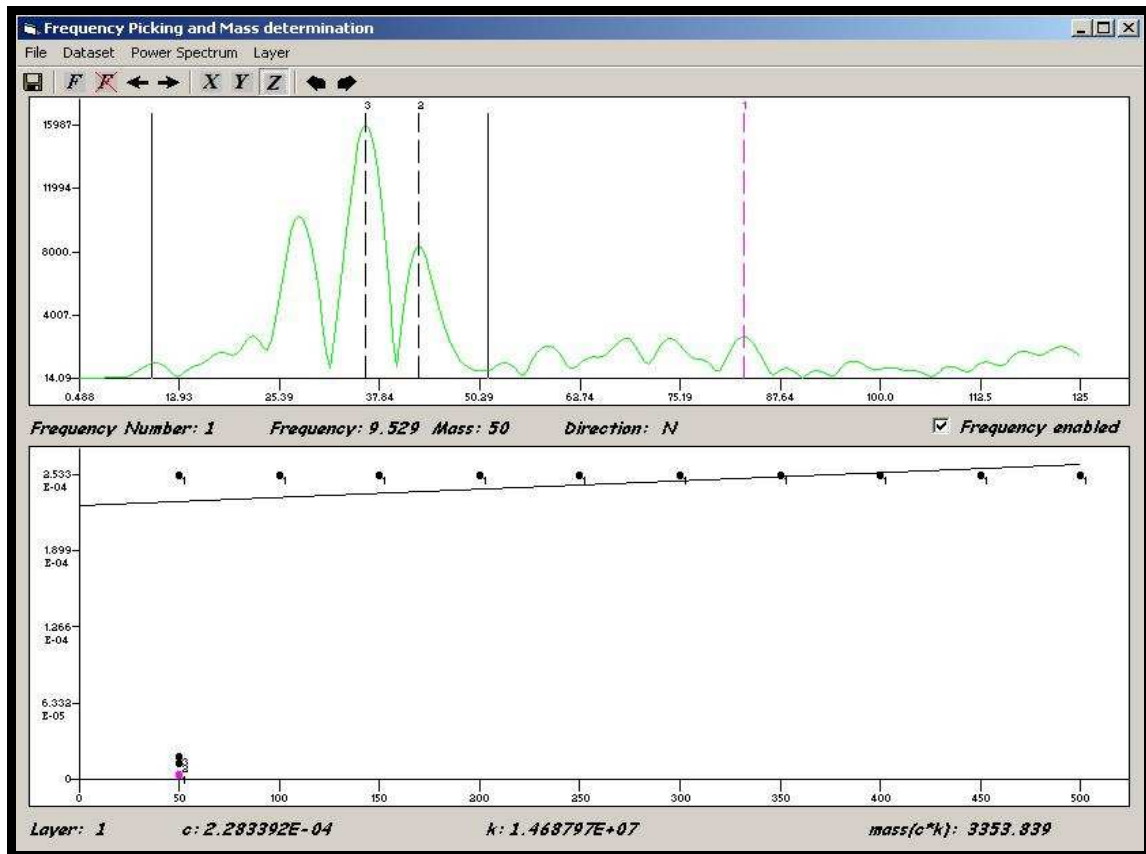


Figure 3.4: Main mass calculation interface.

The next step in the processing is to identify the different frequencies that are associated with the different layers of the weathered zone. Each original trace is then filtered more than once to obtain these dominant frequencies, i.e. if there are three dominant frequencies, three different layers exist. The filtering will then be performed three times to produce three different traces correlating with these frequencies. These traces will be stored inside the “layer1” to “layer 3” directories hosted in the segydata directory. This option can be chosen from the main menu as the “Filter SEG-Y data” option (Figure 3.5).

Figure 3.6 shows the main interface where the filter parameters are chosen for the filter process. The parameters of the traces of all three components can be chosen and filtered by using this window. The next and previous records can be selected by pressing the ► or ◀ buttons.

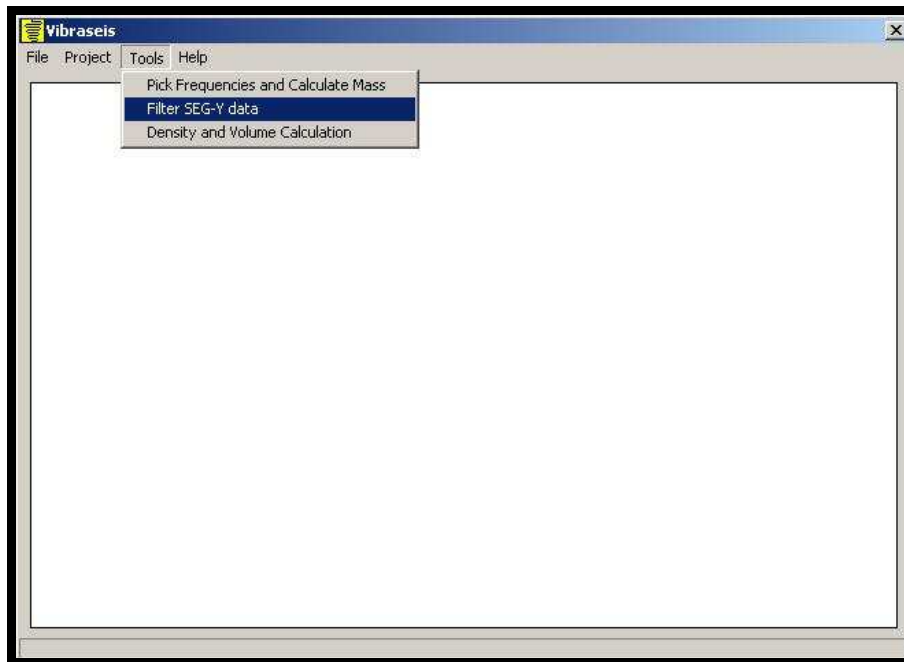


Figure 3.5: Main menu to filter the segy data.

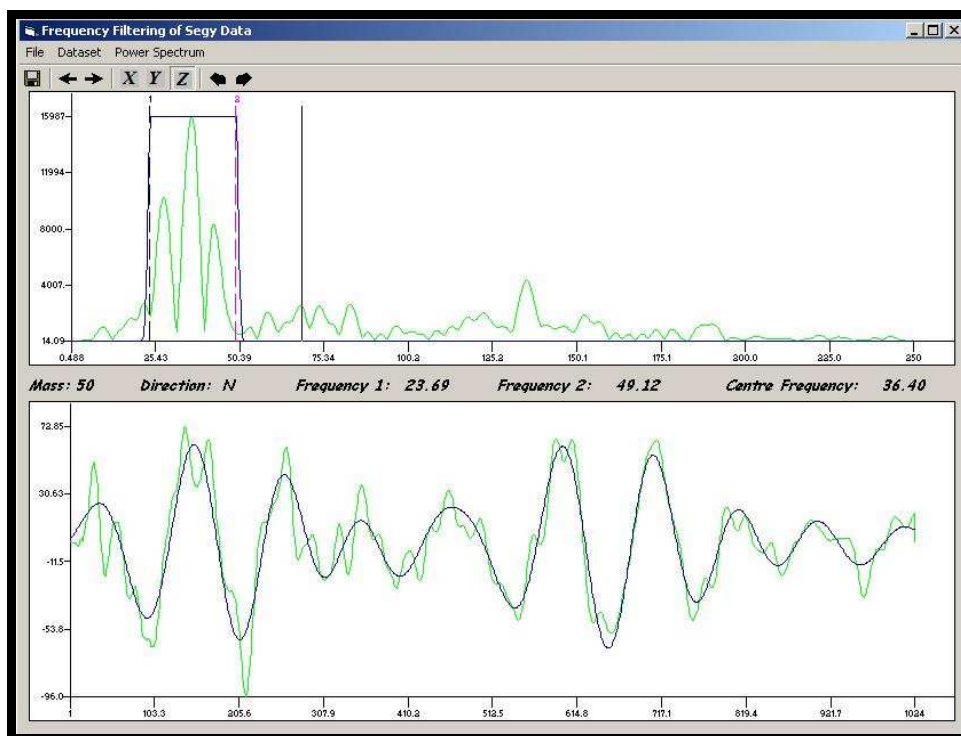


Figure 3.6: Window to filter the segy trace data. The lower and higher frequencies can be selected by pressing the ← or → buttons. The frequencies between the lines are kept.

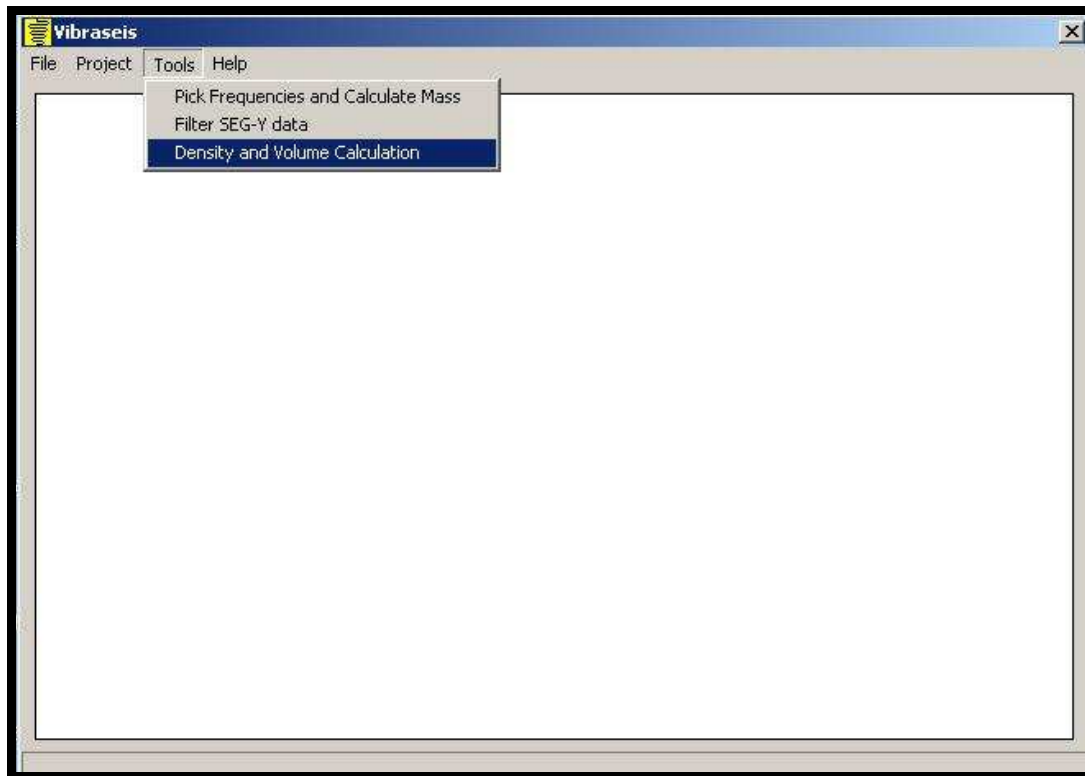


Figure 3.7: Main menu of Density and Volume Calculation.

The last step in the processing sequence is to calculate the volume of the excited mass and then obviously the density. This option can be selected from the main menu (Figure 3.7). The window, in which the main volume and density calculations are performed, is shown in Figure 3.8. This process has to be repeated for each frequency and each trace. Each component is done within its own window.

The top window displays the power spectrum of the filtered trace, as a guide. The middle window displays the filtered trace while the bottom window shows the values of the Q-factor. These Q-factors are calculated on a cycle to cycle basis and it is possible to remove a cycle from the equation if it does not fit in with the data, due to noise. This is done to improve the accuracy and speed of the calculation. The next and previous records can be selected by pressing the ► or ◀ buttons. The k-value (small movement elasticity modulus), the thickness of the layer and also the density of the layer are displayed at the bottom of this window. If the save button is pressed all the data is saved to a CSV file. These files can easily be opened by

Excel. Finally the main menu (Figure 3.9) is used to create a summary file of all the parameters, in a CSV format. These are the final interpretation values of the density sounding.

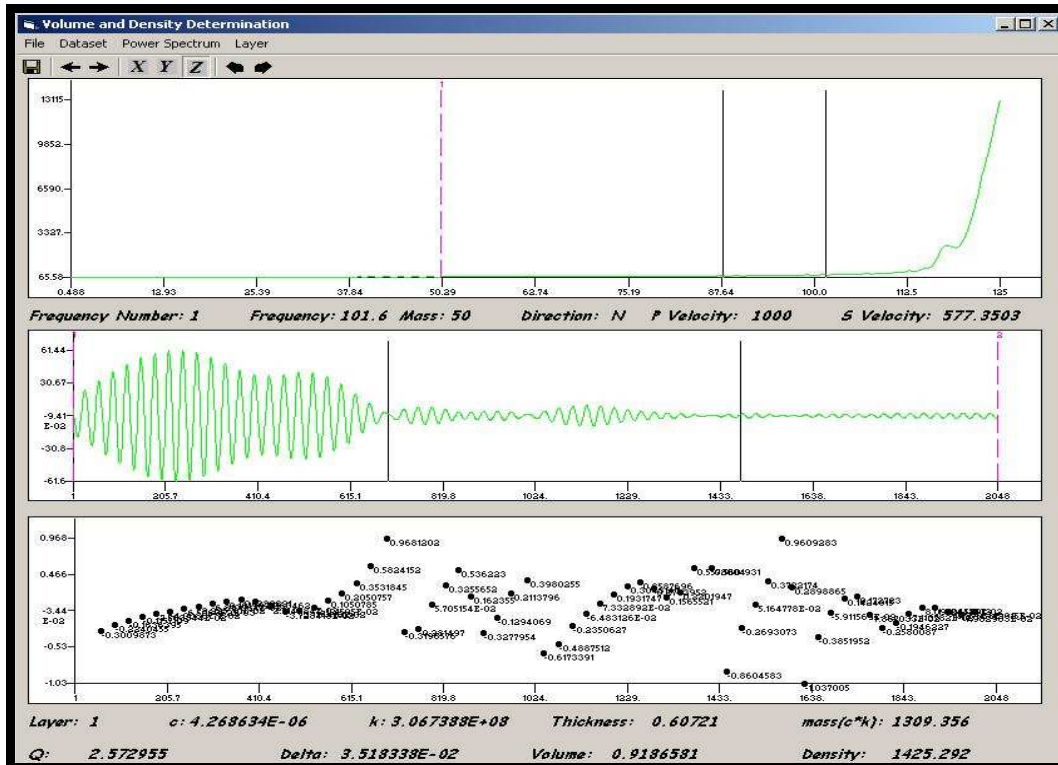


Figure 3.8: Main window to obtain volume and density.

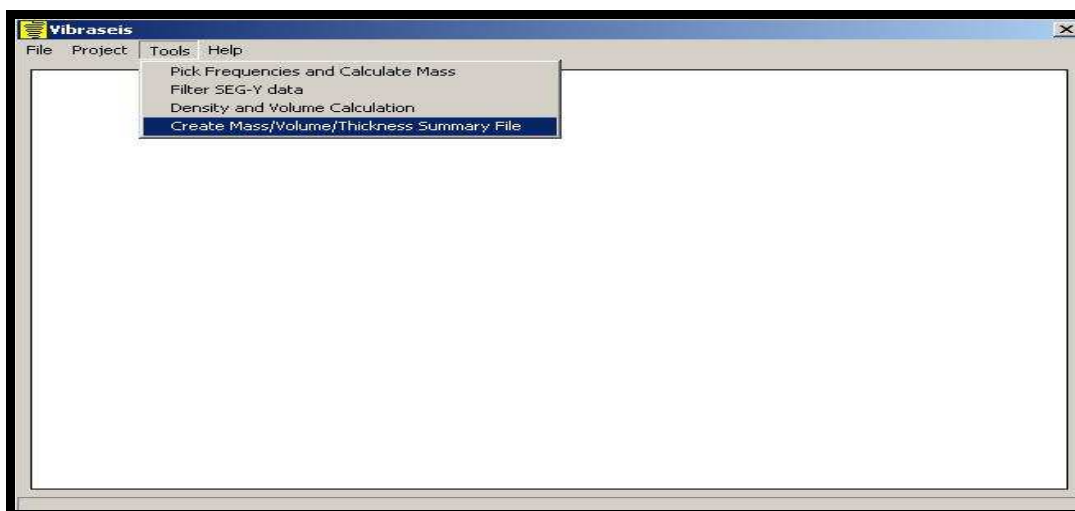


Figure 3.9: Main menu to create summary interpretation file.

CHAPTER 4

Equipment and experimental work

4.1 Introduction

After the initial theoretical development of the method, data had to be collected in the field to test and evaluate the idea. The approach was to first test the method on a single layer situation. It was also important to obtain the density of the subsurface by other means, to have control over the data.

4.2 Development of the trial equipment

In order to save money, trial equipment was put together from different sources. A steel base plate of 50kg was acquired (Figure 4.1). The base plate is a square steel plate of 1.23m and is 5mm thick. The three-component Springheather geophone (Figure 4.2) was mounted onto the base plate. Bags were filled with sand to make weights of 50kg each. These bags are placed onto the base plate to provide the additional mass (Figure 4.2).

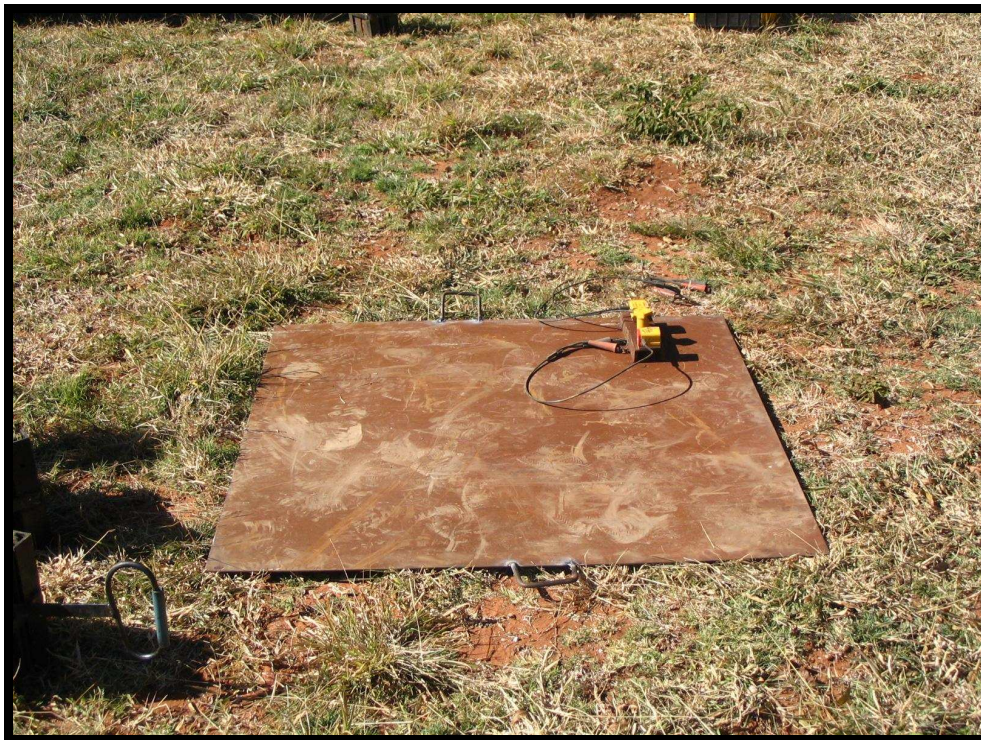


Figure 4.1: Large square 50kg steel base plate of 1.23m by 1.23m.



Figure 4.2: Mounting of Springheather 3-component geophone on base plate, with sand sacks to provide the weight.

The sand bags are put onto the base plate in an incremental fashion. The purpose of the sand bags is to change the weight of the system and hence the natural vibration frequency. The seismograph used for the original experimental equipment was an Ears- α seismograph system developed at the Council for Geoscience (Figure 4.3). The seismograph was originally developed by the Seismology Unit to monitor seismicity. It consists of a personal computer using a PC-104 interface operating from a 12V battery. It stores the data on a small internal hard disk drive. A DC to AC inverter was used to drive the monitor during the process.

The seismic source was a sledge hammer (Figure 4.4) and hammer blows were delivered at the four corners of the base plate. The hammer blows are delivered onto a small baseplate. The trigger is digital. Data recording length was set to 1s.



Figure 4.3: Ears- α seismograph system used which is developed by the CGS.



Figure 4.4: Seismic source was a sledge hammer. A hammer blow was delivered to corners of the plate.

4.3 First field test at Leeuwfontein

In order to verify the developed theory, it was necessary to find a locality which could represent a single layer only situation. The field survey should also be done where both geological and physical property control were good. The best locality found is just north of Pretoria at Leeuwfontein on the 2528CB Silverton sheet (Figure 4.5). The Leeuwfontein Syenites are igneous rocks present as a small outcrop on the farm Leeuwfontein (Figure 4.6) just north of Pretoria. It was mined for dimension stone in the past (Figure 4.7).

The Leeuwfontein syenite is part of the Roodeplaat Syenite Complex, situated in the Magaliesberg quartzites and diabase of the Pretoria Group. The depth extent of this syenite intrusion is more than 10m. This means that for the density sounding technique it can be regarded as a homogeneous single layer only situation.

The base plate was orientated in an N-S orientation. A sledge hammer was used as an energy source and a hammer blow was delivered to corners of the base plate. It was repeated for each weight, which was incremented with 50kg (a single sand sack) after four shots. The data was then recorded with the ears- α system.

The data was processed with a range of different software. The software used included SeisanTM, a package used in seismology. The final plots were done in MS Excel. The main objective of the processing was to calculate the dominant frequency and the attenuation constant.

By plotting the obtained frequency against the added mass, and by substituting the frequency into equation 12 (Chapter 2), the value of the excited mass is obtained. To calculate the sample volume that is excited, the wave velocity is needed. This velocity and attenuation information is substituted into equation 41 (Chapter 2) to obtain the excited volume.

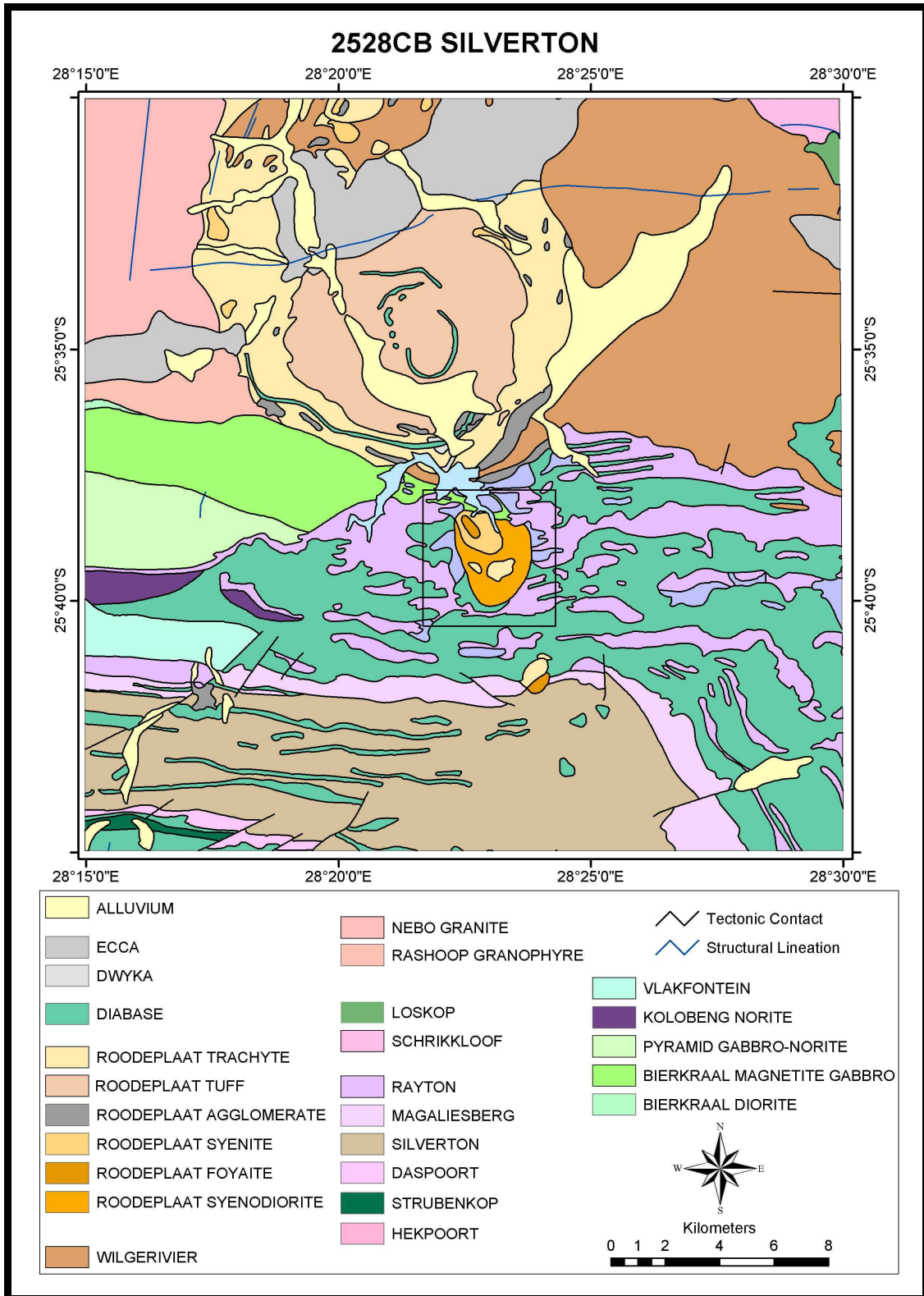


Figure 4.5: The 2528CB Silverton 1: 50 000 sheet. It depicts the geology of the immediate area just north of Pretoria. The Leeuwfontein area is indicated inside the square.

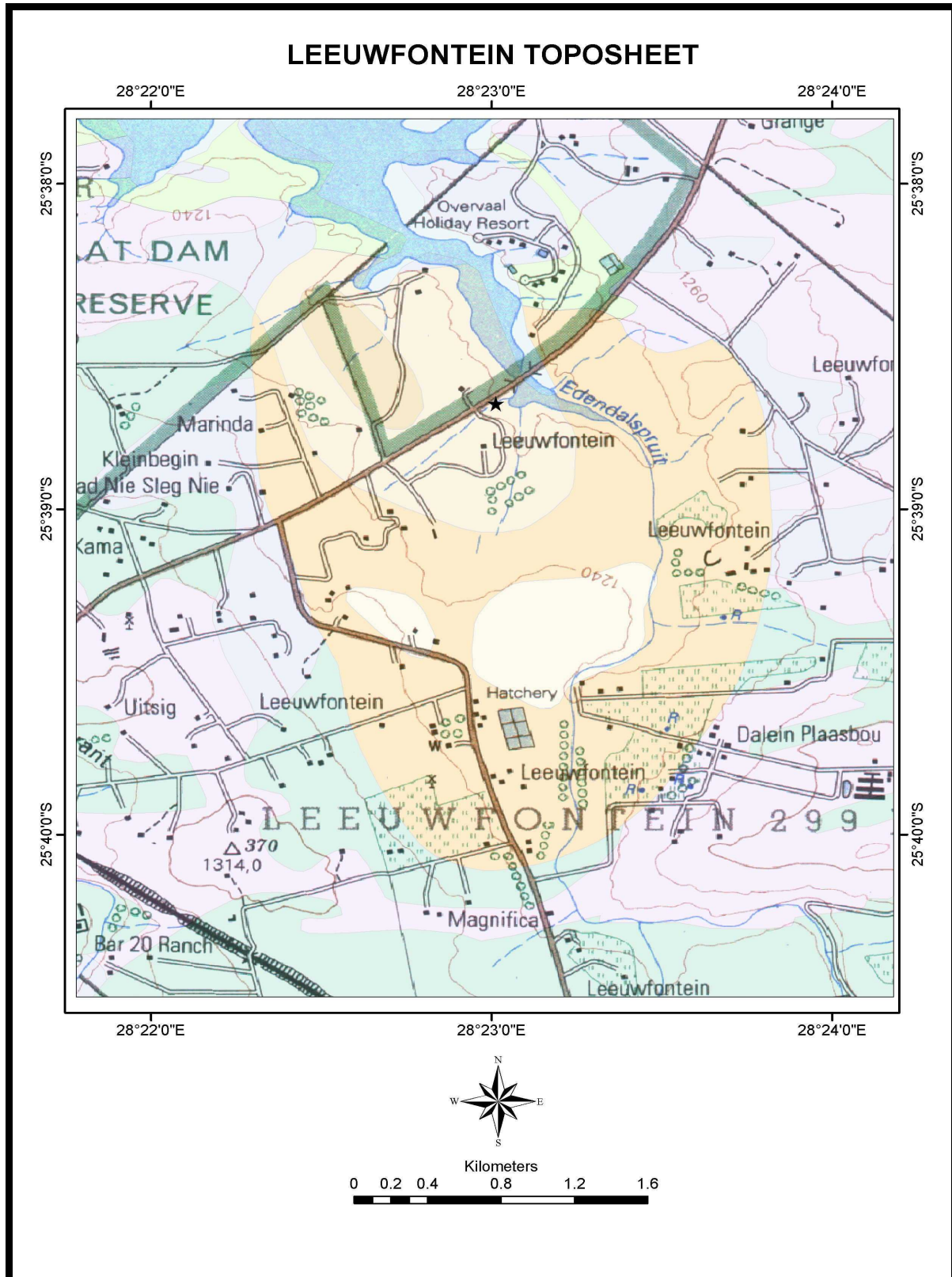


Figure 4.6: The topographic information of Leeuwnfontein overlain on the geology. The quarry site and fieldwork position is indicated with the cross.



Figure 4.7: The quarry site where the first tests were carried out. The depth extent of the syenites is much more than the penetration of the technique: - simulating a single layer situation.



Figure 4.8: Hand held core drill used for sampling. Water with cutting oil is used to ease the drilling process.

To verify the results, it was necessary to obtain some physical property information about the syenites, which included the seismic velocity and density. This was achieved by taking samples of the rock using a small hand held drill (Figure 4.8). The drill uses a diamond tipped drill bit to drill cores of 25mm in diameter up to a length of 30cm. In the physical property laboratory of the CGS the seismic velocities and the densities were measured. Table 4.1 shows the physical property information as measured in the laboratory.

Leeuwfontein Syenite		
Sample Name	Density (g/cm ³)	Seismic Velocity (m/s)
PS1	2.578	4705.9
PS2	2.582	4695.2
PS3	2.595	4692.5
PS4	2.603	4592.6
Average	2.590	4671.6

Table 4.1: Physical property values of Leeuwfontein Syenites as determined in the physical property laboratory of the CGS.

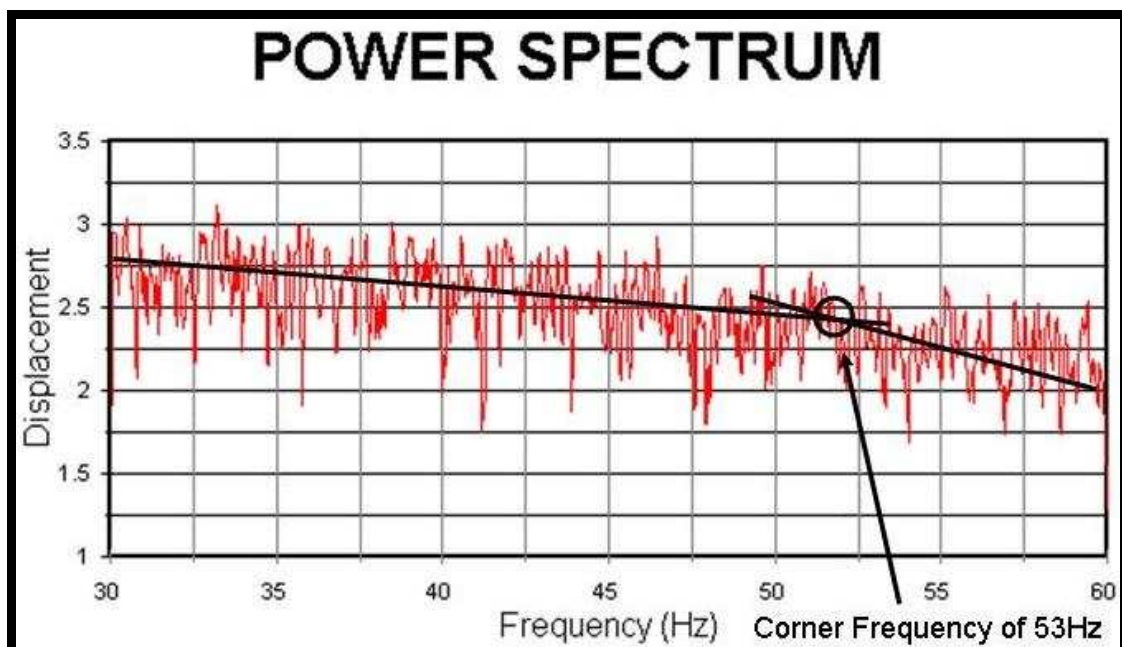


Figure 4.9: Example of a frequency spectrum of the traces that were used to determine the corner frequencies used for the calculation of the masses.

The data was processed using “SeisanTM”. In order to obtain the dominant frequency of the different traces, a power spectrum was calculated for each trace (Figure 4.9). The corner or dominant frequencies were determined on these power spectra, as indicated on Figure 4.9. All these frequencies were plotted against the masses (Figure 4.10). From this figure the excited mass was obtained. This data is given in Table 4.2. This process was repeated for all soundings.

The velocity in Table 4.1 was used in conjunction with an attenuation factor to calculate the depth of penetration. This depth of penetration was used to calculate the volume of mass that was excited. The densities were calculated and compared with the values obtained from the physical property laboratory. Table 4.3 gives the information as generated from both soundings and comparative values obtained from the physical property laboratory.

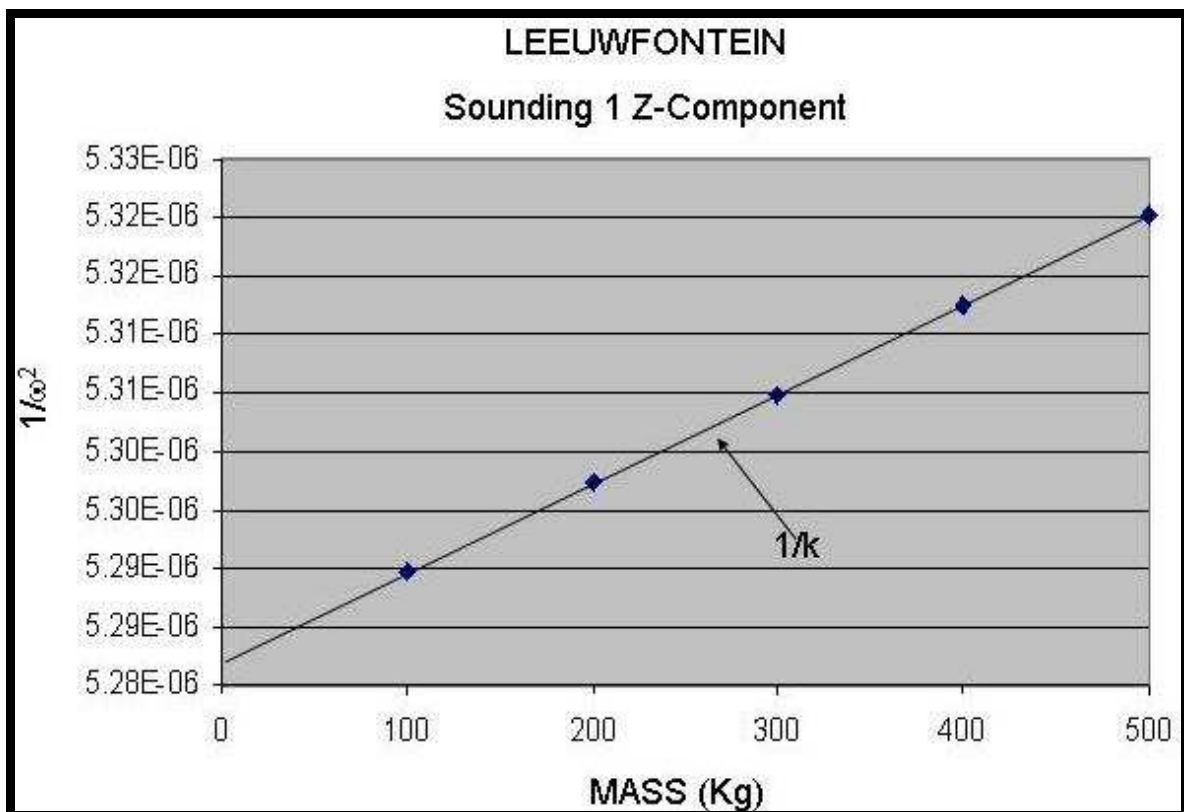


Figure 4.10: Plot to obtain excited mass M_0 from sounding 1 for the Z-component. The gradient is $1/k$.

Sounding 1				
Mass (Kg)	Freq (Hz)	ω	ω^2	$1/\omega^2$
100	69.2	434.7964233	189047.9297	5.29E-06
200	69.15	434.482264	188774.8377	5.3E-06
300	69.1	434.1681047	188501.9432	5.3E-06
400	69.05	433.8539455	188229.246	5.31E-06
500	69	433.5397862	187956.7462	5.32E-06
	K=	571Mpa	Mass=	7042Kg
Sounding 2				
Mass (Kg)	Freq (Hz)	ω	ω^2	$1/\omega^2$
100	73.06	459.0495	210726.4605	4.75E-06
200	72.9	458.0442	209804.4973	4.77E-06
300	72.3	454.2743	206365.1376	4.85E-06
400	72.2	453.646	205794.6744	4.86E-06
500	71.5	449.2477	201823.5404	4.95E-06
	K=	465Mpa	Mass=	7546kg

Table 4.2: Results for both soundings performed at Leeuwfontein.

SOUNDING1					
Mass(kg)	Volume(m³)	Density (g/cm3)	Depth (m)	Lab density (g/cm3)	Difference (g/cm3)
7042	2.718	2.591	1.80	2.580	+0.011
SOUNDING2					
7546	2.908	2.594	1.922	2.599	-0.005

Table 4.3: Final results from Leeuwfontein soundings.

4.4 Discussion of Leeuwfontein experiment and results

The results from the initial experiment at Leeuwfontein proved to be promising for a single layer only situation. The comparison of the analytical results with the laboratory measurements was encouraging, thus justifying further testing of the method.

The instruments used during this experiment was a makeshift setup that consisted of modules from different instrumentation. This instrumentation was large and heavy and proved to be clumsy. This was especially true with the sand bags that were used as weights. Certain modifications had to be done to the instrumentation.

4.5 Second field test at Donkerhoek

Single layer only, igneous basement rock environments, similar to Leeuwfontein are not often encountered. The main application envisaged for this method would be testing ground stability and foundation applications on the weathered layer. The next step was to test the technique on a single layer weathered profile. In order to verify the developed theory, for a weathering layer situation, it was necessary to find a locality representing a single layer only situation where a good geological knowledge existed. It was decided to do the test at Donkerhoek. Some good geological data exist there. The Donkerhoek locality is to the east of Pretoria, on the 2528CD Rietvleidam sheet (Figure 4.11).

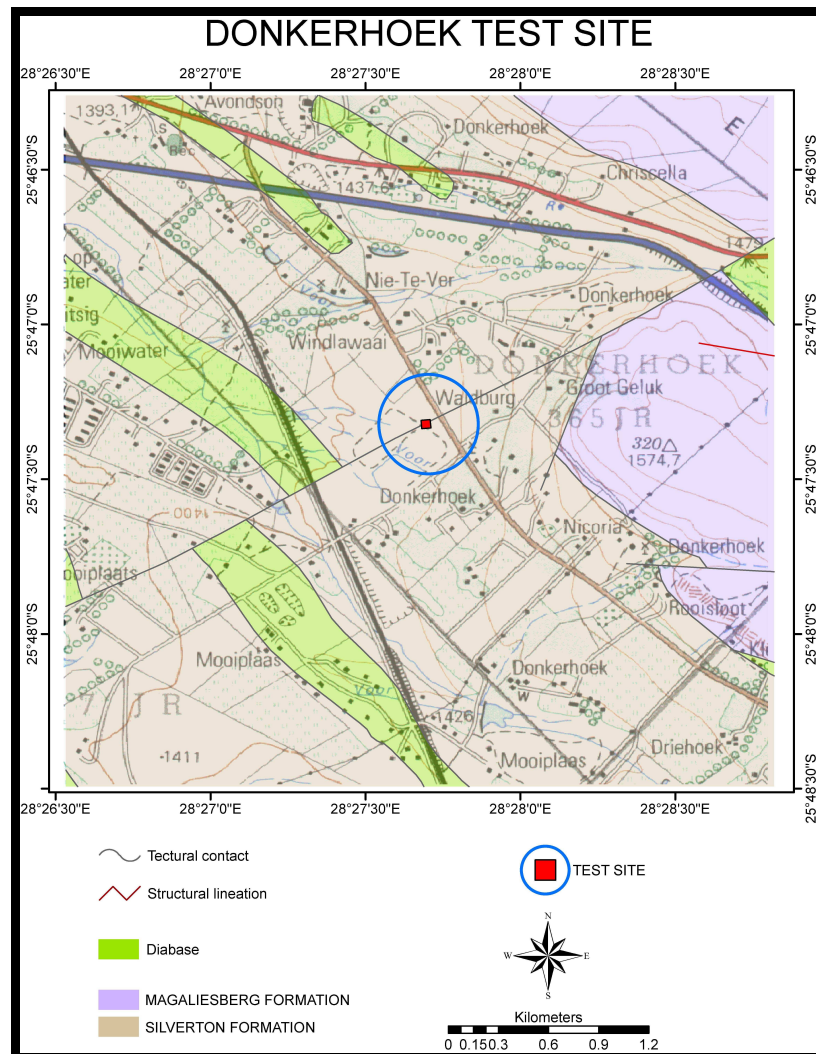


Figure 4.11: The geology of the Donkerhoek area.

The geology of the area consists mainly of shales of the Silverton Formation with bands of the Hekpoort andesitic lavas, lying on top of the Magaliesberg Quartzites. The weathered product in the Donkerhoek area is very thick heaving clay, which originates from the Silverton shales and the andesites. The thickness of this clay varies between 1.2 to 3m, representing a single layer only situation ideal for the testing of the technique (Figure 4.12).



Figure 4.12: Clays weathering product of the Silverton shales at Donkerhoek.

The equipment was modified to make the field operations a bit smoother, more reliable and to increase the quality of the data. The sand bags were substituted by weights (Figure 4.13) and the Ears- α seismograph was replaced by a 24-channel Bison 8024 seismograph (Figure 4.14). Unfortunately the seismograph is not a floating point system and amplitude clipping occurs when the hammer blow is too hard. The single Springheather 3-component geophone was replaced by three SM-6 geophones; one p-wave geophone and two s-wave geophones (Figure 4.15).

Three soundings were executed at Donkerhoek. The data collected from Donkerhoek was tested against a DCP test at each sounding position (Figure 4.16). The data from the DCP test is given in appendix II. At each sounding position a test pit was opened with a backacter. The soil profile was described and an undisturbed sample was taken. The sample was tested at credible soil labs and the results are shown in appendix II.



Figure 4.13: 50Kg weight that was constructed to replace sand sacks.



Figure 4.14: Bison seismograph that replaced ears- α seismograph



Figure 4.15: Geophones that replaced the single Springheather 3-D geophone used in the first experiment.



Figure 4.16: DCP test performed at each sounding position.

The base plate was also orientated in an N-S orientation. A sledge hammer was used as an energy source and a shot was done at all four sides of the base plate. It was repeated for each weight, After four shots it was incremented with 50kg (Figure 4.13) The data was recorded with the Bison seismograph. A very small seismic refraction survey was completed with a 0.5m geophone spacing to determine the velocity of the clay layer.

The data was processed with a range of software that was developed on Matlab and the final plots were done in Excel. The main objective of the processing was to determine the dominant frequency and the attenuation constant.

By plotting the obtained frequency against the added mass, and by substituting the frequency into equation 12 in Chapter 2, the excited mass is obtained. To calculate the excited sample volume, the wave velocity from the small refraction seismic survey is also needed. This velocity and attenuation information is substituted into equation 41 in Chapter 2 to obtain the excited volume. Table 4.4 displays the velocity information as obtained from the small seismic refraction surveys at each sounding position.

Donkerhoek – Silverton shales		
Sounding Number	Geophone spacing (m)	Seismic Velocity (m/s)
1	1	483.2
2	1	490.0
3	1	495.3
Average	1	489.5

Table 4.4: Seismic wave velocity values of Silverton shales as determined by small seismic refraction surveys.

Figure 4.17 shows the excited mass results from sounding 1 in all three directions. From the figure, one can see that it is more difficult to fit a straight line through the data with a low error margin. This is due to the fact that the sounding sites did not represent a true single layer only situation, and the deviations are shown in the data.

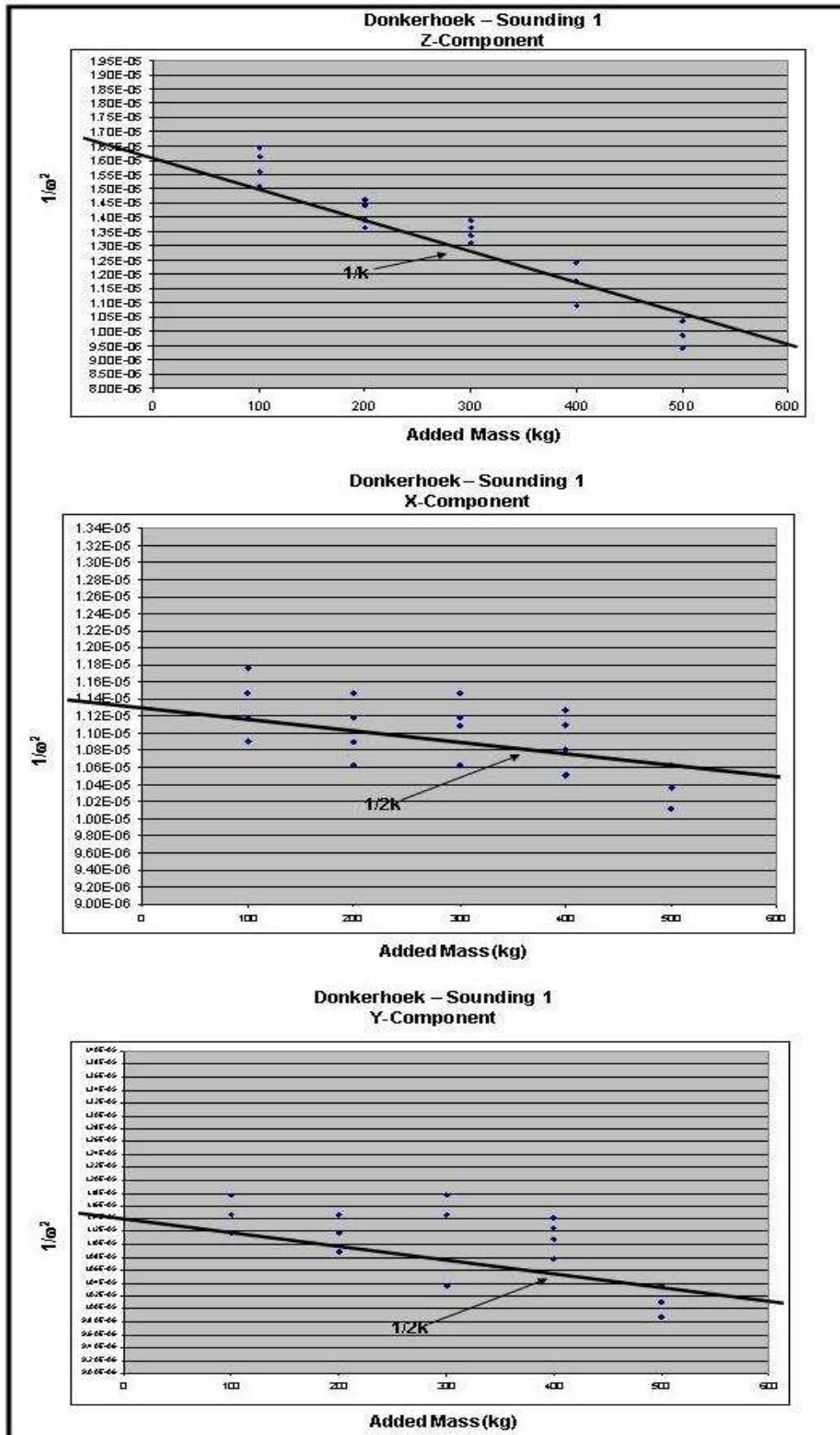


Figure 4.17: Plot to obtain excited mass M_0 from sounding 1. The gradient is $1/k$ for the Z-Component (P-wave) and $1/2k$ for the X and Y-Components (S-wave).

The depth of penetration for the seismic wave at the dominant frequency was calculated for each sounding position by determining the Q-factor. The decay is exponential as indicated in Chapter 2. The density measurements from the results from Soillabs are given in Appendix II. The comparison between the soundings and the results from Soillabs are shown in Table 4.5.

SOUNDING1					
Mass(kg)	Volume(m³)	Density (g/cm3)	Depth (m)	Lab density (g/cm3)	Difference (g/cm3)
6643	4.478	1.830	2.95	1.835	-0.005
SOUNDING2					
6270	4.591	1.634	3.10	1.632	+0.002
SOUNDING3					
6450	4.033	1.695	2.66	1.734	-0.039

Table 4.5: Final results from Donkerhoek soundings.

4.6 Discussion of Donkerhoek experiment and results

The results from the second experiment at Donkerhoek proved to be promising for a single layer only situation on the weathered layer. The comparison between analytical results and the laboratory measurements was encouraging, and justified further investigations. The larger difference between Sounding3 could be due to the fact that no undisturbed sample was taken from the testpit and an average density was taken as the laboratory result. The larger value for the density is assumed because of the larger shear modulus.

The instrumentation used during this experiment was an improved version to the one used for the first trail experiment. This instrumentation is still heavy but somewhat smaller and proved to be less clumsy. The Bison seismograph proved to be much easier to control and to operate and it was easier to produce results. The only major problem is the fact that the Bison is not a floating point instrument, as clipped traces produce inaccurate power spectrums.

The software in Matlab proved to be slightly easier to use than using SeisanTM. It is

however imperative that dedicated software has to be developed for this method.

4.7 Third field test at Country View

The Bison seismograph was replaced by a Geometrics Strataview 24-channel seismograph (Figure 4.18). This seismograph is a floating point system and it will prevent clipping of the traces.

The next step was to test the technique on a multi layer environment where geological control was possible. The area between Johannesburg and Pretoria, mainly underlain by the Halfway House granites, yields a good weathering product. It was decided to do the test at Country View an area earmarked for development. The locality is located on the 2528CC Verwoerdburg sheet (Figure 4.19). The main purpose of the survey was to evaluate the subsurface with the density sounding technique and to compare it with other laboratory techniques and the Troxler test.



Figure 4.18: Geometrics Strataview seismograph with 24 channels that replaced the Bison Geopro seismograph, mainly because it is a floating point system.

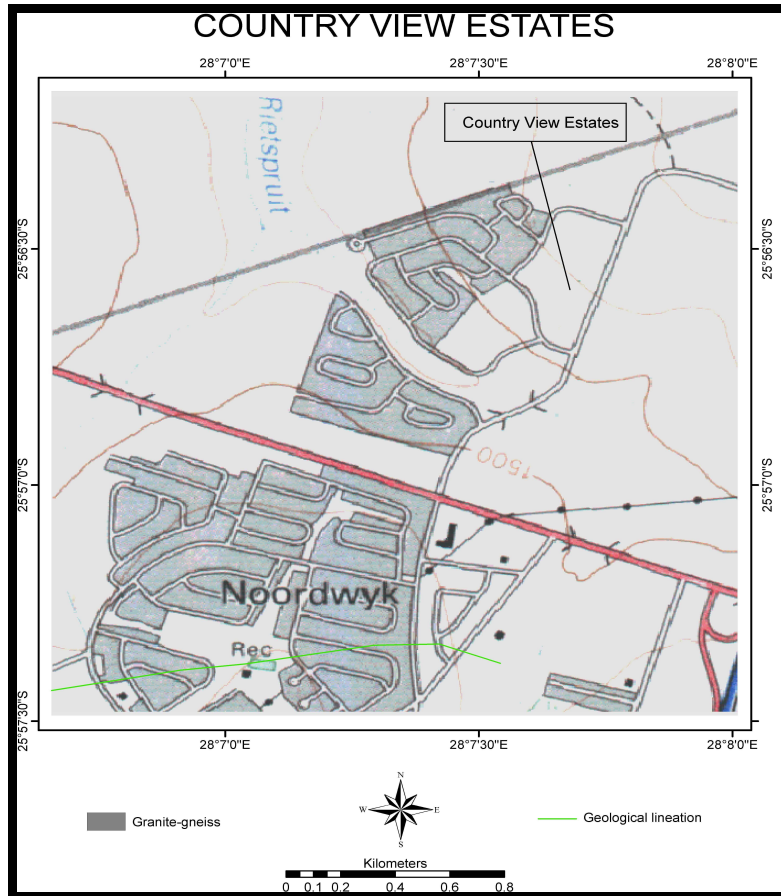


Figure 4.19: Enlarged portion of the 2528CC Verwoerdburg 1:50 000 sheet indicating Country view.



Figure 4.20: Weathering profile of the Halfway House Granites at Country View

The geology of the area consists mainly of Halfway House Granites. It is old Archean aged granite and forms the basement. The granites can be highly weathered and large areas are therefore covered by the weathering product (Figure 4.20). This is the case at Country View estates.

4.8 Fieldwork at Country View

Density soundings were performed on a multi layer weathered profile from the Halfway House Granites. It usually weathers to a soft top layer and a clay rich bottom layer, which transgresses slowly into fresh granite. The purpose of this survey was to determine the density of the layering for development of a small housing complex at Country View (Figure 4.21).

Test pits were dug at each density sounding position. Troxler tests, DCP tests as well as laboratory tests done by Soillab were used to verify the answers obtained from the density sounding technique. Table 4.6 gives the summarised results of the site. All the DCP profiles and laboratory results are given in Appendix II



Figure 4.21: Site at Country View estates.

SOUNDING 2: P-wave											
Layer	Total Mass (kg)	Mass (kg)	Total Volume (m³)	Volume (m³)	Total thick (m)	Thick (m)	Density (kg/m³)	E-Modulus	LAB (kg/m³)	DCP (kg/m³)	Troxler (kg/m³)
1	1309	1309	0.670	0.670	0.443	0.443	1953.73	1.88E9	1891		1661
2	5046	3737	2.33	1.660	1.540	1.079	2211.24	1.63E9			
3	6557	2820	2.81	1.15	1.856	0.777	2452.17	4.89E8	2596	2594	1623
SOUNDING 2: S-wave (North-South)											
Layer	Total Mass	Mass	Total Volume	Volume	Total thick	Thick	Density	E-Modulus	LAB	DCP	Troxler
1	1311	1311	0.680	0.670	0.442	0.442	1952.24	1.09E9	1891		1661
2	5034	3723	2.37	1.560	1.470	1.028	2428.21	1.07E9			
3	6740	3017	2.86	1.32	1.897	0.869	2065.15	4.89E8	2596	2594	1623
SOUNDING 2: S-wave (East-West)											
Layer	Total Mass	Mass	Total Volume	Volume	Total thick	Thick	Density	E-Modulus	LAB	DCP	Troxler
1	1308	1308	0.670	0.670	0.442	0.442	1952.24	1.09E9	1891		1661
2	5096	3788	2.23	1.560	1.470	1.028	2428.21	1.07E9			
3	6514	2726	2.88	1.32	7.897	0.869	2065.15	4.63E8	2596	2594	1632
						Ave1	1954.23	1.35E9			
						Ave2	2280.80	1.25E9			
						Ave3	2356.32	4.80E8			

Table4.6: Summarised results from Country View.

SOUNDING 3: P-wave											
Layer	Total Mass (kg)	Mass (kg)	Total Volume (m³)	Volume (m³)	Total thick (m)	Thick (m)	Density (kg/m³)	E-Modulus	LAB (kg/m³)	DCP (kg/m³)	Troxler (kg/m³)
1	1309	1309	0.670	0.670	0.443	0.443	1957.15	2.87E9			
2	4998	3689	2.33	1.660	1.540	1.079	2222.29	1.04E9			
3	6551	2862	2.81	1.15	1.856	0.777	2488.69	4.28E8			
SOUNDING 3: S-wave (North-South)											
Layer	Total Mass	Mass	Total Volume	Volume	Total thick	Thick	Density	E-Modulus	LAB	DCP	Troxler
1	1307	1307	0.680	0.670	0.442	0.442	1928.68	1.91E9			
2	5195	3888	2.37	1.560	1.470	1.028	2300.59	3.09E9			
3	6415	2527	2.86	1.32	1.897	0.869	2159.83	3.78E8			
SOUNDING 3: S-wave (East-West)											
Layer	Total Mass	Mass	Total Volume	Volume	Total thick	Thick	Density	E-Modulus	LAB	DCP	Troxler
1	1302	1302	0.670	0.670	0.442	0.442	1962.71	1.87E9			
2	5002	3700	2.23	1.560	1.470	1.028	2371.79	3.03E9			
3	6510	2810	2.88	1.32	7.897	0.869	2128.79	4.81E8			
						Ave1	1949.51	2.22E9			
						Ave2	2298.29	2.39E9			
						Ave3	2259.10	4.29E8			

Table 4.6: Summarised results form Country View.

SOUNDING 4: P-wave											
Layer	Total Mass (kg)	Mass (kg)	Total Volume (m³)	Volume (m³)	Total thick (m)	Thick (m)	Density (kg/m³)	E-Modulus	LAB (kg/m³)	DCP (kg/m³)	Troxler (kg/m³)
1	1309	1309	0.681	0.681	0.450	0.450	1920.54	3.67E8	1891		1711
2	4991	3683	2.345	1.664	1.550	1.100	2213.34	3.73E8			
3	6439	1448	2.995	0.651	1.980	0.430	2224.27	3.74E8	2526	2634	1697
SOUNDING 4: S-wave (North-South)											
Layer	Total Mass	Mass	Total Volume	Volume	Total thick	Thick	Density	E-Modulus	LAB	DCP	Troxler
1	1318	1318	0.681	0.681	0.450	0.450	1935.39	3.38E8	1891		1711
2	4966	3648	2.345	1.664	1.550	1.100	2192.31	7.78E8			
3	6427	1461	2.995	0.651	1.980	0.430	2244.24	7.89E8	2526	2634	1697
SOUNDING 4: S-wave (East-West)											
Layer	Total Mass	Mass	Total Volume	Volume	Total thick	Thick	Density	E-Modulus	LAB	DCP	Troxler
1	1313	1313	0.681	0.681	0.450	0.450	1928.05	3.38E8	1891		1711
2	4992	3679	2.232.345	1.664	1.550	1.100	2210.94	1.05E8			
3	6496	1504	2.995	0.651	1.980	0.430	2310.99	4.32E8	2526	2634	1697
						Ave1	1927.99	3.28E8			
						Ave2	2205.53	4.34E8			
						Ave3	2259.83	5.32E8			

Table 4.6: Summarised results from Country View.

SOUNDING 5: P-wave											
Layer	Total Mass (kg)	Mass (kg)	Total Volume (m³)	Volume (m³)	Total thick (m)	Thick (m)	Density (kg/m³)	E-Modulus	LAB (kg/m³)	DCP (kg/m³)	Troxler (kg/m³)
1	1309	1309	0.670	0.670	0.443	0.443	1957.15	2.87E9			1891
2	4998	3689	2.33	1.660	1.540	1.079	2222.29	1.04E9			
3	6551	2862	2.81	1.15	1.856	0.777	2488.69	4.28E8			1645
SOUNDING 5: S-wave (North-South)											
Layer	Total Mass	Mass	Total Volume	Volume	Total thick	Thick	Density	E-Modulus	LAB	DCP	Troxler
1	1307	1307	0.680	0.680	0.450	0.450	1928.68	1.91E9			1891
2	5195	3888	2.37	1.690	1.570	1.120	2300.59	3.09E9			
3	6415	2527	2.86	1.17	1.888	0.768	2159.83	3.78E8			1645
SOUNDING 5: S-wave (East-West)											
Layer	Total Mass	Mass	Total Volume	Volume	Total thick	Thick	Density	E-Modulus	LAB	DCP	Troxler
1	1302	1302	0.670	0.670	0.442	0.442	1962.71	1.87E9			1891
2	5002	3700	2.23	1.560	1.470	1.028	2371.79	3.03E9			
3	6510	2810	2.88	1.32	1.897	0.869	2128.79	4.18E8			1645
						Ave1	1949.51	2.22E9			
						Ave2	2298.29	2.39E9			
						Ave3	2259.10	4.29E8			

Table 4.6: Summarised results from Country View.

4.9 Discussion of Country View experiment and results

Three layers were identified at Country View from the gathered field data. The first is a thin top layer of approximately 0.45m in thickness. The second layer is approximately 1m thick, while a third layer was also interpreted. This data show that the second layer has a lower density and is also softer than the first layer. This relationship was also substantiated by the DCP tests shown in Appendix II. This was also corroborated from visual and physical inspection of the test pits.

The density soundings also revealed that the area is anisotropic with weaker direction North-South relative to the East-West direction. This is obvious from inspection of the modulli in Table 4.6. Where possible, the design of the buildings needs to be altered in such a way that the heavier loads are orientated in the East-West direction to ensure stronger foundations.

From Table 4.6 it is clear that the density sounding technique yielded density values closer to the laboratory results or those obtained by Troxler neutron method. The values obtained from the density sounding technique are in-situ values and a fixed moisture content is always present. Differences in the moisture content may be the largest reason why the values differ. However it is true that the densities sounding methods is no different to any other geophysical method approximating the real situation and in rare occasions yield precisely the same results as the laboratory.

CHAPTER 5

Conclusions and Recommendations

5.1 Conclusions and Recommendations

The development of this method was born from the need to find a way of measuring the density of the substratum using a non-invasive approach. It is believed that the new approach discussed in this thesis can meet this requirement. The method utilizes data in three dimensions; which include vertical pressure waves (P-waves) and horizontal shear waves (S-waves).

Comparison with the laboratory data was favourable. This method was successful in the field and poses some merit. Single layer scenarios where the method can be applied are only encountered in very few cases. Examples of single layer cases are man-made structures, such as road embankments and gravity dam walls. Tests in multi-layer situations, particularly with the weathered profile were also successful. In most cases, the weathered layer is a multi-layered medium.

The accuracy of the proposed method depends largely on the quality of instrumentation, processing accuracy (determining the damping factor (b) of the seismic traces) and of the subsurface. Given that the rocks and soil are strongly, but less than critically damped (Thorne & Wallace 1995) it is evident that the calculated volume depends largely on the damping factor. Various approaches for determining this factor have to be investigated on good-quality data and the processing software (Fourie and Cole, 2004). The coupling of the base plate with the subsurface is not yet perfected. This could lead to a lower determination of the excited mass and volume, and subsequently the density.

As with most other geophysical methods (such as the D.C. electrical resistivity and electromagnetic methods (Griffiths *et al.*, 1969, Telford, 1986, Kearey *et al.*, 1991), it will be impossible to do absolute accurate interpretations without any verification.

The method will yield a good first-order approximation, and if test pits or boreholes are available to verify the interpreted results, the savings may be considerable.

From the experience gained, it is evident that this method works relatively fast. It is possible to perform approximately 10 soundings in one day, depending on accessibility and the terrain. A major negative factor at this stage is that the equipment is still very heavy, which makes it difficult to manipulate. A redesign of the equipment will be necessary to increase the ease of handling and mobility of the equipment. One solution may be to permanently mount the equipment on a specialised vehicle.

Currently, data processing such as the digital signal processing and filtering, are done by means of dedicated in-house developed software in Visual Basic (Fourie and Cole, 2004). This software unifies all the necessary processes and routines to process the data and the display options into one package.

One important addition towards the software can be done. For Q-values that stay more or less constant, a technique was developed by Kjartansson (1979) whereby the Q-factor can be established by means of a relationship between the frequencies of the successive layers and the small movement elasticity moduli of the successive layers. This relationship is given below:

$$\left(\frac{1}{Q}\right) \approx \frac{\Pi}{\log\left(\frac{\omega}{\omega_0}\right)} \left(\frac{1}{2} \frac{k_1 - k_0}{k_0}\right) \quad 5.1$$

The main application from this relationship would be that the Q-values that is needed to calculate the layer thicknesses can already be determined during the mass determination phase. This will save a tremendous amount of time during the processing of the data.

Finally, the main advantages of this method should be emphasized:

- The method is non-invasive/non-destructive.
- The method will be cost effective, by limiting the number of test pits, and large diameter exploration holes.
- Laboratory costs will be reduced.
- The method is fast, and the production rate is relatively high.

Recommendations are that:

- Setup should be mounted on a specialized vehicle for easier operation.
- More weight increments to a larger total mass of 1000Kg should be utilized in order to obtain the small movement modulus more accurately.
- Improvement on the software should be done and the Kjartansson method of Q-factor development should be incorporated into the software.
- Method should be tested for the influence of discontinuities in the soil.

5.2 Acknowledgements

The author is very much indebted to the following persons, which made it possible for this research to be performed:

- Mr. Patrick Cole for the programming of the method in Visual Basic to process the data easily in a single package. He did a sterling job and made it possible to process the data.
- Mr. Gerard Finnie of the University of the Witwatersrand who reviewed the mathematics very meticulously and went through the mathematical derivation with a magnifying glass. He also verified certain relationships with Mathematica. He did a splendid job, and picked all the mistakes, of which there were a lot. This is really appreciated.
- A special word of gratitude is also expressed towards Prof. J.L. van Rooy for



his valuable advice during this project.

- Thanks to Mrs. Leonie Maré of the Physical Property Laboratory at the Council for Geoscience for performing the laboratory tests on the control samples and for helping with the preparation of some of the figures.
- Gratitude is also expressed towards Messrs C. R. Randall and I. Saunders of the Council for Geoscience for fruitful and sometimes heated discussions.
- The author also wishes to thank Ms Zahn Nel, language consultant of the Council for Geoscience, for proofreading the document and for the French translations during publications

6. REFERENCES

- Abbiss, C.P., 1979:** A comparison of the stiffness of the chalk at Mundford from a seismic survey and a large scale tank test; *Geotechnique* Vol. 29, no. 4, pp. 461-468.
- Abbiss, C.P., 1981:** Shear wave measurements of the elasticity of the ground; *Geotechnique*, Vol 31, no.1, p. 91-104.
- Allred, B.J., Redman, J.D., McCoy E.L. and Taylor R.S., 2005:** Golf Course Applications of Near-Surface Geophysical Methods: A Case Study; *Journal of Environmental and Engineering Geophysics*, Vol.10, Issue 1
- Auld, B., 1977:** Cross - hole and down - hole V_s by mechanical impulse; *Journal of Geotechnical Engineering*, Vol. 103, no. GT12, pp. 1381 - 1398.
- Baguelin F., Jézéquel, J.F. and Shields, D.H., 1978:** The Pressure meter and Foundation Engineering (First Edition). Series on Rock and Soil Mechanics (Vol. 2, No. 4): Trans Tech Publications.
- Brown, P.D. and Robertshaw, J., 1953:** The in-situ measurement of Young's modulus for rock by a dynamic method; *Geotechnique* Vol. 3, no. 7, p.283.
- Byrne G., Everett J.P., Schwartz K., Friedlaender E.A., Mackintosh N., Wetter C., 1995:** A Guide to Practical Geotechnical Engineering in Southern Africa. Third Edition, Franki, 1995.
- Classical Mechanics lecture notes, 1980:** University of Stellenbosch, South Africa.
- Clayton C.R.I. and Heyman G., 2001:** Stiffness of geomaterials at very small strains; *Geotechnique*, Vol. 51, no. 3, pp. 245-255.

Craill, C, etal, 1993: Donkerhoek (Pretoria); Resultate van alle geofisieseopnames gedoen op die terrein tot en met 31 Januarie 1993, Verslag Geologiese Opname van Suid Afrika.

Design of Small Dams, 1965: United States Department of the Interior, Bureau of Reclamation.

Darracott, B.W., 1976: Seismic surveys and civil engineering; The Civil Engineer in South Africa, February, 1976.

Davis E.H. and Poulos H.G., 1966: Laboratory investigations of the effects of sampling; Proc. Symp. on Site Investigation, Sydney, Australia.

Fourie C.J.S., 2005: Three-dimensional in-situ density estimations using a seismic technique. Africa Geoscience Review, Vol.12, no. 1&2.

Fourie C.J.S. and Cole P., 2004: Development of an In-situ Density Geophysical method using a Seismic Technique. Internal report to the CGS, report number 2004-0095.

Fourie C.J.S. and Cole P., 2004: Three Dimensional In-situ Density Estimations using a Seismic Technique. Geoscience Africa Conference, University of the Witwatersrand, Johannesburg South Africa, 12-16 July.

Franki, 1995: A Guide to Practical Geotechnical Engineering in Southern Africa. Third Edition.

Griffiths, D.H. and King R.F., 1969: Applied Geophysics for Engineers and Geologists; Pergamon Press.

Heyman G., Clayton C. R. I. and Reed T., 1997: Laser Interferometry to evaluate the performance of local displacement transducers; Geotechnique Vol. 47, no.

3, pp. 399-405.

Heyman G., 2003: The Seismic Cone Test; Journal of the South African Institution of Civil Engineering, Vol 45, no.2, p.26-31, Paper 552.

Horton, C.W., 1953: Rayleigh waves on the surface of visco-elastic solid, Geophysics Vol. 18, no.1, pp. 70-74.

Jardin R.J., Potts D.M., Fourie A.B. and Burland J.B., 1986: Studies of the influence of non-linear characteristics in soil-structure interaction; Geotechnique Vol.36, no. 3, pp. 377-396.

Kearey, Phillip and Brooks, Michael, 1991: An introduction to Geophysical Exploration, Second Edition, Blackwell Scientific Publications.

Kibble T.W.B., 1985: Classical Mechanics, Third Edition, Longman Scientific & Technical Press, London.

Kjartansson, E., 1979: Constant Q wave propagation and attenuation; Journal of Geophysical Research, Vol. 84, pp.4737-4748.

Mavko, K., Mukerji, T. and Dvorkin, J., 2003: The Rock Physics Handbook, Cambridge University Press, Edinburgh.

Moya, A., Schmidt, V., Segura, C., Boschini, I. And Atakan, K., 2000: Empirical evaluation of site effects in the metropolitan area of San José, Costa Rica; Soil Dynamics and Earthquake Engineering Vol.20, no.1-4.

Nasseri-Moghaddam, A., Cascante, G. And Hutchinson, J, 2005: A New Quantative Procedure to Determine the Location and Embedment Depth of a Void Using Surface Waves; Journal of Environmental and Engineering

Geophysics, Vol.10, Issue 1.

Safak, E., 2000: Characterisation of seismic hazard and structural response by energy flux; Soil Dynamics and Earthquake Engineering, Vol. 20, no. 1-4.

Sears, Zemansky and Young, 1987: University Physics (Seventh Edition).
Massachusetts: Addison-Wesley Publishing Company.

Shtivelman, V., Marco, S., Reshef, M., Agnon, A. And Hamiel, Y., 2005: Using trapped waves for mapping shallow fault zones; Near Surface Geophysics, Vol. 3 no.2.

Telford, W.M., 1986: Applied Geophysics, Cambridge University Press.

Thanassoulas, C. and Tsokas, G.N., 1985: A microcomputer program for Tsuboi's method of gravimetric interpretation; First Break Vol. 3, No.6, 1985.

Thorne, L, and Wallace, T C, 1995: Modern Global Seismology. San Diego: Academic Press.

Tsuboi, C., 1983: Gravity, p.254; George Allen and Unwin, London.

Turesson, A. and Lind, G., 2005: Evaluation of electrical methods, seismic refraction and ground penetrating radar to identify clays below sands – Two case studies in SW Sweden; Near Surface Geophysics, Vol. 3 no.2.

United States Department of the Interior, Bureau of Reclamation, 1965: Design of Small Dams.

Waters, K.H., 1981: Reflection Seismology, A tool for Energy Exploration, Wiley and Sons, New York.



Wilson M.G.C and Anhaeusser, C.R., 1998: The Mineral Resources of South Africa. Council for Geoscience, Sixth Edition.

Yilmaz, O, 1989: Seismic Data Processing, Society of Exploration Geophysicists, U.S.A.



Appendix I

Accepted and Published Paper



Three-dimensional *in-situ* subsurface density estimations using a seismic technique

C. J. S. FOURIE

Geophysics Division, Council for Geoscience, Private Bag X112, Pretoria, 0001, South Africa
stoffel@geoscience.org.za

Abstract - Various geophysical methods, such as seismic refraction and gravity techniques, are intended to measure or to give an estimation of the density of a subsurface. However, these methods, at best, yield only an average value, because of the large size of the sampling volume. Depending on the degree of accuracy needed, an undisturbed sample may well be the only solution. If it is the case, test pits need to be made or large diameter holes need to be drilled. The cost of the operation will necessarily then increase in accordance with the number of samples that need to be taken at a specific site. The entirely new geophysical method proposed in this article entails measuring the *in-situ* density of the subsurface. It utilises seismic energy by recording seismic traces in three dimensions, and measuring the density vertically, rather than laterally. Although only a few experiments have been performed so far in a “single layer” situation, the results seem promising.

Keywords: In-situ, density, P-wave, S-wave, Seismic

Résumé - Plusieurs méthodes géophysiques, telles que les techniques de réfraction sismique et gravimétrique, visent à mesurer ou à évaluer la densité de la surface. Cependant, ces méthodes, aux mieux, ne rendent qu'une valeur moyenne à cause du volume considérable du matériel prélevé. D'après le degré de précision requise, il se peut bien que la seule solution soit d'utiliser un échantillon non traité. Le cas échéant, il faudra creuser des puits d'exploration ou forer de grands trous de diamètre. Le coût de l'opération montera forcément en flèche, conformément au nombre d'échantillons qui devront être prélevés à tout site particulier. La méthode de géophysique tout à fait innovatrice proposée dans cet article nécessite que les dimensions de la densité *in-situ* du sous-sol soient mesurées. Elle se sert d'énergie sismique en enregistrant des traces sismiques à trois dimensions, et en mesurant la densité de façon verticale plutôt que latérale. Même s'il n'y a qu'un nombre limité d'expériences effectuées jusqu'au présent dans un domaine se composant d'une couche unique, les résultats de celles-ci semblent prometteurs.

INTRODUCTION

There are various methods (e.g. the Dynamic Penetrometer Test or DPT and the Cone Penetrometer Test (Baguelin *et al.*, 1978 and Franki, 1995) used today that enable structural engineers and engineering geologists to gain some understanding of the density distribution of the subsurface. These methods are, however, qualitative and give only

estimates of the variations of the densities. At present the only way of obtaining conclusive measurements entails using “undisturbed samples” from the geological horizons, which can be expensive and difficult to handle. In addition to the laboratory costs, test pits or large diameter holes have to be drilled. Moreover, the unavailability of rapid laboratory results further delays the process.

A few established geophysical methods are used to determine subsurface rock densities. These include:

- the seismic method (usually refraction seismics (Kearey and Brooks, 1991)),
- the gravity method (Griffiths and King, 1969, Telford, 1986),
- and the neutron source or Troxler test (Byrne *et al.*, 1995).

The main disadvantage of the first two methods is that the sampling volume of the subsurface is often prohibitively large. Seismic refraction geophone spreads can be as large as 240m. This gives rise to a density measurement that has to be averaged over a large sample volume with resulting loss of resolution. The main concerns and difficulties with the Troxler test are safety (radioactive sources), moisture content of the subsurface and the relatively shallow depths to which it can be employed (30 cm–60 cm). Best employment are usually obtained inside testpits.

Owing to these reasons, it was thus necessary to develop a new geophysical methodology or method that would not only address these needs, but that would be, as an added advantage, non-invasive (Fourie and Cole, 2004). Important advantages of such a new geophysical method would be:

- The method would require fewer test pits, large diameter holes and undisturbed samples to verify the geophysics and to construe the interpretation.
- Current structures, such as road embankments and gravity dam walls, could be investigated without compromising their integrity.
- The depth of investigation is 2 m to 5 m.

UNDERSTANDING THE PROBLEM

All geophysical methods that are currently used to measure the density of the subsurface do so in an indirect manner. The gravity method is an exception. For example, from the seismic refraction method the P-wave velocity can be measured, and this velocity allows the scientist or engineer to derive a density (Griffiths and King, 1969, Telford, 1986, Yilmaz, 1989).

This new proposed method also measures

the density of the subsurface indirectly. It is also a seismic method. It attempts to measure the amount of mass that is excited by the seismic source, as well as the volume of this mass, thereby making it possible to calculate the density of the subsurface. A much smaller sampling volume is used, which in turn improves the resolution of the density measurement.

DESCRIPTION OF THE CONCEPT

During any seismic survey, the subsurface is set into vibration by a seismic source, such as a hammer or explosives. These vibrations are then recorded using sensitive sensors, such as geophones (Telford, 1986, Yilmaz, 1989).

In order to estimate the density of the subsurface, it is essential to obtain the mass (M_0) and the volume (V_0) of the sample area (figure 1). The challenge herein entails being able to determine M_0 and V_0 from indirect sources of measurement, without physically removing samples of the subsurface soils.

The proposed method calculates the mass and the volume of the sample to be investigated through the use of seismic waves. The seismic waves are recorded by using a three-component geophone system, mounted on a bearing plate on the surface (figure 1). The seismic energy is recorded in three dimensions, utilising the P- and S-waves, where the P-wave is the vertical wave and the S-waves are the horizontal waves. Weights are added in increments of 50 kg on top of the bearing plate to change the total mass (bearing plate plus added weights plus subsurface) and hence the frequency of vibration. The seismic source is a hammer. The P-waves and the S-waves are generated using a hammer. The hammer blows are delivered just next to the bearing plate, to simulate a zero offset (Yilmaz, 1989).

In an attempt to derive a descriptive mathematical model, it is assumed that the system can be represented by a simple model; a mass attached to a spring, which is equal to the mass of the subsurface underneath the bearing plate. The other end of the spring is fixed to an edifice (figure 2). All symbols are explained in the list of symbols (Table 1).

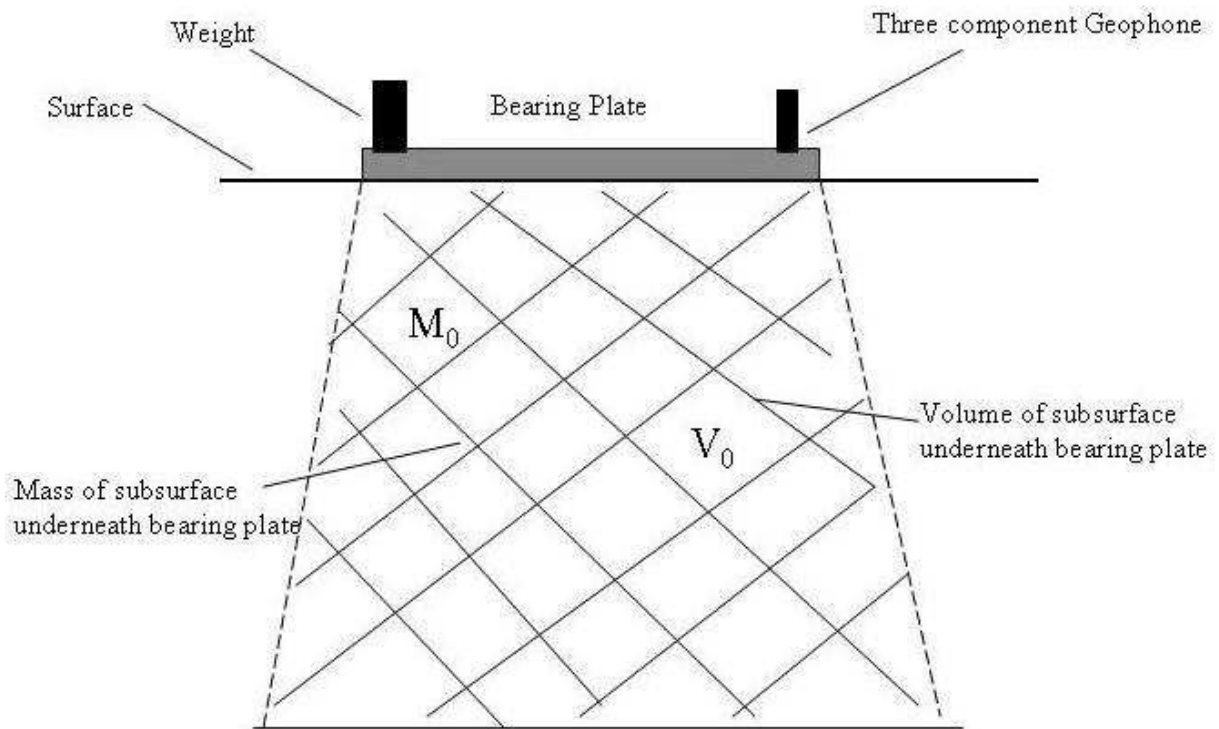


Figure 1. Schematic representation of the problem.

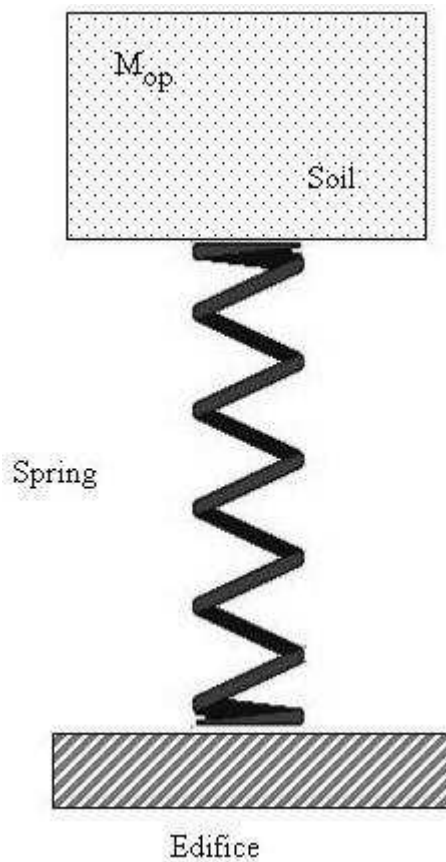


Figure 2: Simplified schematic P-wave physical model.

Table 1. List of symbols.

SYMBOL	EXPLANATION	SYMBOL	EXPLANATION
F_p	P-wave force	M_{TZ}	Total mass from P-wave
k_p	P-wave spring constant	$A(t)$	Amplitude with time
z	P-wave amplitude	A_{0z}	Initial Aplitude
M_{0p}	Groundmass	ω_{0z}	Initial Angular Frequency
\ddot{z}	P-wave acceleration	E_{kp}	Vertical Kinetic Energy
ω_p	Angular Frequency of the P-wave	ρ_p	Vertical density
Δm	Additional mass	λ_p	P-Wave length
A_p	Area of influence	F_s	S-wave force
L	Length of base plate	K_s	S-wave spring constant
h_p	Depth below base plate	x	S-wave amplitude
α	Influence angle	M_{0s}	Groundmass
V_{0p}	Volume of excited mass	\ddot{x}	S-wave acceleration
b_p	Damping factor of the P-wave	ω_s	Angular Frequency of the s-wave
V_p	Velocity of the P-wave	M_{TX}	Total mass from S-wave

Determination of the mass M_0 using the P-wave

Following the above assumption, Hooke's Law (Sears *et al.*, 1987) can be written as:

$$F_p = -k_p z \quad 1$$

where F_p is the force k_p is the spring constant and z is the vertical amplitude. The "p" subscript indicates the P-wave.

The differential wave equation (Kibble, 1985) that describes the movement of the mass is given in equation 2.

$$M_{0p} \ddot{z} + k_p z = 0 \quad 2$$

By solving this equation and allowing for the addition of extra mass (Δm), the following equation follows (Fourie and Cole, 2004):

$$k_p = \omega_p^2 (M_{0p} + \Delta m) \quad 3$$

and ω is the angular frequency.

By using equation 3 the following diagram (figure 3) represents the computation of M_0 (Fourie and Cole, 2004).

Determination of the volume V_0 using the P-wave

If a square base plate with dimensions L is used, the resulting area underneath the plate is L^2 . If we assume that the influence will not only come from directly underneath the plate, the new area (A_p) at a depth (h_p) below the base plate, if the angle of influence from the plate is α , is (Fourie and Cole, 2004) (figure 4)

$$A_p = (L + 2h_p \tan \alpha)^2 \quad 4$$

where the new length is $L + 2x$ and $\tan \alpha = x/h_p$

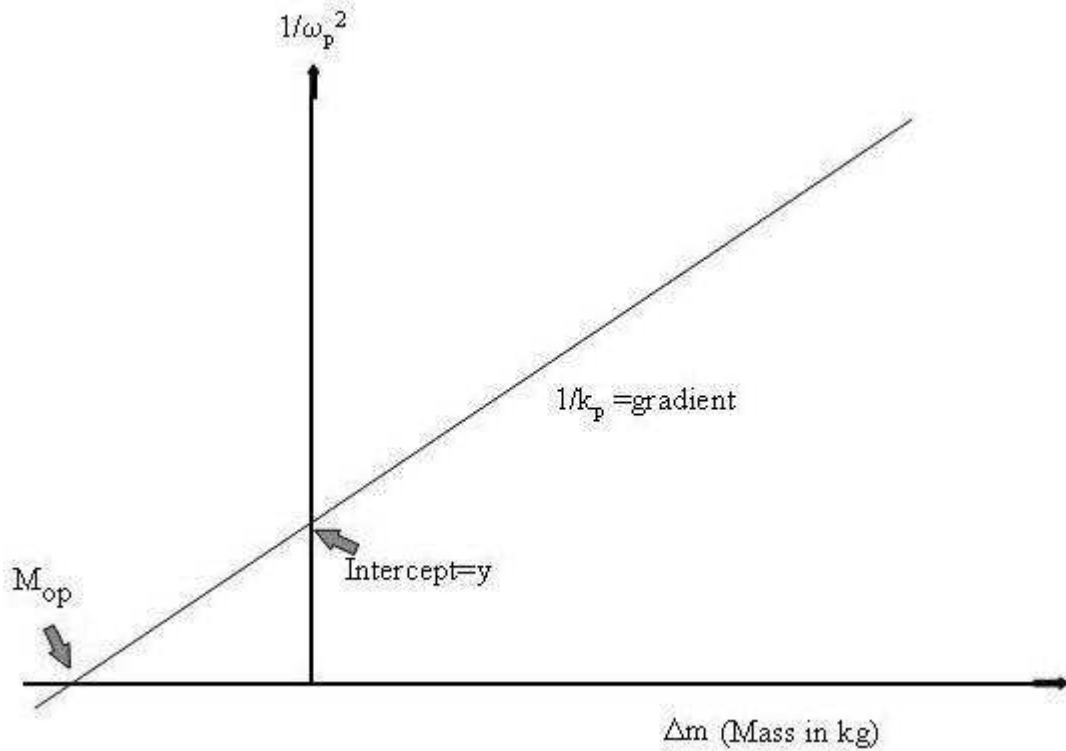


Figure 3. Schematic representation of the determination of the excited mass using the P-wave.

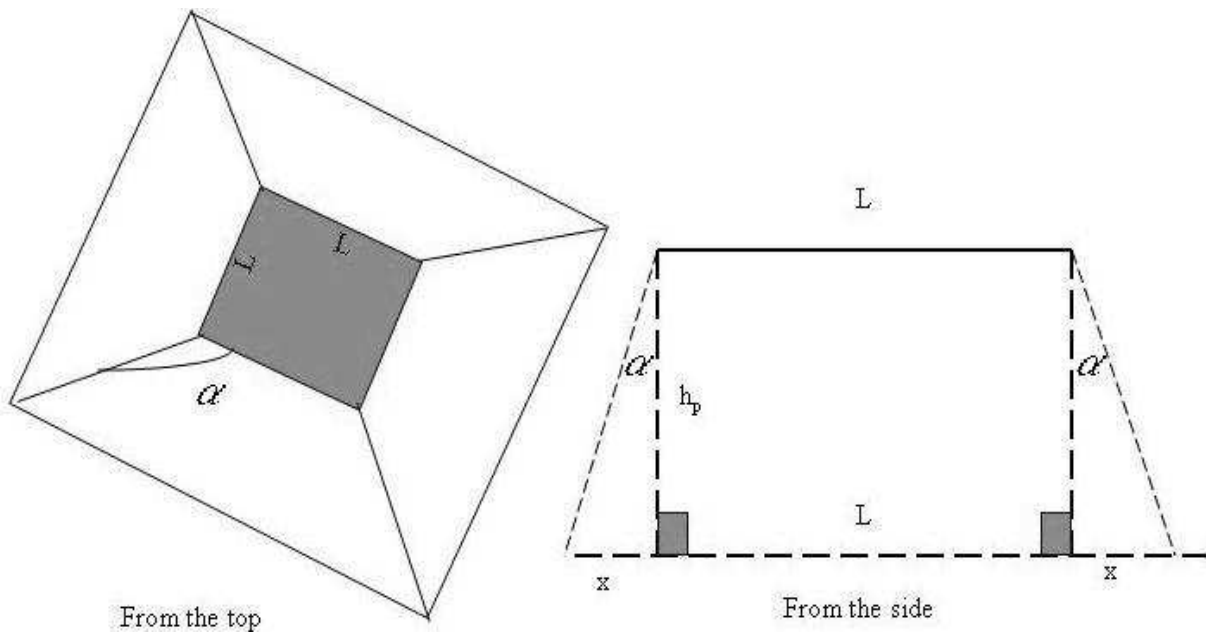


Figure 4. Determination of volume underneath the bearing plate.

The volume of the vibrating column $V_{op} = A_p \cdot h_p$. The height, h_p , of the vibrating volume as well as the angle α , are unknown. The following deduction is based on the assumption that α is very small. The objective is to express the height of the volume in terms of measurable parameters, such as the wavelength or the

velocity of seismic waves.

After the excitation of the groundmass, the movement is damped or attenuated. The following equation expresses the system with damping as follows (Kibble, 1985):

$$F_p + b_p V_p = -k_p z \quad 5$$

where b is the damping factor and V is the velocity of the medium.

The amount of damping depends on the velocity of the movement (Kibble, 1985). If z is the movement of a differential volume under the plate, then:

$$M_{TZ} \frac{d^2 z}{dt^2} + b_p \frac{dz}{dt} + kz = 0 \quad 6$$

where M_{TZ} is the total mass.

A solution to this differential equation is (Thorne and Wallace, 1995):

$$A(t) = A_{0z} e^{-b\omega_0 t} \sin \omega_0 t \sqrt{1 - b_p^2} \quad 7$$

where $A(t)$ is the amplitude with time.

If the assumption is made that the system is strongly damped, but less than critically damped, equation 7 reduces to (Thorne & Wallace 1995):

$$A(t) = A_{0z} e^{-b\omega_0 t} \quad 8$$

This is a harmonic oscillation that decays exponentially with time.

If we assume that all the energy in the vertical direction (P-wave or pressure wave) is transferred from the seismic source to the ground, the kinetic energy of the source will be equal to the energy of the excited mass column. The kinetic energy (E_{kp}) in the vertical direction of the vibrating column is calculated, by using the following relationship (Fourie and Cole, 2004):

$$E_{kp} = \frac{1}{2} M_{0p} V_p^2 \quad 9$$

The kinetic energy (E_{kp}) of a differential volume at a depth h_p , together with the facts that the mass (M_{0p}) = $\rho_p * V_p$ and the volume (V_{0p}) = $A_p * h_p$ are substituted into equation 9 results in:

$$dE_{kp} = \frac{1}{2} \rho_p A_p V_p^2 dh_p \quad 10$$

The following equation is derived by substituting equations 4 and 8 into equation 10:

$$dE_{kp} = \frac{1}{2} \rho_p (A_0 \omega_{0z})^2 (L + 2h_p \tan \alpha)^2 e^{-\frac{2kh}{\lambda_p}} dh_p \quad 11$$

By solving equation 11, a mathematical relationship for the volume is derived. This volume is used with the mass to obtain the density (Fourie and Cole 2004):

$$V_{0p} = \frac{L^2 \lambda_p}{2k_p} + 2L \left(\frac{\lambda_p}{k_p} \right)^2 \tan \alpha + \frac{5}{2} \left(\frac{\lambda_p}{k_p} \right)^3 \tan^2 \alpha \quad 12$$

The density is thus calculated by using the following relationship (Fourie and Cole, 2004):

$$\rho_{0p} = \frac{M_{0p}}{\frac{L^2 \lambda_p}{2k_p} + 2L \left(\frac{\lambda_p}{k_p} \right)^2 \tan \alpha + \frac{5}{2} \left(\frac{\lambda_p}{k_p} \right)^3 \tan^2 \alpha} \quad 13$$

Determination of the mass M_0 using the S-wave

In order to derive a mathematical model for the S-wave, the assumption is made of a mass attached to a spring at each side, to obtain a simple model. The mass attached to the springs oscillates in the S-wave (lateral) direction with host rock on both sides. Figure 5 presents this scenario schematically.

Assuming that the values of the spring constants are the same, it is then possible to write from the classical mechanics (Classical Mechanics Lecture Notes, University of Stellenbosch, 1980):

$$F_s + k_s x = -k_s x \quad 14$$

where k_s are the spring constants and x is the horizontal amplitude. The “s” subscript indicates the S-wave. All symbols are explained in the list of symbols (Table 1). The differential wave equation that describes the movement of the mass is (Classical Mechanics Lecture Notes, University of Stellenbosch, 1980):

$$M_{0s} \ddot{x} + 2k_s x = 0 \quad 15$$

By solving equation 15, and allowing for the addition of mass, the following equation is derived (Fourie and Cole, 2004):

$$\frac{1}{\omega_s^2} = \frac{1}{2k_s} (M_{0s} + \Delta m) \quad 16$$

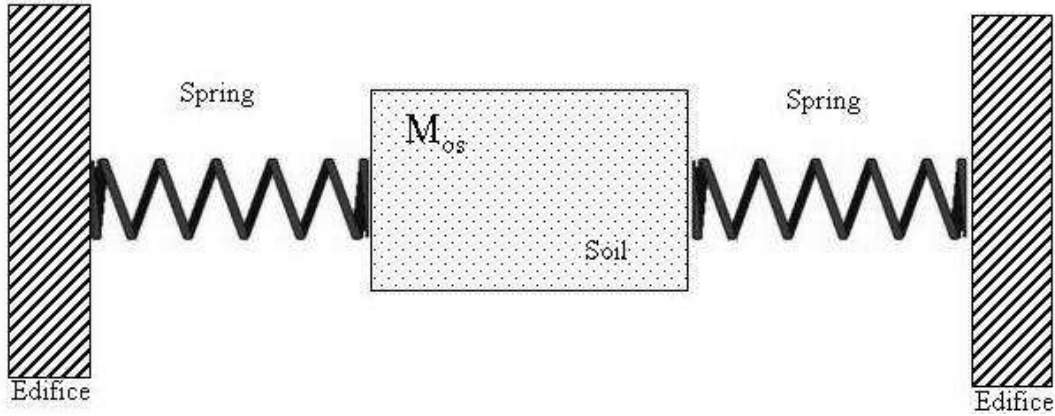


Figure 5. Simplified schematic S-wave physical model.

Equation 16 can then be used to calculate the mass that is excited by the S-wave in a similar fashion as is shown in figure 3.

Determination of the volume V_0 using the S-wave

Similarly, if the same square base plate with dimensions L is used, and the angle of influence from the plate is α , the resulting area underneath the plate (figure 4) will be expressed by equation 4.

During the excitation of the groundmass, the movement is damped. The following differential equation expresses the system with damping (Classical Mechanics Lecture Notes, University of Stellenbosch, 1980):

$$F_s + b_s V_s + k_s x = -k_s x \quad 17$$

where b_s is the damping factor and V_s is the S-wave velocity of the medium.

The differential wave equation describing the situation is then:

$$M_{TX} \frac{d^2 x}{dt^2} + b_s \frac{dx}{dt} + 2k_s = 0 \quad 18$$

where M_{TX} is the total mass.

By going through the same process as with the P-wave, an expression for the volume of mass that is excited by the energy source can be calculated (Fourie and Cole, 2004):

$$V_{0s} = \frac{L^2 \lambda_s}{2k_s} + 2L \left(\frac{\lambda_s}{k_s} \right)^2 \tan \alpha + \frac{5}{2} \left(\frac{\lambda_s}{k_s} \right)^3 \tan^2 \alpha \quad 19$$

The density is thus calculated by using the following relationship (Fourie and Cole, 2004):

$$\rho_{0s} = \frac{M_{0s}}{\frac{L^2 \lambda_s}{2k_s} + 2L \left(\frac{\lambda_s}{k_s} \right)^2 \tan \alpha + \frac{5}{2} \left(\frac{\lambda_s}{k_s} \right)^3 \tan^2 \alpha} \quad 20$$

FIRST FIELD TEST ON IGNEOUS ROCKS

Field procedure

The first density soundings were performed on an igneous complex, situated just north of Pretoria referred to in the literature as the Leeuwfontein Syenites (Wilson *et al.*, 1998) (figure 6). This site was chosen for the following reasons:

- It is a single geological layer environment.
- It was easy to drill samples from the rocks, for laboratory measurements (figure 7).

Two density soundings were performed, using a large hammer as a seismic source and a large base plate (figure 8a). P-waves (figure 8a) and S-waves (figure 8b) were generated, using the hammer. A modified base plate with steel pens is struck at the side parallel to the surface to generate the S-waves. The seismic traces (figure 9) were recorded in three directions to obtain information in three dimensions. A laptop computer was used for the process control and the data processing. The final results are displayed in a table format.



Figure 6. The Leeuwfontein Syenites just north of Pretoria. It is more than 10m thick.
For the purpose of this experiment it represents a single layer.



Figure 7. Diamond core drill used for taking laboratory samples.

RESULTS

Seismic traces and calculations were used to determine the amount of mass that had been

excited by the source in three dimensions. Figure 10 shows an example of how the Z-component (P-wave) were utilised to calculate the mass..



Figure 8a. Base plate, weights and seismic hammer source to generate the P-wave.



Figure 8b: The S-wave base plate. The holes are for the steel pens. It is struck on the side.

Figure 10 shows the amount of mass that was excited to amount to 7 042 kg. A seismic P-wave velocity of 4 650 m/s was measured on the core samples in the laboratory. The attenuation factor was also calculated on the seismic traces obtained during the fieldwork. These parameters were substituted into the equation to

calculate the volume, which in this case was 2,718 m³. The density calculated for this sounding was 2 591 kg/m³. Since the area of the base plate was 1,513 m², depth of investigation was 1,796 m. Table 2 shows a summary of the results for the two soundings performed on the Leeuwfontein Syenite.

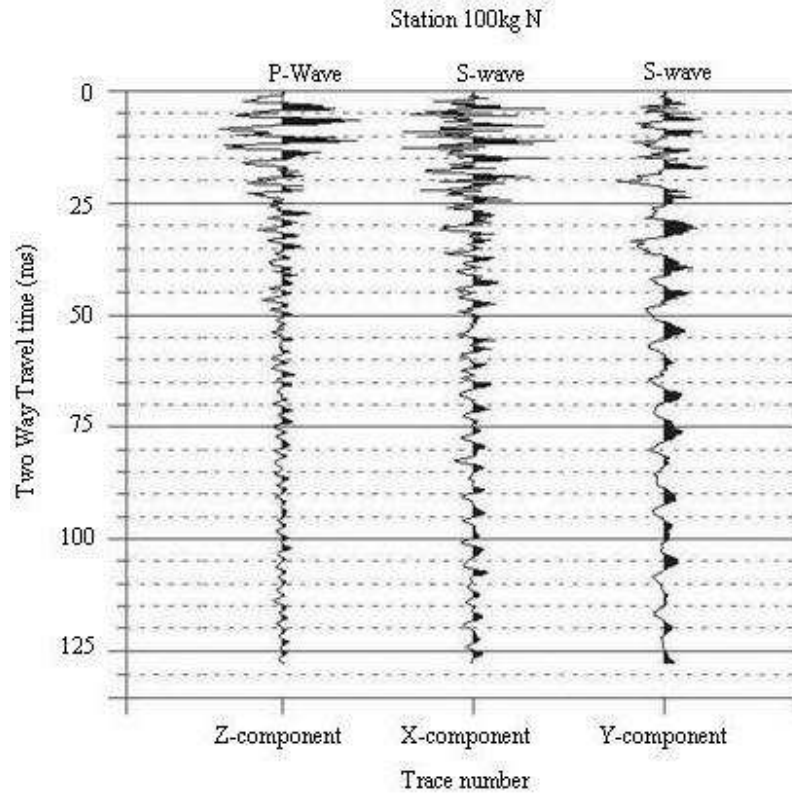


Figure 9. Seismic traces used to calculate the density.

Sounding 1 Leeuwfontein
P-wave or Z-component

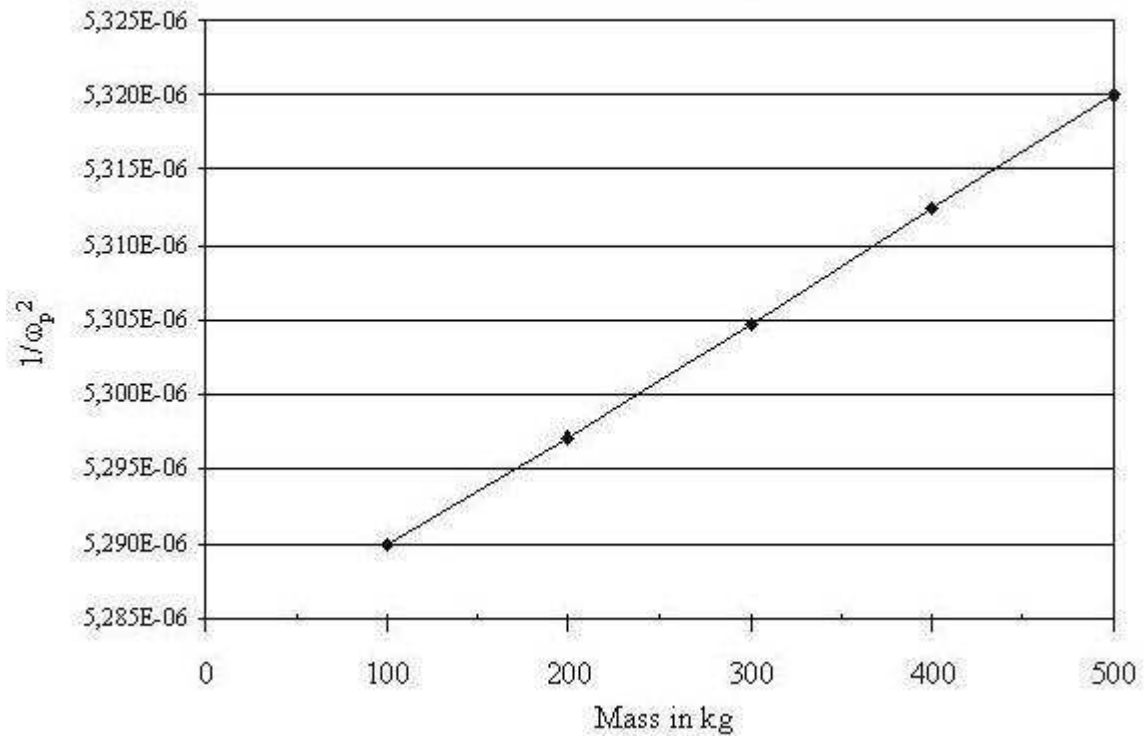


Figure 10: Plot to obtain amount of excited mass.

Table 2: Comparison between field and laboratory results

SOUNDING 1					
Mass (kg)	Volume (m ³)	Density (kg/m ³)	Depth (m)	Lab density (kg/m ³)	Difference (kg/m ³)
7 042	2,718	2591	1,80	2580	+11
SOUNDING 2					
Mass (kg)	Volume (m ³)	Density (kg/m ³)	Depth (m)	Lab density (kg/m ³)	Difference (kg/m ³)
7 546	2,908	2594	1,922	2599	-5

DISCUSSION OF RESULTS AND THE WAY FORWARD

The development of this method was born from the need to find a way of measuring the density of the ground using a non-invasive approach. It is proposed that the new approach discussed in this paper can meet this requirement. The method uses data in three dimensions; which include the vertical pressure waves (P-waves) and horizontal shear waves (S-waves).

Comparison with the laboratory data was favourable. From Table 2 it is clear that this method was successful in the field and poses some merit, at least in a single layer situation. However, it is true that a single layer situation is encountered in very few cases. Examples of single layer cases are man-made structures, such as road embankments and gravity dam walls. It is important that the method be tested in multi-layer situations, which do not consist of igneous rock, as the method is particularly applicable to the weathered layer. In most cases, the weathered layer is a multi-layered medium.

The accuracy of the proposed method depends largely on the quality of instrumentation, processing accuracy (determining the damping factor (b)) of the seismic traces and of the subsurface. Given that the rocks and soil are strongly, but less than critically damped (Thorne & Wallace 1995) it is evident that the calculated volume depends largely on the damping factor. Various approaches to determining this factor have to be investigated on good-quality data. The coupling of the base plate with the subsurface is not perfect. This could lead to a lower determination of the excited mass and volume, and subsequently the density.

As with most of the other geophysical methods (such as the D.C. electrical resistivity and electromagnetic methods (Griffiths *et al.*, 1969, Telford, 1986, Kearey *et al.*, 1991), it will be impossible to do absolutely accurate interpretations without any verification. The method will yield a good first-order approximation, and if test pits or boreholes are available to verify the interpreted results, the savings may be considerable.

From the experience gained, it is evident that this method is fast. It is possible to perform about 10 soundings in one day, depending on accessibility and the terrain. A major negative factor at this stage is that the equipment is very heavy, which makes it difficult to manipulate. A redesign of the equipment will be necessary to increase the ease of handling and mobility of the equipment. One solution may be to permanently mount the equipment on a specialised vehicle.

Currently, data processing, such as the digital signal processing and filtering, are done by means of modules of various software packages. The development of dedicated software has started. This software envisages unifying all the necessary processes and routines to process the data and the display options into one package.

Finally, the main advantages of this proposed method should be emphasised:

- The method is non-invasive/non-destructive.
- The method will be cost effective, by limiting the number of test pits, and large diameter holes. It will save on laboratory costs.
- The method is fast, and the production rate is relatively high.
-

Acknowledgements - The author wishes to thank Mrs Leonie Maré of the Physical Property Laboratory at the Council for Geoscience for performing the laboratory tests on the control samples. Gratitude is also expressed towards Dr A. Kijko, Messrs C. R. Randall, I. Saunders, J.G. Barkhuizen of the Council for Geoscience for fruitful and sometimes heated discussions. The author also wishes to thank Ms Z. Nel, language consultant of the Council for Geoscience, for proofreading the document and for the French translation.

REFERENCES

- Baguelin, F., Jézéquel, J. F. and Shields, D. H. 1978. *The Pressure meter and Foundation Engineering* (First Edition). Series on Rock and Soil Mechanics (Vol. 2, No. 4). Trans Tech Publications.
- Byrne, G., Everett, J. P., Schwartz, K., Friedlaender, E. A., Mackintosh, N. and Wetter, C. 1995. *A Guide to Practical Geotechnical Engineering in Southern Africa*. Third Edition, Franki, 1995.
- Classical Mechanics lecture notes, 1980, University of Stellenbosch, South Africa.
- Fourie, C. J. S. and Cole, P. 2004. Development of an *in-situ* Density Geophysical method using a Seismic Technique. Report 2004-0095, Council for Geoscience, Pretoria, South Africa.
- Fourie, C. J. S. and Cole, P. 2004. Three – dimensional *in-situ* subsurface Density estimations using a Seismic Technique. Geoscience Africa, 2004, Abstracts. (Johannesburg, South Africa).
- Griffiths, D.H. and King, R.F. 1969. *Applied Geophysics for Engineers and Geologists*. Second Edition, Pergamon Press.
- Kearey, Phillip and Brooks, Michael, 1991. *An introduction to Geophysical Exploration*. Second Edition, Blackwell Scientific Publications.
- Kibble, T. W. B. 1985. *Classical Mechanics*. Third Edition, Longman Scientific & Technical Press, London.
- Sears, Zemansky and Young, 1987. *University Physics* (Seventh Edition). Massachusetts, Addison-Wesley Publishing Company.
- Telford, W. M. 1986. *Applied Geophysics*. Cambridge University Press.
- Thorne, L. and Wallace, T. C. 1995. *Modern Global Seismology*. San Diego, Academic Press.
- Wilson, M. G. C. and Anhaeusser, C. R. 1998. *The Mineral Resources of South Africa*. Council for Geoscience, South Africa, Sixth Edition.
- Yilmaz, O. 1989. *Seismic Data Processing*, Society of Exploration Geophysicists, U.S.A.



UNIVERSITEIT VAN PRETORIA
UNIVERSITY OF PRETORIA
YUNIBESITHI YA PRETORIA

Appendix I

Accepted and Revised to be Published Paper

Three-dimensional *in-situ* small movement elasticity modulus estimations of the subsurface using a seismic technique

C. J. S. FOURIE^{1*}, P. COLE² and J. L. VAN ROOY³

¹Applied Geoscience, NRE Division, CSIR, South Africa
P.O. Box 395, Pretoria 0001, South Africa

²Geophysics Division, Council for Geoscience, South Africa
Private Bag X112, Pretoria 0001, South Africa

³Department of Geology, University of Pretoria, Pretoria 0002, South Africa

*Previously with Council for Geoscience

(First received 28 July, 2006; modified version accepted 25 October, 2006)

Abstract – All civil engineering projects require information from the subsurface for design purposes. Usually this information is considered in the development of foundations of the structure. The size of the structure requires different information, mainly because foundations are smaller, shallower and located in the weathered layer for smaller structures, and deeper and larger into the base rock for larger structures. Usually collapsibility and the heaving potential play a large role in design parameters, but the small movement elasticity modulus (SMEM) is the most important constraint. Different techniques exist to measure this parameter. The most obvious one is to measure the modulus in a laboratory on an undisturbed sample. Another option recently proposed by the authors is to measure the P-wave and S-wave velocity and derive the modulus from these velocities. A new approach is to use the density sounding technique to measure the small movement elasticity modulus in three directions. In this paper we present some new experimental evidence obtained by this method.

Keywords: *In-situ*, density, P-wave, S-wave, small movement elasticity modulus

La technique de sondage de densité pour mesurer le module d'élasticité de petits mouvements dans trois directions

Résumé - Tout projet de génie civil requiert de l'information sur la subsurface aux fins du dessin. D'habitude, cette information est considérée en vue du développement des fondations de la structure. Les dimensions de la structure nécessitent d'autres informations, surtout du fait que les fondations sont plus petites, moins profondes et situées dans la couche altérée pour des structures de dimensions moins importantes, alors qu'elles sont enfoncées plus profondément et plus largement dans la roche de base pour les structures de taille plus importante. Normalement, bien que la tendance à l'effondrement et le potentiel de la boursouffure jouent un rôle important concernant les paramètres de conception, c'est le module d'élasticité de petits mouvements (SMEM) qui y est la contrainte la plus importante. Il y a différentes techniques qui servent à mesurer ce paramètre dont le plus évident est la mesure du module dans un laboratoire en utilisant un échantillon non remanié. Une autre possibilité récemment postulée par les auteurs serait de mesurer la vitesse des ondes P et S et d'en déduire le module. Une nouvelle démarche consiste à utiliser la technique de sondage de densité pour mesurer le module d'élasticité de petits mouvements dans trois directions. Dans cet article nous visons à présenter une nouvelle évidence expérimentale obtenue par cette méthode.

Mots clés – *In-situ*; densité; la vitesse des ondes P et S le module d'élasticité de petits mouvements



INTRODUCTION

Modern developments in geophysics, geology and engineering have resulted in increasingly sophisticated techniques of analysis of problems in soil mechanics. The reasons for this are threefold:

- better and more sophisticated technology that is now more readily available.
- The need to determine parameters more accurately, to prevent large over designing.
- The need to decrease the cost of development projects.

These improved methods have also highlighted the problems inherent in conventional sampling and laboratory testing procedures. Frequently, these testing procedures cannot supply suitably accurate parameters either for sophisticated techniques of analysis (such as finite element analysis) or even for modern design calculations.

Various authors (e.g., Brown and Robertshaw, 1953; Davis and Poulos, 1966) have shown that the action of ‘sampling’ causes significant disturbance due both to mechanical deformation and to the inevitable difference in stress history between a sampled element of subsurface and a similar element in the field. This confirms the need to sample physical properties *in-situ* (for example density and small movement elasticity modulus), in particular for the construction and engineering industry.

Although tests like the Dynamic Cone Penetrometer Test and the consolidation test can give an indication of the density variations of the subsurface, accurate *in-situ* density determinations can actually only be determined up to a shallow depth by using the neutron based Troxler equipment. Variations in the moisture content can however influence the determinations. If accurate subsurface parameters were needed from greater depths, an undisturbed sample would be needed.

Physical properties derived from field geophysical techniques tend to be much greater than those obtained from conventional laboratory testing, for example stiffness derived from field seismics (Clayton and Heyman, 2001). A laser interferometry system was developed to evaluate the sensitivity and accuracy of displacement transducers (Heyman, Clayton and Reed, 1997) in order to investigate the extent of the linear-elastic range of geomaterials in triaxial stress space.

This argument has led in the past to the belief that geophysical measurements are useful in design problems associated with large events like earthquakes where large movements occur, but could not be used in engineering calculations of small ground movements around foundations and structures. This now raises the question: Is it worthwhile to develop and investigate any geophysical techniques for engineering applications?

It was argued (Auld, 1977) that seismic methods are dynamic, giving negligible time for plastic or creep strains to occur and that the induced strains are very small. It was only recently that it was appreciated that stresses and strains around tunnels are actually very small and that it follows that geophysical techniques might be capable of yielding the parameters (Jardin *et al.*, 1986).

Clayton and Heyman (2001) showed that the results of the very-small-strain stiffness measured in the laboratory by using a Fabry-Perot laser interferometer under high pressure were comparable with geophysical data from the same sites where the samples were taken. The movements during the seismic experiments were measured using displacement transducers. This proves that the use of geophysical techniques is suitable in deriving *in-situ* engineering parameters and that the development of such geophysical techniques is necessary and advisable. In order to emphasize the importance of accurate *in-situ* measurements on all the physical properties that are of importance to engineers, important issues from literature should be discussed.

The Seismic Refraction method can be used to determine the densities of the subsurface (Griffiths and King, 1969; Darracott, 1976) and the small movement elasticity modulus. The densities and the small movement elasticity moduli are obtained indirectly by measuring the velocities of the P-waves and S-waves.

During a P-wave or longitudinal wave the particle movement is in the same direction as the wave propagation, in other words a pressure wave. During the S-wave or transverse wave the particle movement is perpendicular to the wave propagation. The equations describing these velocities are:

$$V_p = \sqrt{\frac{k + \frac{4}{3}G}{\rho}} \quad 1$$

and

$$V_s = \sqrt{\frac{G}{\rho}} \quad 2$$

where k is the bulk or incompressibility modulus. G is the shear or rigidity modulus, and ρ is the density.

From the above equations it is obvious that larger modulus values are associated with higher velocities. By using this method, the density and modulus are measured *in-situ*. These values are however only an indication of the real value due to the large sampling volume, which is directly proportional to the size of the seismic spread (6,12,24 channel). The sampling volume can be reduced if smaller geophone spacing is used.

Engineers routinely use the ratio of V_p/V_s to give them an indication of the density and “hardness” of

the subsurface, and generally the following hold true (Darracott, 1976):

- High V_p and a V_p/V_s ratio of approximately $\sqrt{3}$ indicates unweathered bedrock.
- Low V_p and a V_p/V_s ratio of approximately $\sqrt{3}$ indicates sandy or gravel fill.
- Low V_p and a high V_p/V_s ratio indicate clayey material, usually above the water table.
- V_p velocity about 1500 m/s, high V_p/V_s ratio may indicate soft clay material, below the water table.

It is impossible to distinguish between minor layers inside the weathering layer if the velocity contrasts are small. For most rocks there is an empirical relationship between the V_p and the rock quality, namely the higher the velocity the better the rock quality (Brown and Shaw, 1953). They showed the empirical relationship between Young's modulus (E) and V_p :

$$E = 111.15V_p^{2.34} \quad 3$$

where the unit for E is in Pa.

Poisson ratios can be obtained from seismic velocities. It is the ratio between compression strain and extension strain in the direction of stretching force. Extensive (stretching) deformation is considered positive and compressive deformation is considered negative. The definition of Poisson's ratio contains a minus sign so that normal materials have a positive ratio.

$$\nu = \frac{-\mathcal{E}_{compressive}}{\mathcal{E}_{extensive}} \quad 4$$

where

$$\frac{V_p}{V_s} = \sqrt{\frac{1-\nu}{\frac{1}{2}-\nu}} \quad 5$$

If the subsurface is compacted, it is found that the elastic modulus K and G increase more rapidly than does the density, which makes the determination of the density difficult (Griffiths and King, 1969).

Since it is difficult to assign a specific velocity and a density to a rock type, it is however possible to quote a range of velocities which would cover a certain lithology. Table 1 shows the general trend of increasing velocity with increasing density (i. e., decreasing porosity). The large areas of overlap indicate the insensitivity of the seismic velocity to small variations in density.

Materials of exceptionally low velocity are usually encountered near the surface (weathered layer) and are of considerable importance to the civil engineer. Properties such as its elasticity (especially the small movement elasticity modulus), plasticity, strength and density are the most important. Young's

modulus can only be determined if the velocity, density and Poisson's ratio are known.

The seismic cone test (Heyman, 2003) is used to measure the *in situ* S and P waves of the soil. The largest advantage of this test is that it allows for the measurement of the void ratio on undisturbed material at the *in situ* stress condition. Heyman (2003) used the seismic cone test on a gold tailings dam and compared it with an undisturbed sample from the daywall of the same dam. According to Heyman (2003) the small strain stiffness and Poisson's ratio can also be calculated from the velocity measurements where small movements occur, such as foundations.

Shear waves provide a direct way of determining the dynamic shear modulus of the ground that is independent of Poisson's ratio (Abbiss, 1981). Two shear wave methods have been applied to determine *in situ* properties as a function of depth on three clay sites. The first method was shear wave refraction and the second measured the velocity of Rayleigh waves



Table1. P-wave velocities for certain rock types (after Griffith and King, 1969).

Tableau 1 . in French

Lithology	P-wave velocity (km/s)	Density (g/cm ³)
Clastic rocks, unconsolidated	0.3-1.8	1.5-2.2
Clastic rocks, consolidated and cemented	1.5-3.7	2.0-2.6
Clastic rocks in orogenic belts	3.1-6.2	2.5-2.8
Metamorphic rocks	4.6-6.2	2.7-3.0
Limestone	3.1-6.2	2.4-2.7
Igneous rocks	4.6-4.2	2.4-3.0

generated by vibrators. In addition pressure wave velocities were measured enabling the dynamic Poisson's ratio to be calculated.

Shear waves methods have the advantage that the shear modulus is directly related to the shear wave velocity (Equation 2, Abbiss, 1981). This is not necessarily the case for the p-wave velocity where the modulus may depend to a large extent on Poisson's ratio.

The modulus of chalk at Munford was compared from a seismic survey and a large scale tank test (Abbiss, 1979). A steel tank of 18.3m in diameter and approximately 20m high was filled with water to produce a pressure of 179kNm⁻². Displacements under the tank were measured in vertical shafts, by means of very accurate displacement transducers. In this way strains were measured at various levels down to 16.3m below the tank, nearly to the water table. It was found that the dynamic Young's moduli calculated from a seismic refraction survey of the chalk are proportional to the moduli determined from the full scale tank loading test. The moduli showed an approximately linear increase with depth similar to a modified Gibson soil of the first kind.

The main problem of a shear wave refraction survey is to identify the s-wave arrivals between the p-waves. The best way to remedy the situation is to use a source that is rich in s-waves in the direction of the survey (Abbiss, 1981). The signal to noise ratio can also be improved by stacking the signal on a seismograph. By reversing the connections of the s-wave geophone will help stacking of the s-wave but zero the p-wave (Abbiss, 1981).

The seismic sounding technique (Fourie, 2005, Fourie and Cole, 2004b) uses seismic waves in three directions to obtain the moduli in three directions. A large base plate is used and the mass on top of the base plate is increased incrementally. From this graph the moduli are calculated, without the necessity to obtain seismic velocities.

UNDERSTANDING THE PROBLEM

All geophysical methods that are currently used to measure the moduli of the subsurface do so in an indirect manner. From the seismic refraction method the P-wave velocity can be measured, and this velocity allows the scientist or engineer to derive a modulus if the density is known (Griffiths and King, 1969; Telford, 1986; Yilmaz, 1989). If an S-wave velocity is known, the process is even easier.

This new proposed method also measures the modulus of the subsurface indirectly. It is also a seismic method (Fourie, 2005; Fourie and Cole, 2004a). It attempts to measure the amount of mass that is excited by the seismic source. By adding weights to a base plate, the vibration frequency of the system is changed, thereby making it possible to calculate the elasticity modulus of the subsurface. A much smaller sampling volume is used, which in turn improves the accuracy of the measurement.

In order to estimate the small movement elasticity modulus of the subsurface, the same process as determining the density of the subsurface is followed. During the process of obtaining the mass (M_0) of the density sounding technique (Fourie, 2005) the small movement elasticity modulus is acquired.

DESCRIPTION OF THE CONCEPT

The P- and S- seismic waves are recorded by using a three-component geophone system, mounted on a bearing plate on the surface (Figure 1). Weights are added in increments of 50 kg on top of the base plate to

change the total mass (base plate plus added weights plus subsurface) and hence the frequency of vibration (Fourie, 2005). For a complete description of the method see Fourie, 2005.

The equation that describes the calculation of the modulus versus the addition of extra mass (Δm) after Fourie (2005) is:

$$k_p = \omega_p^2 (M_{0p} + \Delta m) \quad 6$$

where ω is the angular frequency.

By using equation 6, the computation of the bulk modulus k_p (Fourie, 2005) is achieved (Figure 2). All symbols are explained in the list of symbols (Table 2).



Fig. 1. Large bearing plate with geophones mounted for measurements in three directions.

Fig. 1 . in French

Table 2: List of symbols.

Tableau 2. in French

SYMBOL	EXPLANATION	SYMBOL	EXPLANATION
F_p	P-wave force	M_{TZ}	Total mass from P-wave
k_p	P-wave spring constant	M_{TX}	Total mass from S-wave
z	P-wave amplitude	ω_{0z}	Initial Angular Frequency
M_{0p}	Groundmass	ω_s	Angular Frequency of the s-wave
\ddot{z}	P-wave acceleration	F_s	S-wave force
ω_p	Angular Frequency of the P-wave	K_s	S-wave spring constant
Δm	Additional mass	x	S-wave amplitude
\ddot{x}	S-wave acceleration	M_{0s}	Groundmass

In a similar fashion, the equation that describes the calculation of the shear modulus (k_s) versus the addition of extra mass (Δm) after Fourie (2005) is:

$$\frac{1}{\omega_s^2} = \frac{1}{2k_s} (M_{os} + \Delta m) \quad 7$$

Equation 7 can then be used to calculate the shear modulus (k_s) versus the addition of extra mass (Δm) in a similar fashion and is shown in Figure 2.

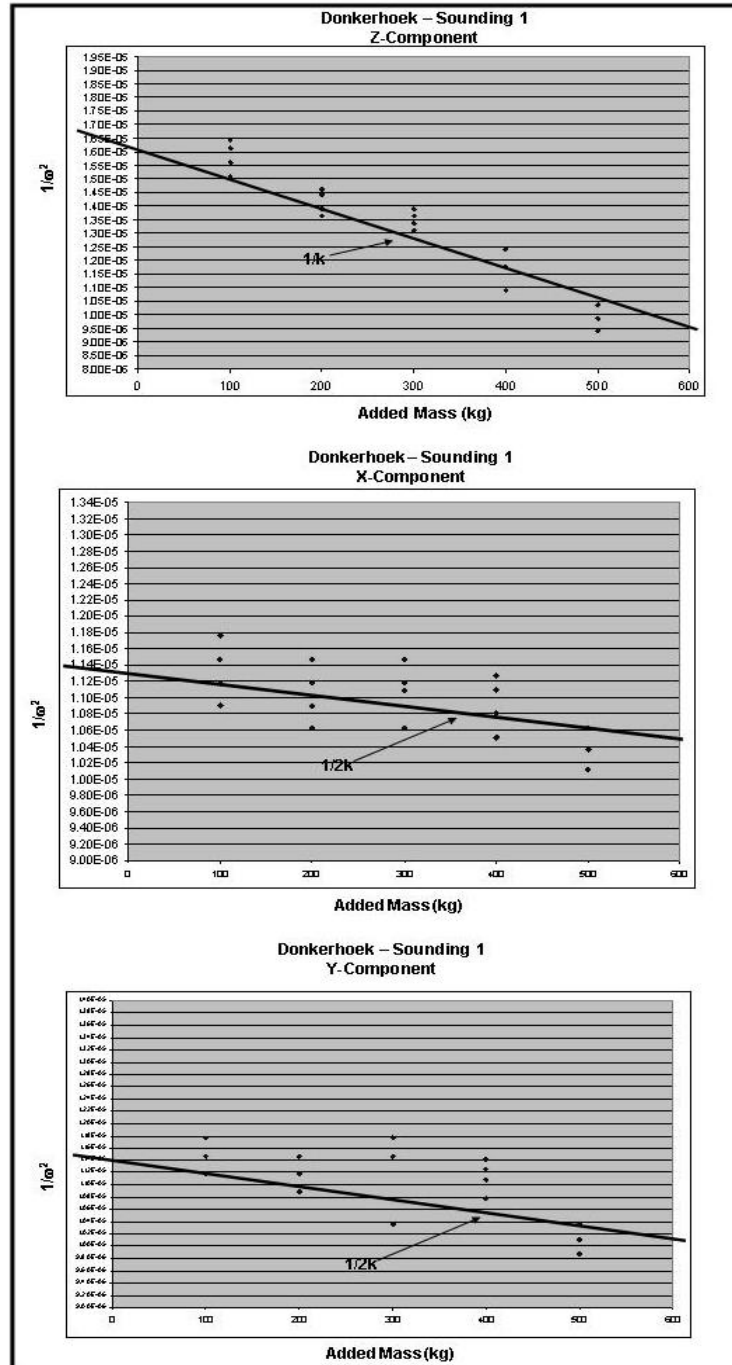


Fig. 2. Example of calculation of the excited mass and the modulus for each direction. Note that modulus is $1/k$ for the P-wave and $1/2k$ for the S-wave.

Fig. 2. in French

FIELD TEST ON WEATHERED MIDRAND GRANITES

Field procedure

The density soundings were performed on the weathered layer of an igneous complex, situated just south of Pretoria referred to in the literature as the Midrand Granites (Wilson *et al.*, 1998) (Fig. 3).

These granites are Archean basement and weathers to an *in-situ* clay (Fig. 4). The purpose of the survey was to compare this geophysical method with laboratory results for this area as part of an urban development.

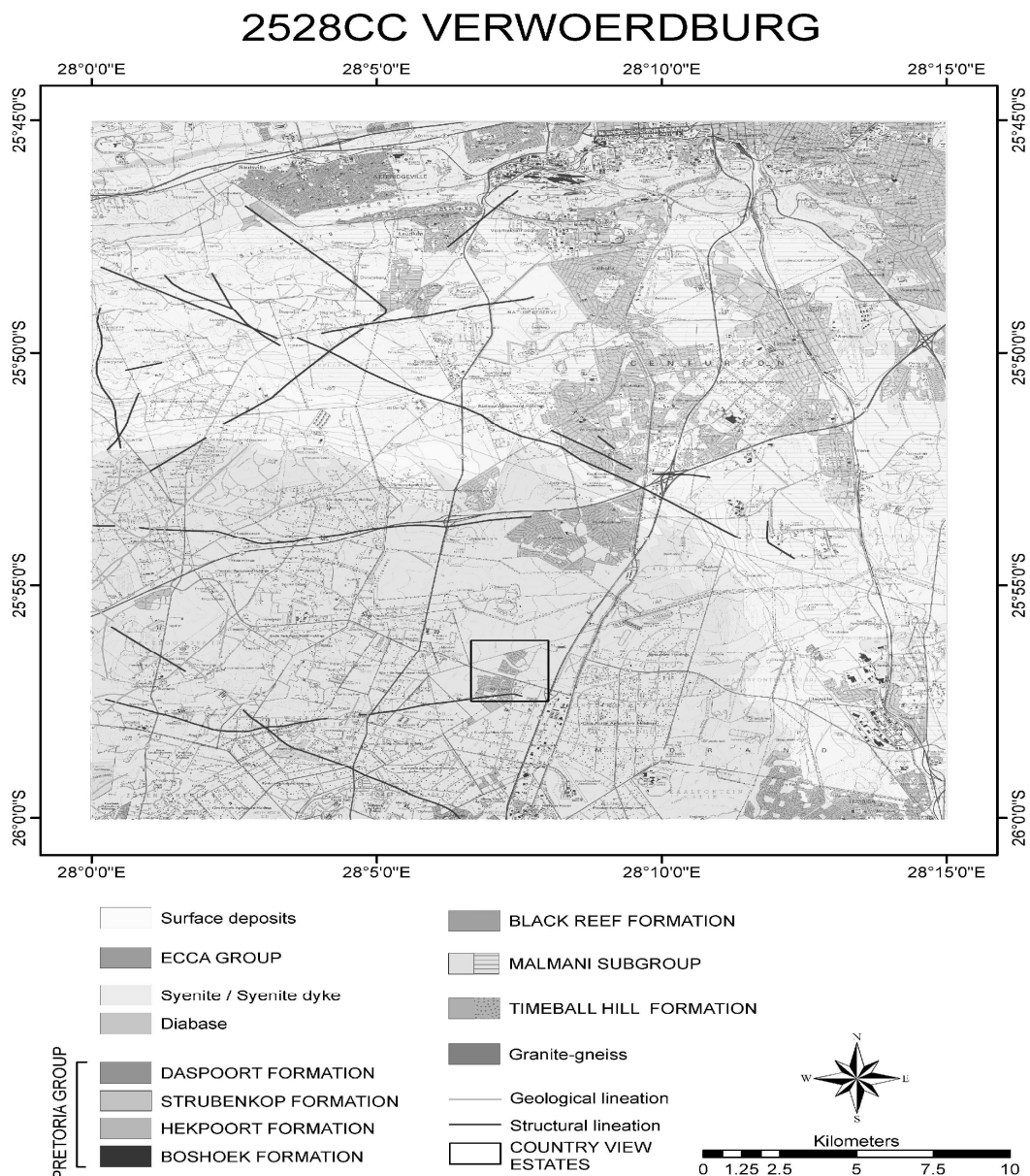


Fig. 3. 1:50 000 sheet indicating the survey area inside the rectangle.

Fig.3. in French



Fig. 4. Weathering profile of the Midrand Granites. From this figure the different layers can be seen.

Fig. 4. in French

Five density soundings were performed, using a large hammer as a seismic source and a large base plate (Fig. 1). P-waves and S-waves were generated, using the hammer. The seismic traces were recorded in three directions to obtain information in three dimensions. A seismograph was used to record the data. The data were processed using an in-house developed software package called Seisrho.

The seismic record data from the seismograph is read into Seisrho. A Fourier transform is then calculated on each trace to obtain a frequency spectrum. This frequency spectrum is then used to pick the frequencies that correspond to each applied mass and layer. The process is repeated till a straight line can be constructed to obtain the modulus values and the excited masses. All this processing is done in the window of Seisrho that is displayed in Figure 5.

RESULTS

Figure 5 shows the window in Seisrho where the excited masses are calculated for each layer. Each line represents a different layer. The modulus values are also estimated inside this window of Seisrho, by calculating the gradients

of each line. This is achieved by calculating the frequency response for each trace at different applied masses on the base plate. An example of the final results is displayed in Table 3. A comparison of the field data to the laboratory results of Soillab is also given in Table 3. The modulus values were obtained in the laboratory on undisturbed samples by using the double odometer test.

Seismic traces and the calculations in Seisrho were used to determine the amount of mass that had been excited by the source in three dimensions and also the modulus values. The results indicate that the second layer of the area is weaker in the E-W direction than the first and third layers. The results thus indicate the anisotropic nature of the site, meaning that the structural support of the foundations by the weathered layer will be larger in the N-S direction as in the E-W direction. Otherwise the foundations must be deeper than the second layer to avoid possible sagging problems. This information indicates towards the civil engineer that the design should incorporate this by rotating the structures in such a way that the largest strains are in the stronger E-W direction, or that special instructions are given for the construction.

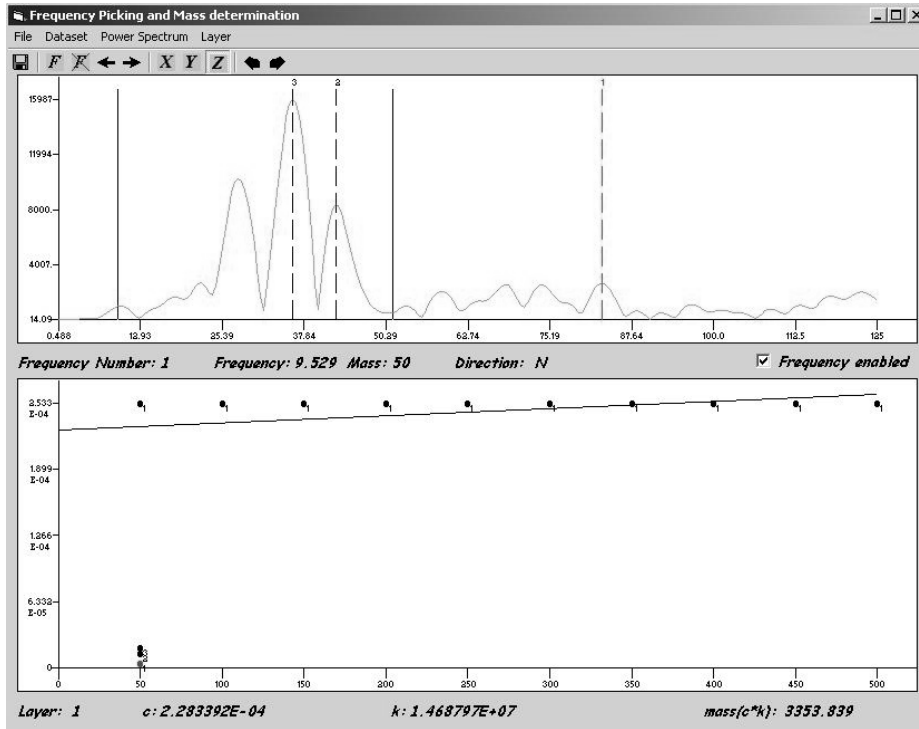


Fig. 5. Processing window in Seisrho where the modulus values are calculated.

Table 3. Comparison of field data with laboratory data.

P-Wave				
Layer	Total Mass	Mass	E-Modulus	E-Mod(lab)
1	1309	1309	367MPa	400MPa
2	4991	3683	373MPa	
3	6439	1448	374MPa	
S-Wave (N-S Direction)				
Layer	Total Mass	Mass	E-Modulus	E-Mod(lab)
1	1318	1318	338MPa	
2	4966	3648	778MPa	800MPa
3	6427	1461	789MPa	
S-Wave (E-W Direction)				
Layer	Total Mass	Mass	E-Modulus	E-Mod(lab)
1	1313	1313	338MPa	
2	4992	3679	105MPa	
3	6496	1504	432MPa	
		Ave1	328MPa	
		Ave2	434MPa	
		Ave3	532MPa	

CONCLUSIONS

The development of this method was born originally from the need to find a way of measuring the density of the ground using a non-invasive approach (Fourie, 2005). Other than the seismic refraction method, the determination of the modulus, without having a seismic velocity, is an extra benefit from the method. Four different surveys should be done if the seismic refraction method is to be used to obtain data in three directions. This method acquires data in three dimensions at the same time, saving a lot of time. Information about the anisotropy of the subsurface is also recorded at the same time.

Comparison with the laboratory results was favourable, as can be seen from Table 3. The accuracy of this method depends largely on the quality of instrumentation, processing accuracy of the seismic traces and of the subsurface. The coupling of the base plate with the subsurface is not perfect. This could lead to a lower determination of the excited mass and subsequently the modulus. It will be impossible to do absolute accurate interpretations without any verification. If test pits or boreholes are available to verify the interpreted results, the financial and time savings may be considerable.

Finally, the main advantage of this proposed method is that it is an alternative to the seismic refraction and the seismic cone test methods. Triggering problems can introduce errors in seismic velocities, which in turn can give faulty modulus values. The largest advantage of this test is that no knowledge of the seismic velocity is needed.

Acknowledgements -The authors wish to thank his colleagues for fruitful discussions about the concept. The authors also wish to thank Ms Z. Nel, language consultant of the Council for Geoscience, for proofreading the document and for the French translation. The authors also wish to thank Ms. L.P. Marè for the preparation of the geology map.

REFERENCES

- Abbiss, C. P. 1979. A comparison of the stiffness of the chalk at Mundford from a seismic survey and a large scale tank test. *Geotechnique* **29**, no. 4, 461-468.
- Abbiss, C. P. 1981: Shear wave measurements of the elasticity of the ground. *Geotechnique* **31**, no.1, 91-104.
- Auld, B. 1977: Cross - hole and down - hole V_s by mechanical impulse. *Journal Geotechnical Engineering* **103**, no. GT12, 1381-1398.
- Brown, P. D. and Robertshaw, J. 1953. The *in-situ* measurement of Young's modulus for rock by a dynamic method. *Geotechnique* **3**, no. 7, 283.
- Davis, E. H. and Poulos H. G. 1966: Laboratory investigations of the effects of sampling; *Proceedings. Symposium on Site Investigation*, Sydney, Australia.
- Clayton, C. R. I. and Heyman, G. 2001. Stiffness of geomaterials at very small strains. *Geotechnique* **51**, no. 3, 245-255.
- Darracott, B. W. 1976. Seismic surveys and civil engineering. *The Civil Engineer in South Africa*, February, 1976.
- Fourie, C. J. S. 2005. Three-dimensional *in-situ* subsurface density estimations using a seismic technique. *Africa Geoscience Review* **12**, nos 1 & 2, 1-12.
- Fourie, C. J. S. and Cole, P. 2004a. Development of an *In-situ* Density Geophysical method using a Seismic Technique. Report 2004-0095, Council for Geoscience, Pretoria, South Africa.
- Fourie, C. J. S. and Cole, P. 2004b. Three-dimensional *In-situ* subsurface Density estimations using a Seismic Technique. Geoscience Africa, 2004, *Abstracts*. (Johannesburg, South Africa).
- Griffiths, D. H. and King, R. F. 1969. *Applied Geophysics for Engineers and Geologists*. Second Edition, Pergamon Press.
- Heyman, G. 2003. The Seismic Cone Test; *Journal South African Institution Civil Engineering* **45**, no.2, p.26-31, Paper 552.
- Heyman, G., Clayton, C. R. I. and Reed, T. 1997. Laser Interferometry to evaluate the performance of local displacement transducers. *Geotechnique* **47**, no. 3, 399-405.
- Jardin, R. J., Potts, D. M., Fourie, A. B. and Burland, J. B. 1986. Studies of the influence of non-linear characteristics in soil-structure interaction. *Geotechnique* **36**, no. 3, 377-396.
- Telford, W. M. 1986. *Applied Geophysics*. Cambridge University Press, U. K..
- Wilson, M. G. C. and Anhaeusser, C. R. 1998. *The Mineral Resources of South Africa*. Council for Geoscience, South Africa, Sixth Edition.
- Yilmaz, O. 1989. *Seismic Data Processing*, Society of Exploration Geophysicists, U.S.A.



Appendix II

Donkerhoek

DONKERHOEK TEST PIT PROFILE



**UNIVERSITEIT VAN PRETORIA
UNIVERSITY OF PRETORIA
YUNIBESITHI YA PRETORIA**

TP1		
0 - 0,2	Slightly moist, brown, loose, open, sandy SILT. Colluvium. Roots.	
0,2 - 0,82	Dry, grey brown, stiff, intact, sandy silty CLAY. Colluvium.	
0,82 - 1,60	Dry, yellow olive brown with grey blotches, stiff to very stiff, slickensided, silty CLAY. Colluvium.	
1,60 - 1,80	Yellow brown with grey and white blotches, completely weathered soft rock SHALE. Residual shale.	
	Notes:	
	Refusal on completely weathered shale.	
	No water.	
	Undisturbed sample at: 1,1 m.	
	Disturbed sample at: 1,1 m.	

TP2		
0 - 0,25	Dry, light brown, medium dense, intact, sandy SILT. Colluvium. Roots.	
0,25 - 0,8	Dry, yellow brown with grey and orange blotches, stiff, shattered, sandy silty CLAY. Colluvium. Elluviated at top of layer.	
0,8 - 1,5	Slightly moist, yellow with grey and black and orange blotches, stiff to very stiff, slickensided, silty CLAY. Colluvium.	
	Notes:	
	Refusal.	
	No water.	
	Disturbed sample at: 1,1 m.	

TP3		
0 - 0,3	Dry, light brown, medium dense, intact, sandy SILT. Colluvium. Roots.	
0,3 - 1,0	Dry, yellow brown with grey and orange blotches, stiff, shattered, sandy silty CLAY. Colluvium. Elluviated at top of layer.	
1,0 - 1,5	Slightly moist, yellow brown with grey and black and orange blotches, stiff to very stiff, slickensided, silty CLAY. Colluvium.	
	Notes:	
	Refusal.	
	No water.	
	Undisturbed sample at: 1,1 m.	
	Disturbed sample at: 1,1 m.	



SOILAB (Pty) LTD.

230 ALBERTUS STREET, LA MONTAGNE, PRETORIA
P O BOX 72928, LYNNWOOD RIDGE, 0040

FACSIMILE TRANSMITTAL SHEET

TO: Leon Croucamp	FROM: Zelda Smit
FAX NUMBER: 012 841 1148	DATE: 2003-01-28
COMPANY: Council for Geoscience	TOTAL NO. OF PAGES INCLUDING COVER:
PHONE NUMBER:	SENDER'S REF NO: S03-036
RE / PROJECT: <i>Results</i>	

URGENT

FOR REVIEW

PLEASE REPLY

MISS Z SMIT

Tel: 012-481 3801 Fax: 012-481 3812

E mail: smitz@soilab.co.za



SOIL ANALYSIS BY : SOILLAB (Pty) Ltd - Pretoria

Page : 1

Lab reference No. : S03-036

Date Printed : 2003-01-28

Customer : COUNCIL FOR GEOSIENCE

Job Number : S03-036

Job Description : DONKERHOEK

Contract Number :

Road Number :

Date : 2003-01-15

SAMPLE DESCRIPTION

Sample Number	07461	07462	07463
Sample Position	TP 1	TP 2	TP 3
Sample Depth (mm)	1200	1100	1100
Material Description	LIGHT OLIVE CLAY	DARK YELLOW CLAY	LIGHT BROWN CLAY

Max size of boulder (mm) : -

SCREEN ANALYSIS (% PASS)

Screen Size (mm)	07461	07462	07463
75,00 mm	100	100	100
63,00 mm	100	100	100
53,00 mm	100	100	100
37,50 mm	100	100	100
26,50 mm	100	100	100
19,00 mm	100	100	100
13,20 mm	100	100	100
4,750 mm	100	100	100
2,000 mm	99	100	99
0,425 mm	95	98	95
0,075 mm	73	83	77

SOIL MORTAR

Material	07461	07462	07463
Coarse Sand 2,000-0,425	5	2	4
Coarse Fine Sd 0,425-0,250	8	5	7
Medium Fine Sd 0,250-0,150	7	5	6
Fine Fine Sand 0,150-0,075	6	5	5
Material <0,075	74	83	78

CONSTANTS

Property	07461	07462	07463
Grading Modulus	0.33	0.19	0.29
Liquid Limit	34	36	38
Plasticity Index	13	13	15
Linear Shrinkage (%)	6.0	6.0	7.0
Sand Equivalent			
Classification - TRB	A-6 (9)	A-6 (9)	A-6 (10)
Classification - TRH14			

CBR / UCS VALUES**MOD. AASHTO**

Max Dry Density (kg/m ³)			
Optimum Moisture Cont (%)			
Moulding Moisture Cont (%)			
Dry Density (kg/m ³)			
% of Max Dry Density			
100% Mod CBR/UCS			
% Swell			

NRB

Dry Density (kg/m ³)			
% of Max Dry Density			
100% NRB CBR/UCS			
% Swell			

PROCTOR

Dry Density (kg/m ³)			
% of Max Dry Density			
100% Proc CBR/UCS			
% Swell			

CBR / UCS VALUES

100% Mod AASHTO			
98% Mod AASHTO			
97% Mod AASHTO			
95% Mod AASHTO			
93% Mod AASHTO			
90% Mod AASHTO			

SOILLAB

(PTY) LTD

Reg No 1971/00112/07

 230 Albertus Street
 La Montagne
 Tel (012) 481-3999

 P O Box 72928
 Lynnwood Ridg 0040
 Fax (012) 481-3812

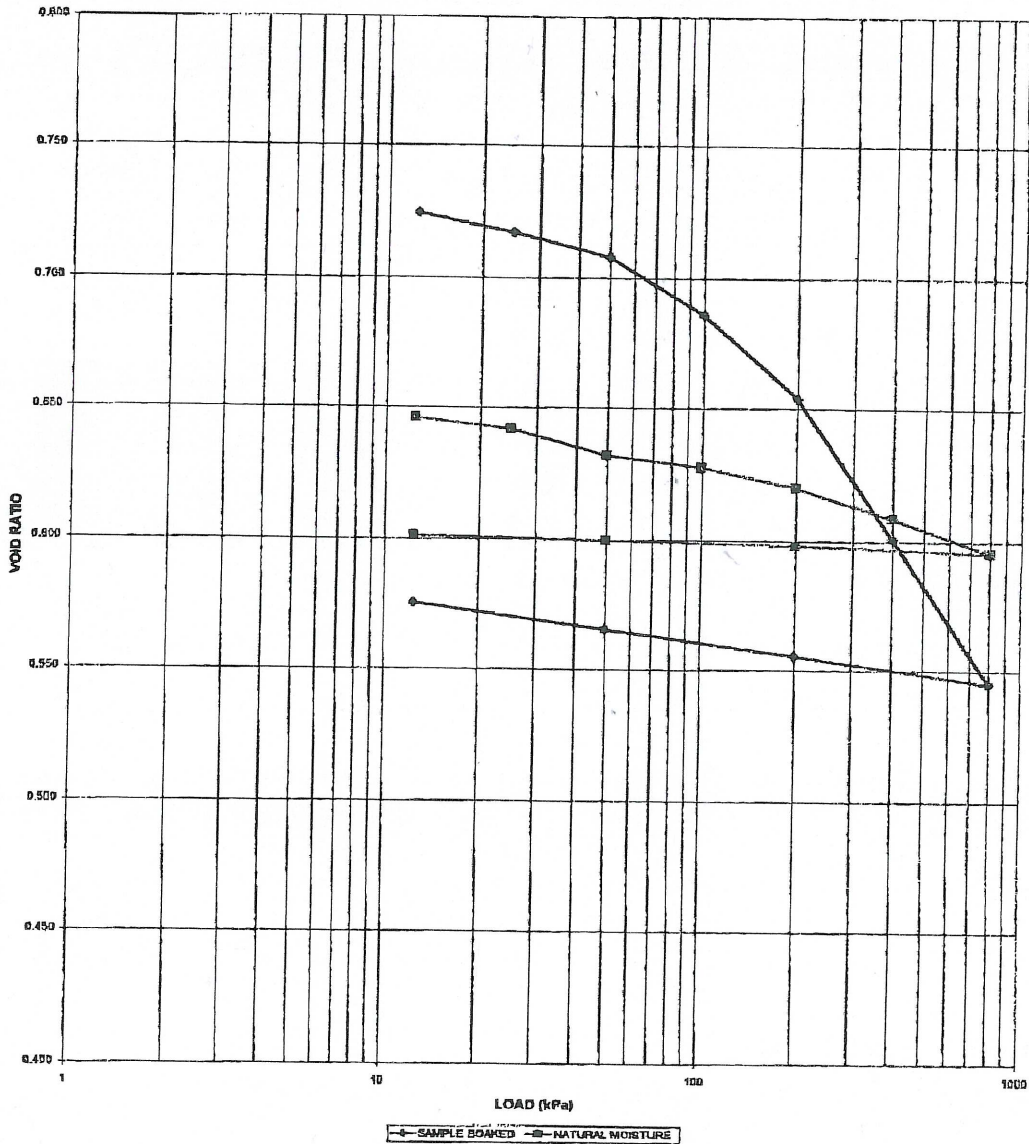


DOUBLE CONSOLIDATION TEST

PROJECT:	DONKERHOEK	INITIAL DRY DENSITY (kg/m ³):	1632				
SAMPLE NO:	TP 9	INITIAL MOISTURE CONTENT (%):	<table border="1"><tr><td>SAMPLE SOAKED</td><td>NATURAL MOISTURE</td></tr><tr><td>18.5</td><td>17.9</td></tr></table>	SAMPLE SOAKED	NATURAL MOISTURE	18.5	17.9
SAMPLE SOAKED	NATURAL MOISTURE						
18.5	17.9						
DEPTH (m):	1.1	MOISTURE CONTENT AFTER TEST (%):	<table border="1"><tr><td>22.2</td><td>16.2</td></tr></table>	22.2	16.2		
22.2	16.2						
INITIAL HEIGHT OF SAMPLE (mm):	19.4	RELATIVE DENSITY:	2.696				
SAMPLE STATE:	UNDISTURBED	INITIAL VOID RATIO:	0.652				
		VOID RATIO AFTER SOAKING:	0.728				

LOAD (kPa):	0	12.5	25	50	100	200	400	800	2000	4000	12.5
HEIGHT (mm):	19.40	20.30	20.25	20.17	20.06	19.80	19.42	18.80	18.15	18.27	18.39
VOID RATIO	0.652	0.728	0.724	0.717	0.708	0.686	0.654	0.601	0.545	0.556	0.568

LOAD (kPa):	0	12.5	25	50	100	200	400	800	2000	4000	12.5
HEIGHT (mm):	19.10	19.03	18.98	18.87	18.82	18.73	18.60	18.45	18.48	18.50	18.51
VOID RATIO	0.652	0.646	0.642	0.632	0.627	0.620	0.608	0.595	0.598	0.600	0.601



KONS/KONSOLIDASIE-DUIDELI03-02

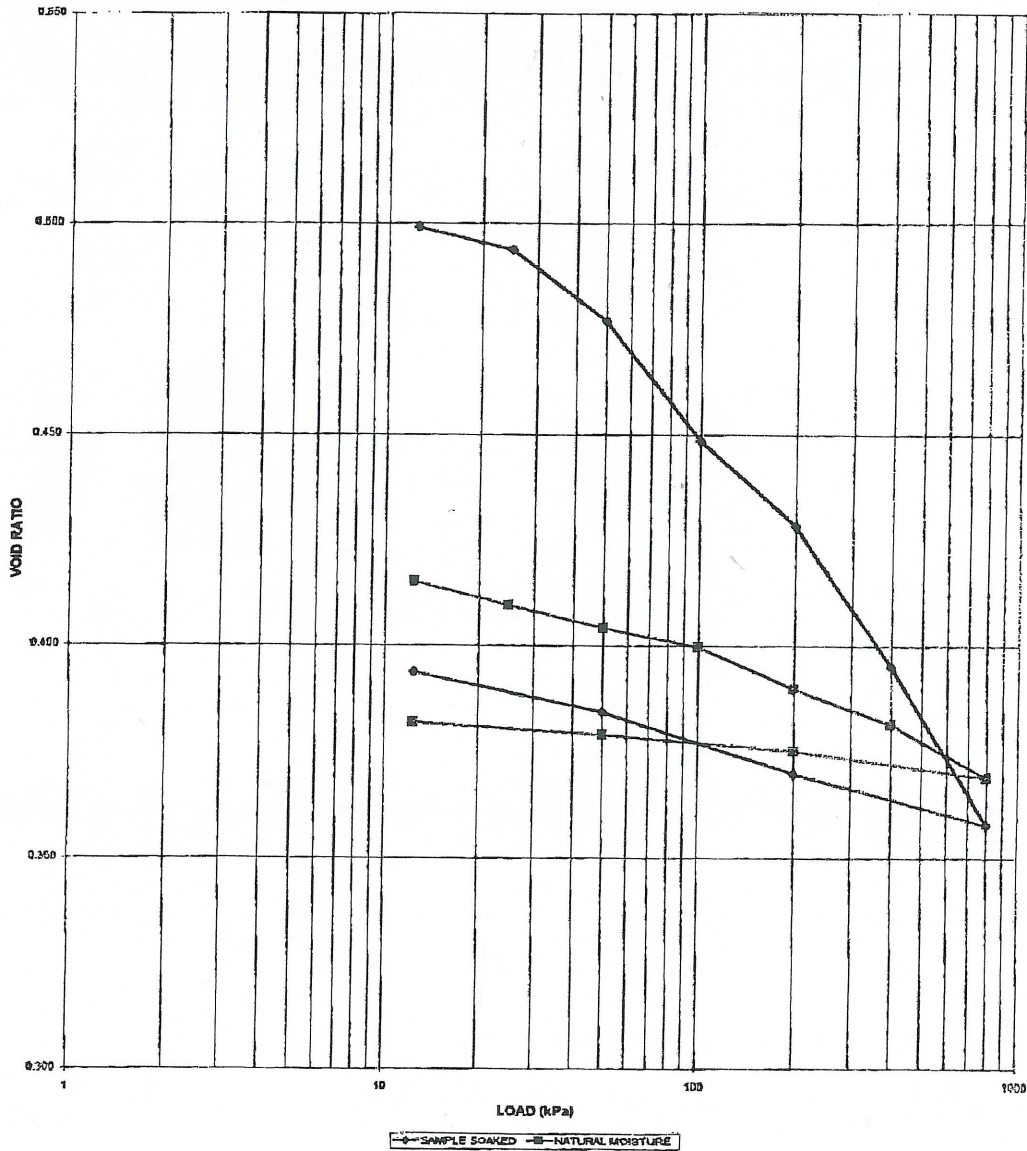


DOUBLE CONSOLIDATION TEST

PROJECT:	DONKERHOEK	INITIAL DRY DENSITY (kg/m ³):	1835				
SAMPLE NO:	TP 1	INITIAL MOISTURE CONTENT (%):	<table border="1" style="display: inline-table; vertical-align: middle;"><tr><th>SAMPLE SOAKED</th><th>NATURAL MOISTURE</th></tr><tr><td>12.5</td><td>11.8</td></tr></table>	SAMPLE SOAKED	NATURAL MOISTURE	12.5	11.8
SAMPLE SOAKED	NATURAL MOISTURE						
12.5	11.8						
DEPTH (m):	1.1	MOISTURE CONTENT AFTER TEST (%):	17.6 10.1				
INITIAL HEIGHT OF SAMPLE (mm):	19.4	RELATIVE DENSITY:	2.599				
SAMPLE STATE:	UNDISTURBED	INITIAL VOID RATIO:	0.416				
		VOID RATIO AFTER SOAKING:	0.508				

LOAD (kPa):	0	12.5	25	50	100	200	400	800	200	50	12.5	
HEIGHT (mm):	19.40	20.66	20.54	20.46	20.37	19.84	19.57	19.11	18.60	18.77	18.98	19.09
VOID RATIO	0.416	0.508	0.499	0.494	0.487	0.449	0.429	0.395	0.358	0.370	0.384	0.394

LOAD (kPa):	0	12.5	25	50	100	200	400	800	200	50	12.5
HEIGHT (mm):	19.50	19.49	19.41	19.34	19.27	19.14	19.02	18.85	18.94	18.99	19.03
VOID RATIO	0.416	0.415	0.410	0.404	0.400	0.390	0.382	0.369	0.375	0.379	0.382



KONSKONSOLIDASIE-DUBBELK03B-01



Appendix II

Country View

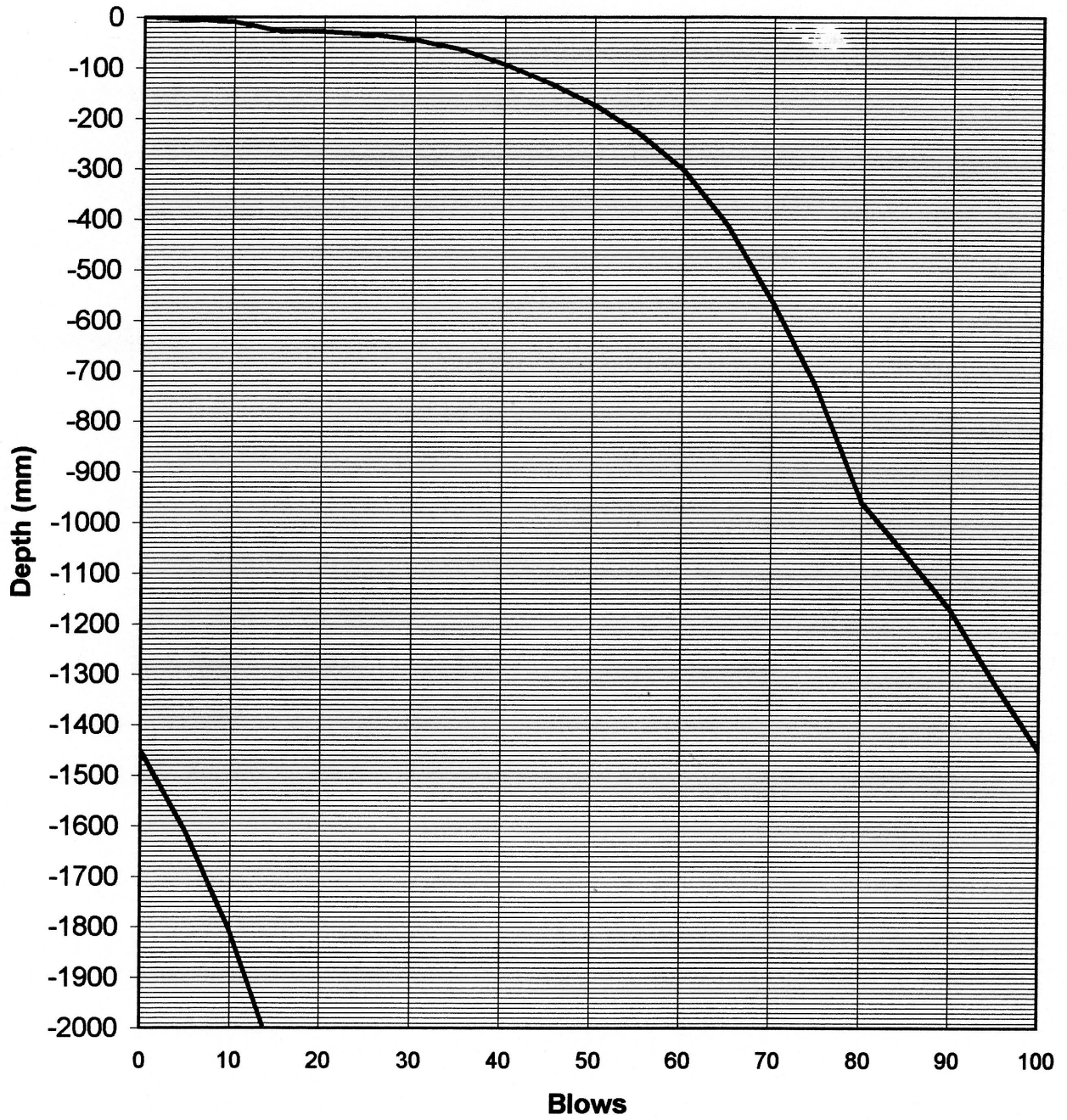


COUNTRY VIEW ESTATE Testpit (TP 1)	
DEPTH TO mm	ENGINEERING GEOLOGICAL PROFILE DESCRIPTION
0-200	Imported construction material- Light brown/grey horizon –combination of fine aggregate and cement - Fine aggregate light-brown silty sand with cement DCP derived SPT value > 40
200-900	Slightly moist, light brown, dense becoming loose with depth, open-textured silty sand. Fine colluvium. DCP derived SPT value 8 to 12 Estimated bearing capacity 60kPa to 90kPa
900-1 400	Slightly moist yellow, mottled red and black loose to very loose nodular ferricrete in a very loose open-textured sandy matrix. Traces of pebble marker and large quartz fragments DCP derived SPT value 8 to 15 Estimated bearing capacity 60kPa to 110kPa NOTES Excavated to 1.4m only - No refusal- See DCP graph 1B DCP refusal at 2.7m No groundwater intersected, but traces of perched watertable at 1.0m (Ferricrete)
Profiled: September/2004 by P.L. Roux	



GEOPRO

DCP 1

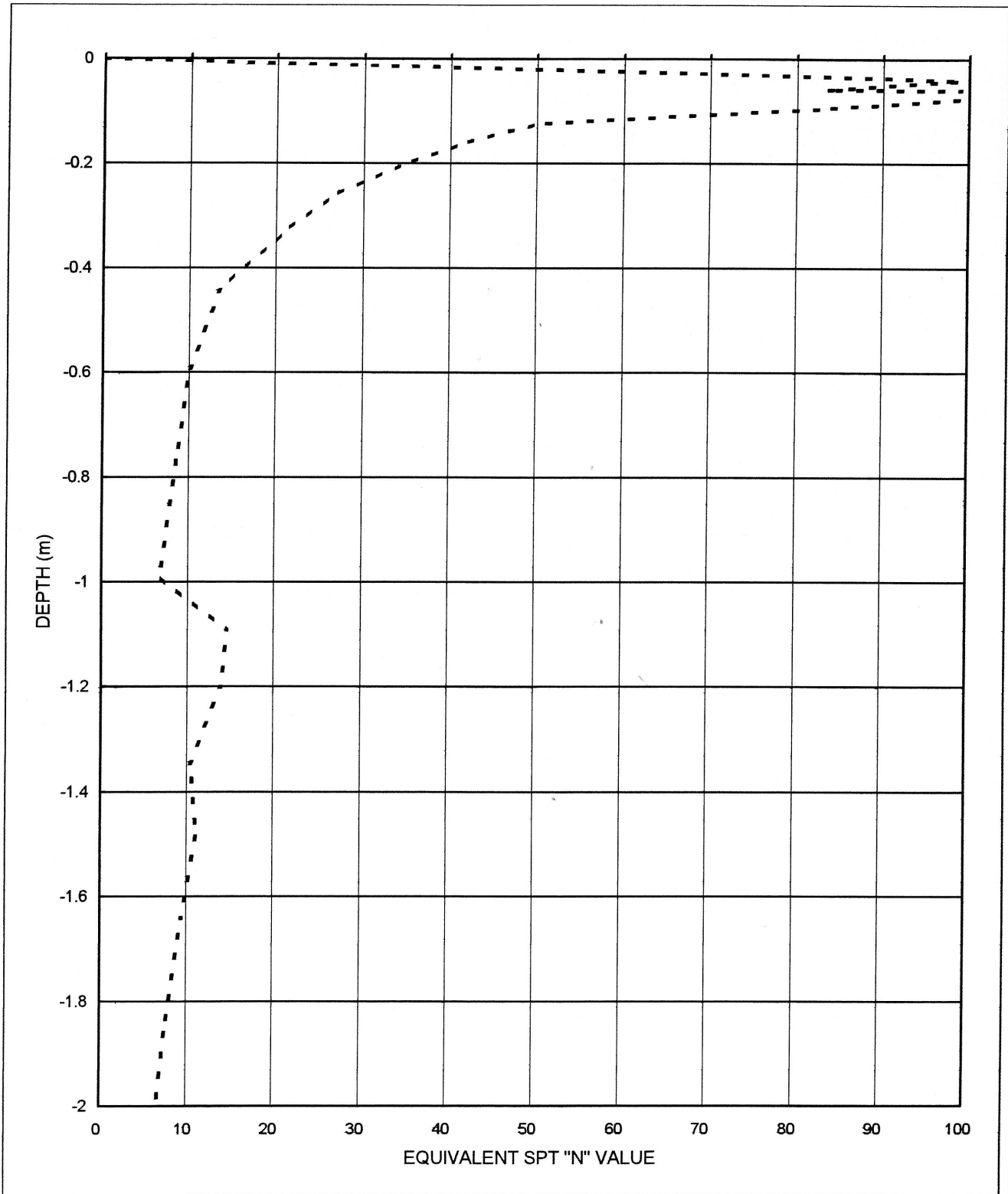


NOTA:

DKP/790-01



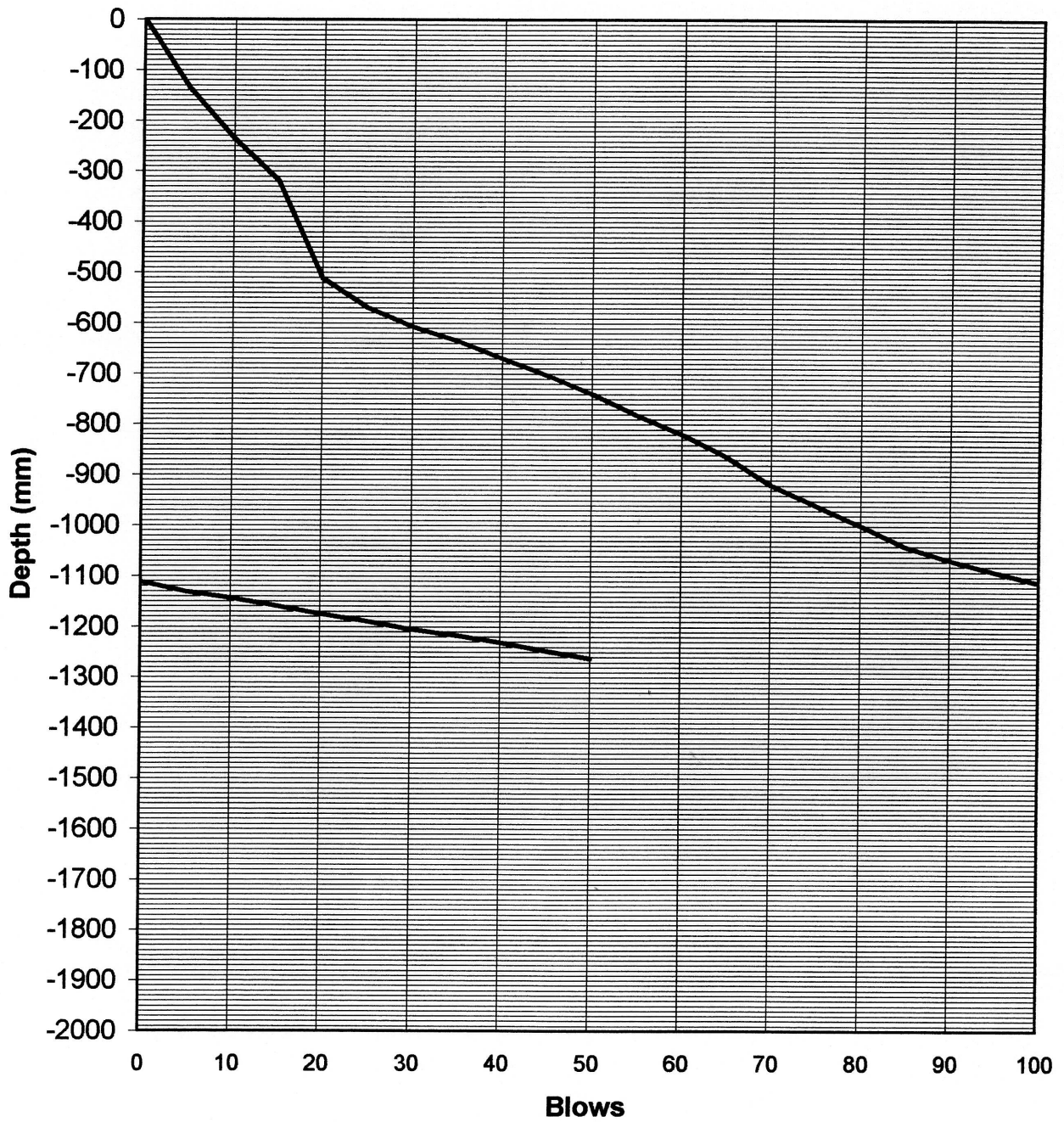
CLIENT:
PROJECT COUNTRYVIEW GARDENS
PROJECT NO.: S04-790
DATE: 30/05/2004
POSITION: DCP 1



DKP/790-11



GEOPRO DCP 1(B)

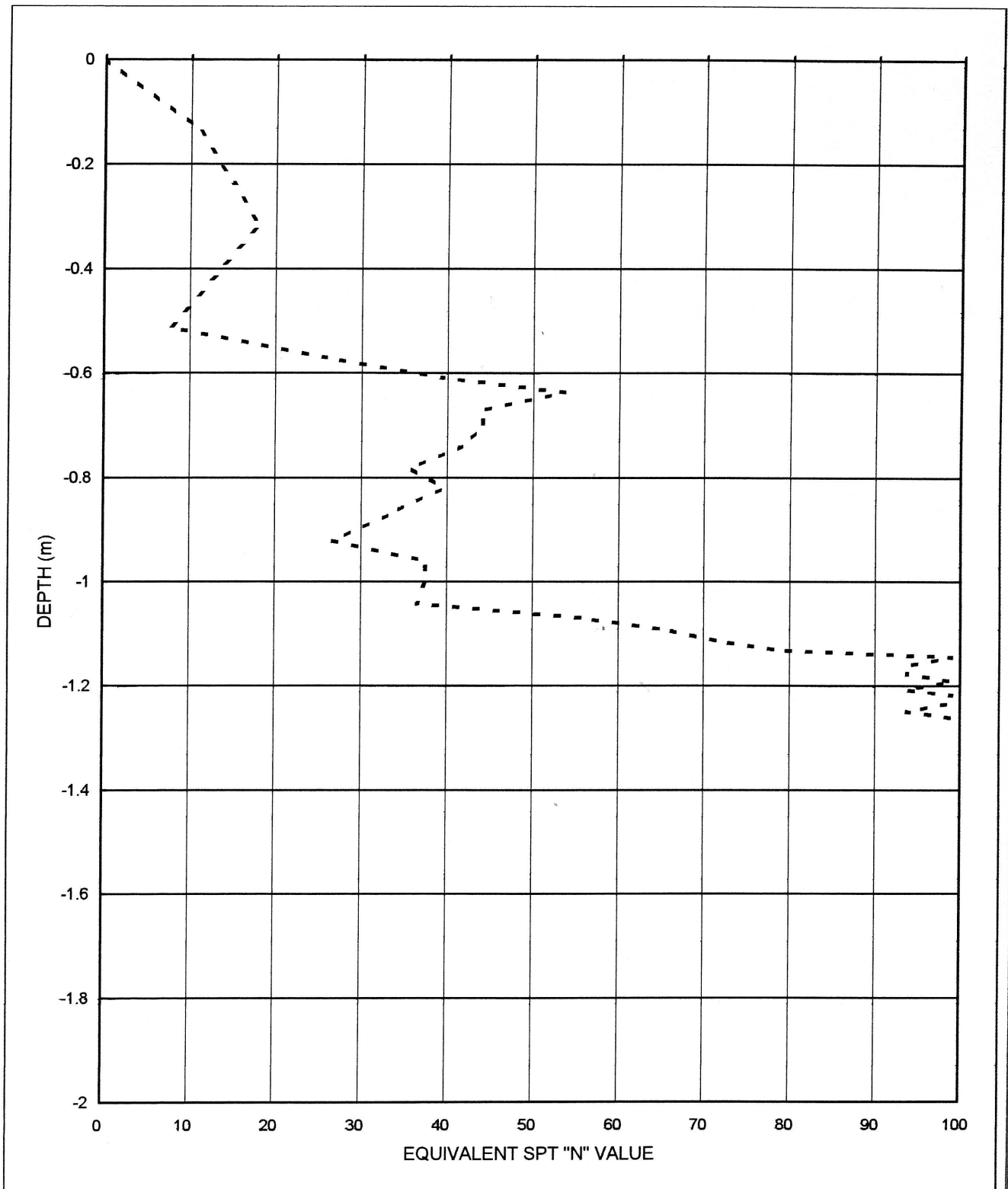


NOTE : DCP STARTED IN BOTTOM OF TP (- 1.5m)

DKP/790-02



CLIENT:
PROJECT COUNTRYVIEW GARDENS
PROJECT NO.: S04-790
DATE: 30/05/2004
POSITION: DCP 1 (B)



DKP/790.12



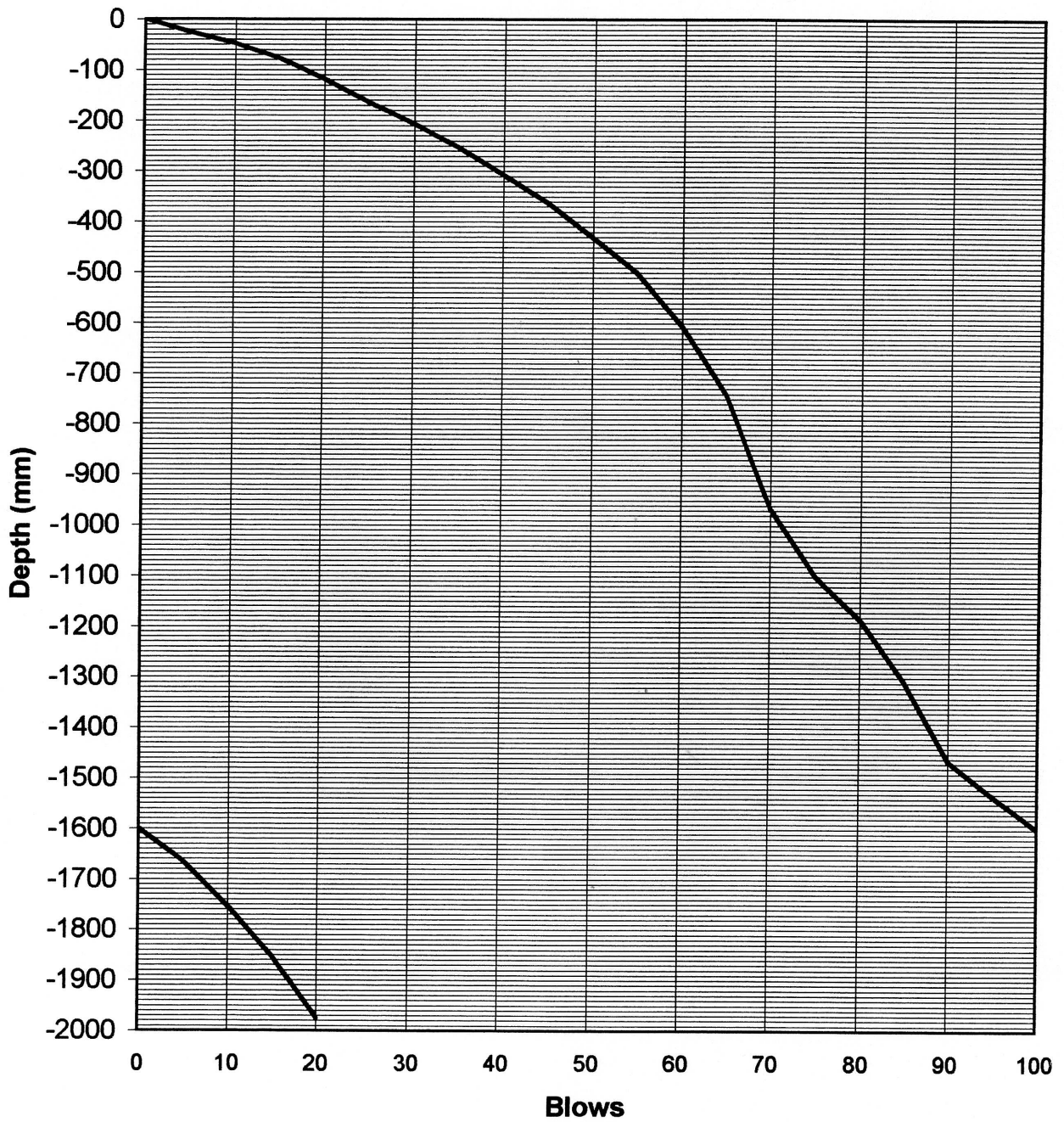
COUNTRY VIEW ESTATE Testpit (TP 2)	
DEPTH TO mm	ENGINEERING GEOLOGICAL PROFILE DESCRIPTION
0-300	Slightly moist, brownish-yellow, open textured silty sand-Fine colluvium DCP derived SPT value > 30 Troxler Nuclear Density Measurements 0-300mm
300-800	Slightly moist, yellowish red dense becoming loose with depth, open textured silty Sand. Fine colluvium- DCP derived very variable SPT 30 to 10 value Estimated bearing capacity 225kPa (drier state) to 75kPa Highly susceptible horizon to collapse settlement on moisture ingress
800-900	Slightly moist yellow, mottled red and black loose to very loose nodular ferricrete in a very loose open-textured sandy matrix. Traces of pebble marker and large quartz fragments DCP derived SPT value 9 Estimated bearing capacity 68kPa
900-1500	Slightly moist, yellow and red highly weathered granite-very soft rock-with soil characteristics DCP derived SPT value 9 Estimated bearing capacity 68kPa Bulk sample taken from 700 to 1 500 for compaction characteristics Troxler Nuclear Density Measurements bottom of testpit 1.5 to 1.8 (300mm) <u>NOTES</u> Excavated to 1.5 only - No refusal- See DCP graph 2B DCP no refusal up to 3.5, but more competent material from 2.7m onwards with SPT values of between 20 -50 No groundwater intersected, but traces of perched watertable at 900mm (Ferricrete)

Profiled: September/2004 by P.L. Roux



GEOPRO

DCP 2

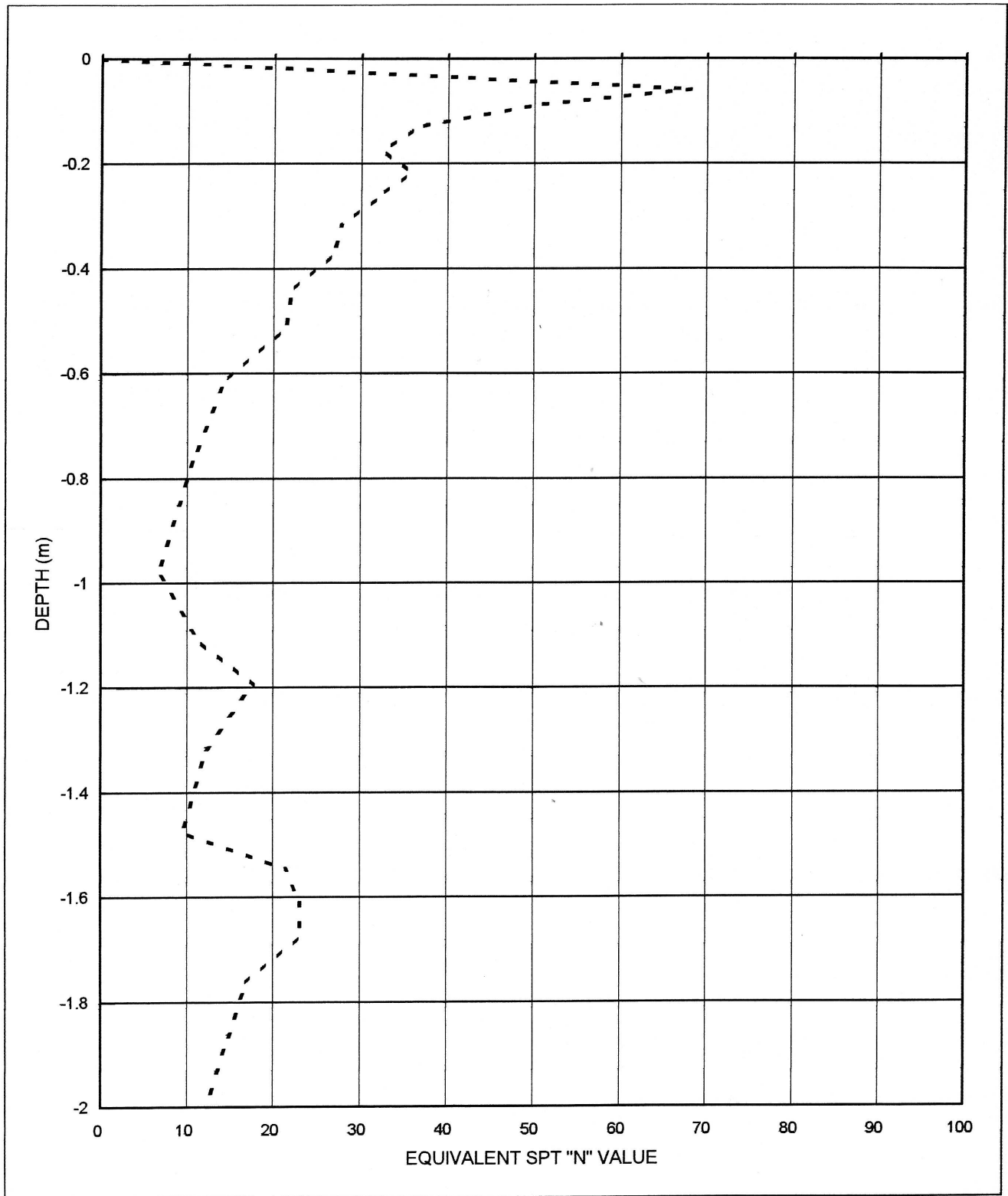


NOTE :

DKP/790-03



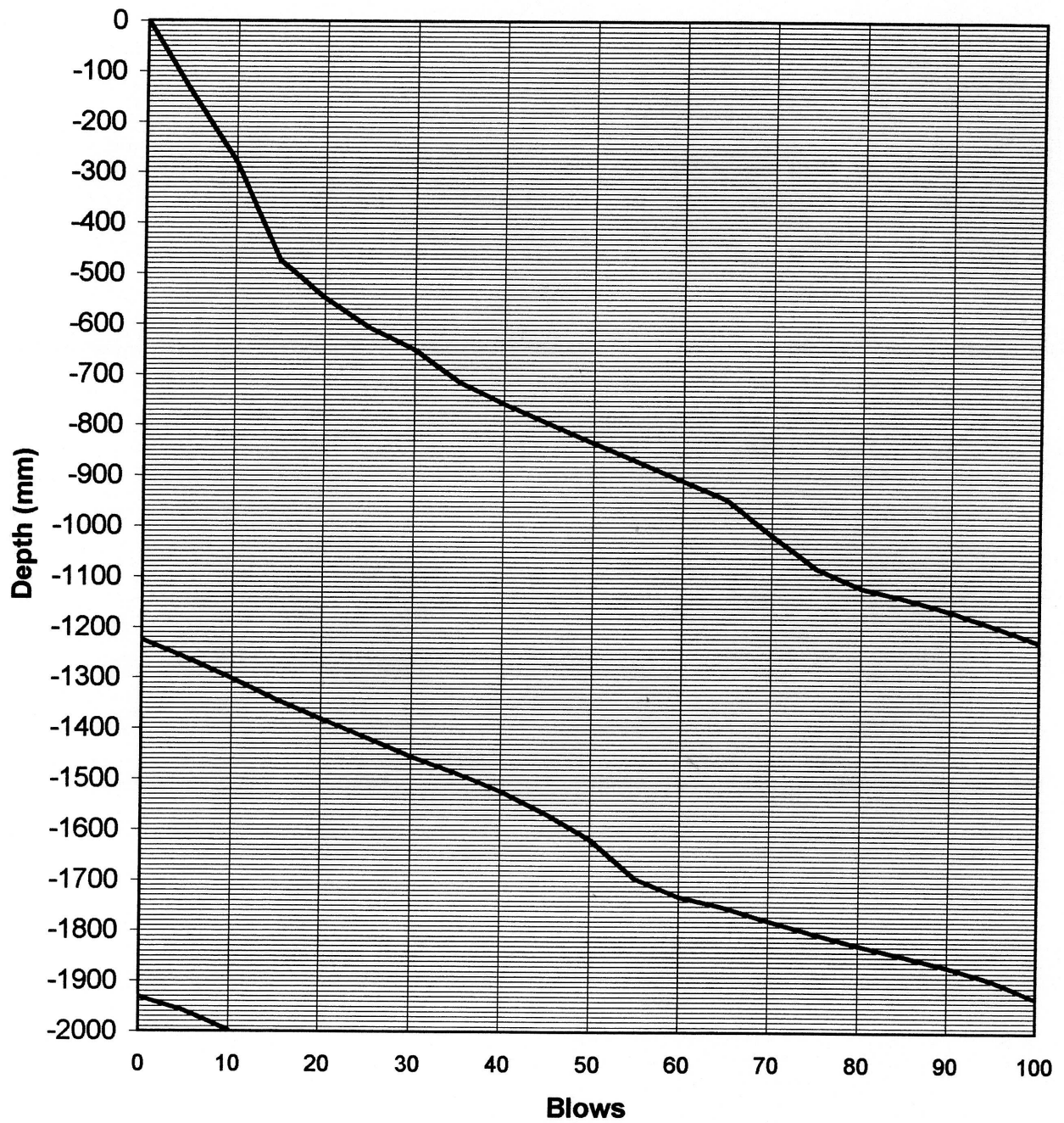
CLIENT:
PROJECT COUNTRYVIEW GARDENS
PROJECT NO.: S04-790
DATE: 30/05/2004
POSITION: DCP 2



DKP/790-13



GEOPRO
DCP 2 (B)

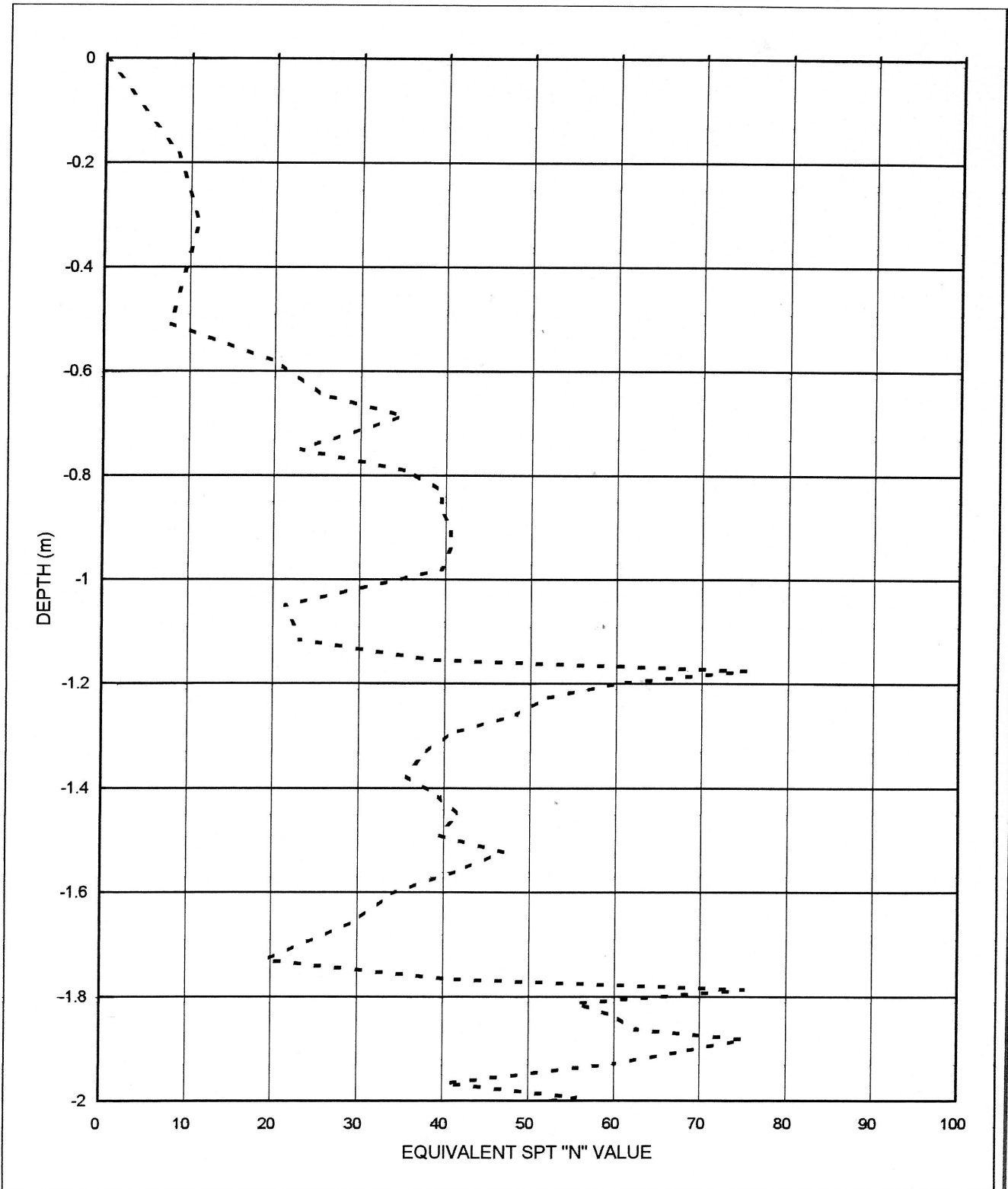


NOTE : DCP STARTED IN BOTTOM OF TP (- 1.5m)

DKP/790-04



CLIENT:
PROJECT COUNTRYVIEW GARDENS
PROJECT NO.: S04-790
DATE: 30/05/2004
POSITION: DCP 2 (B)



DKP/790-14



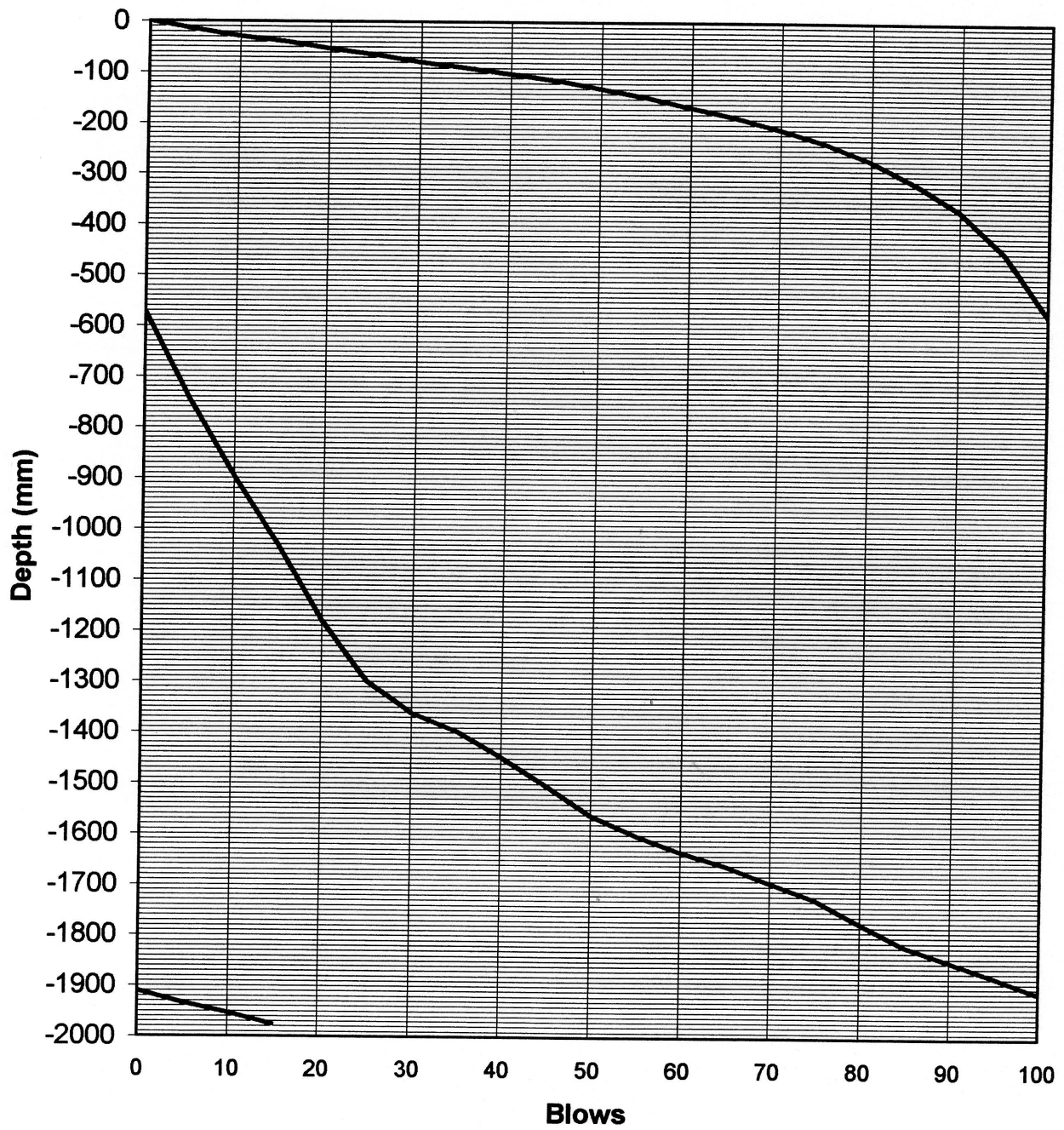
COUNTRY VIEW ESTATE Testpit (TP 3)	
DEPTH TO mm	ENGINEERING GEOLOGICAL PROFILE DESCRIPTION
0-400	Slightly moist, brownish-yellow, open textured silty sand-Fine colluvium DCP derived SPT value > 25 Pebble marker and quartz fragments noticed at 400mm
400-1400	Slightly moist, yellow and red highly weathered granite-very soft rock-with soil characteristics DCP derived SPT value 10 Estimated bearing capacity 75 kPa NOTES Excavated to 1.40only no refusal See DCP graph 3B DCP refusal at 2.4m with SPT value >50 No groundwater intersected
900-1500	

Profiled: September/2004 by P.L. Roux



GEOPRO

DCP 3

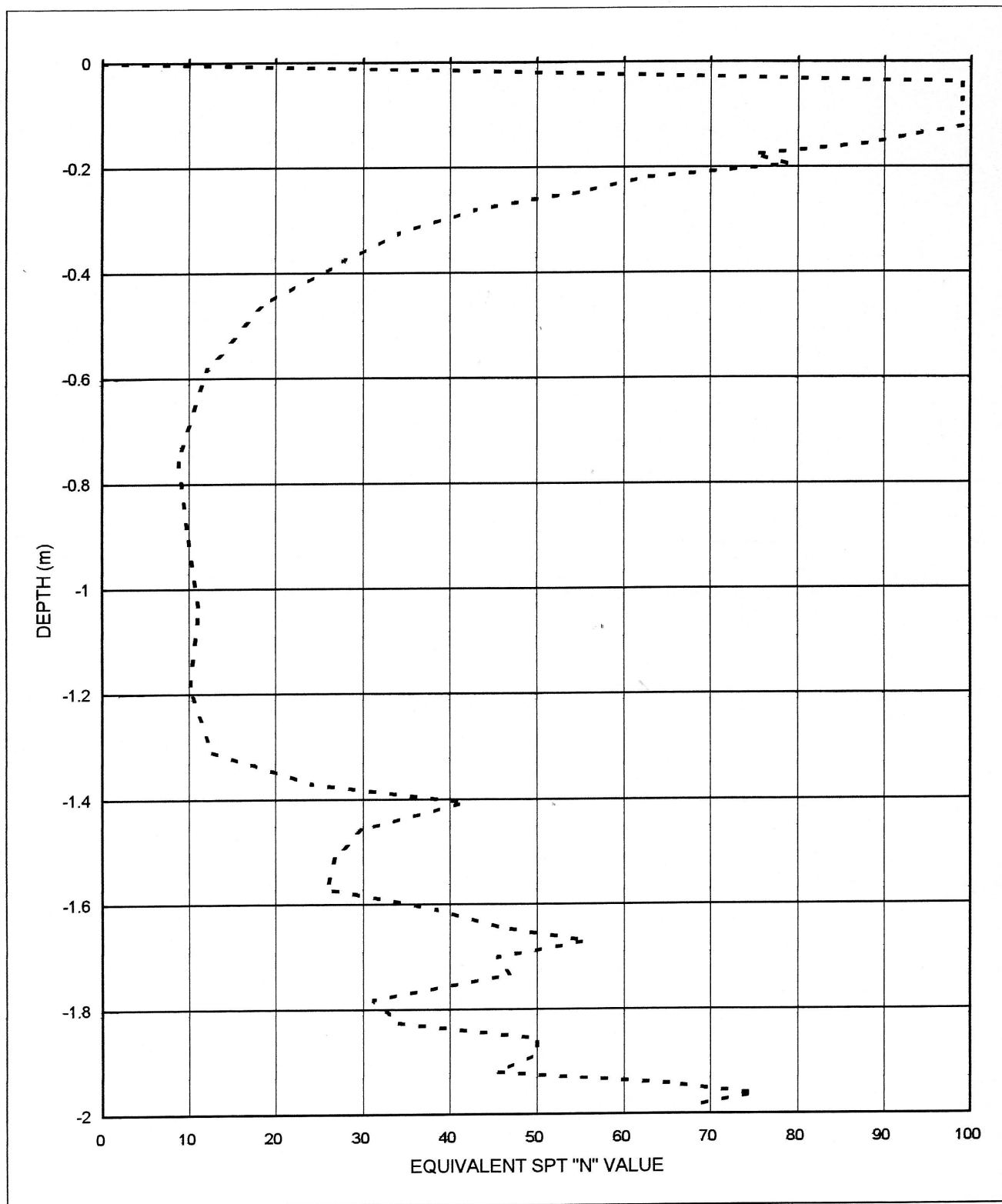


NOTE :

DKP/790-05



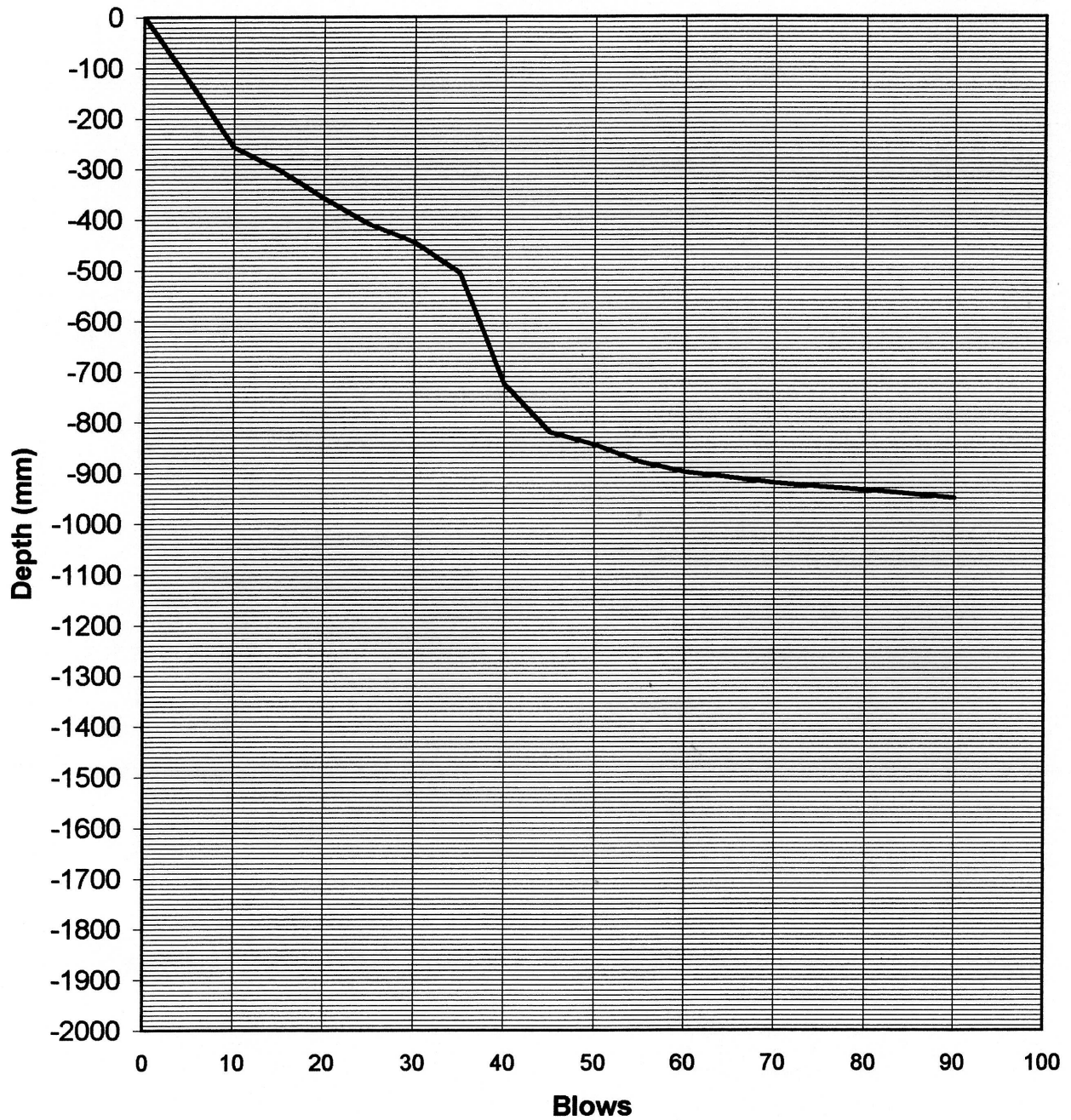
CLIENT: SECURUS
PROJECT: COUNTRYVIEW GARDENS
PROJECT NO.: S04-790
DATE: 30/05/2004
POSITION: DCP 3



DKP/790-15



GEOPRO
DCP 3 (B)

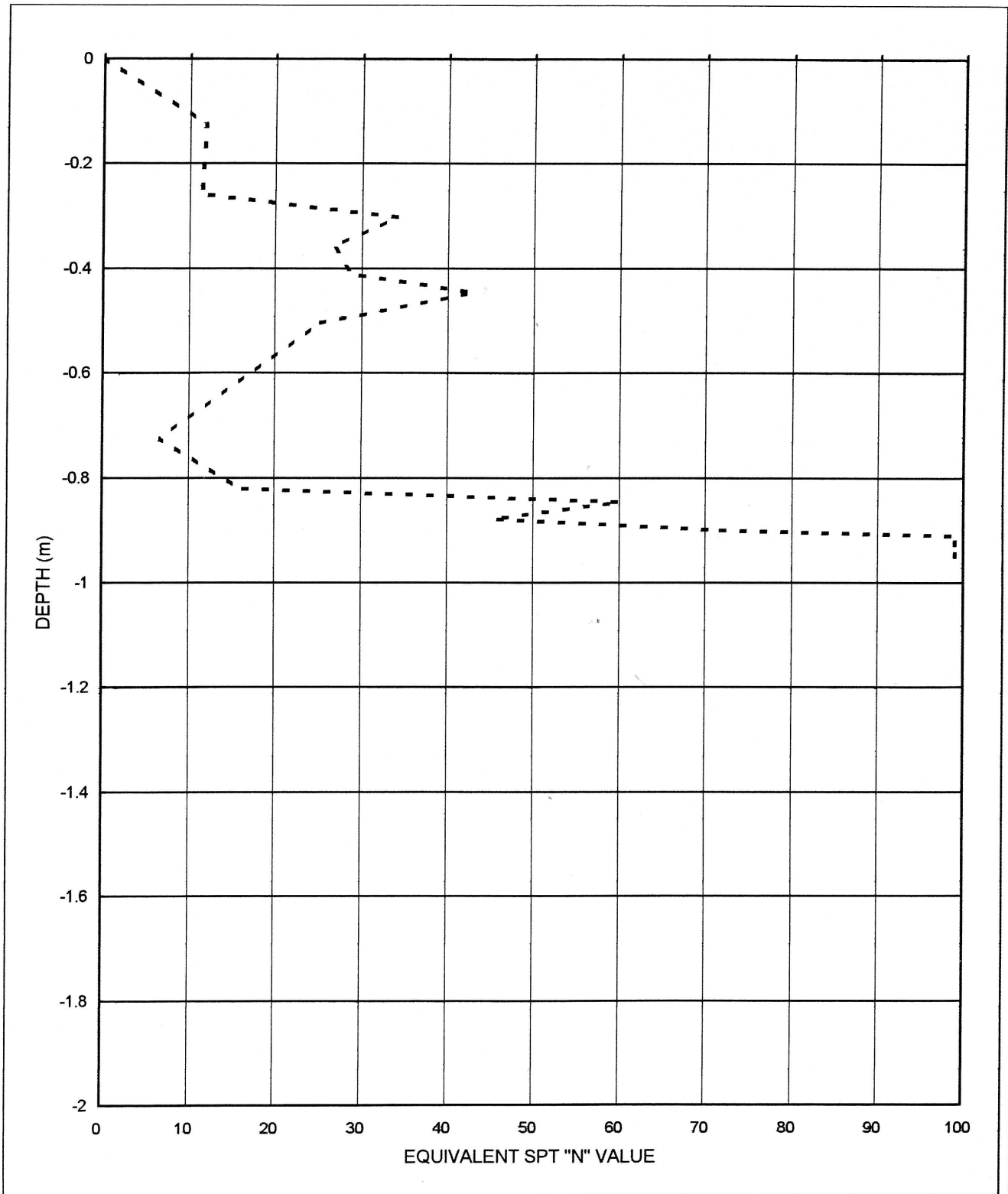


NOTE : DCP STARTED IN BOTTOM OF TP (- 1.5m)

DKP/790-06



CLIENT: [REDACTED]
PROJECT COUNTRYVIEW GARDENS
PROJECT NO.: S04-790
DATE: 30/05/2004
POSITION: DCP 3 (B)



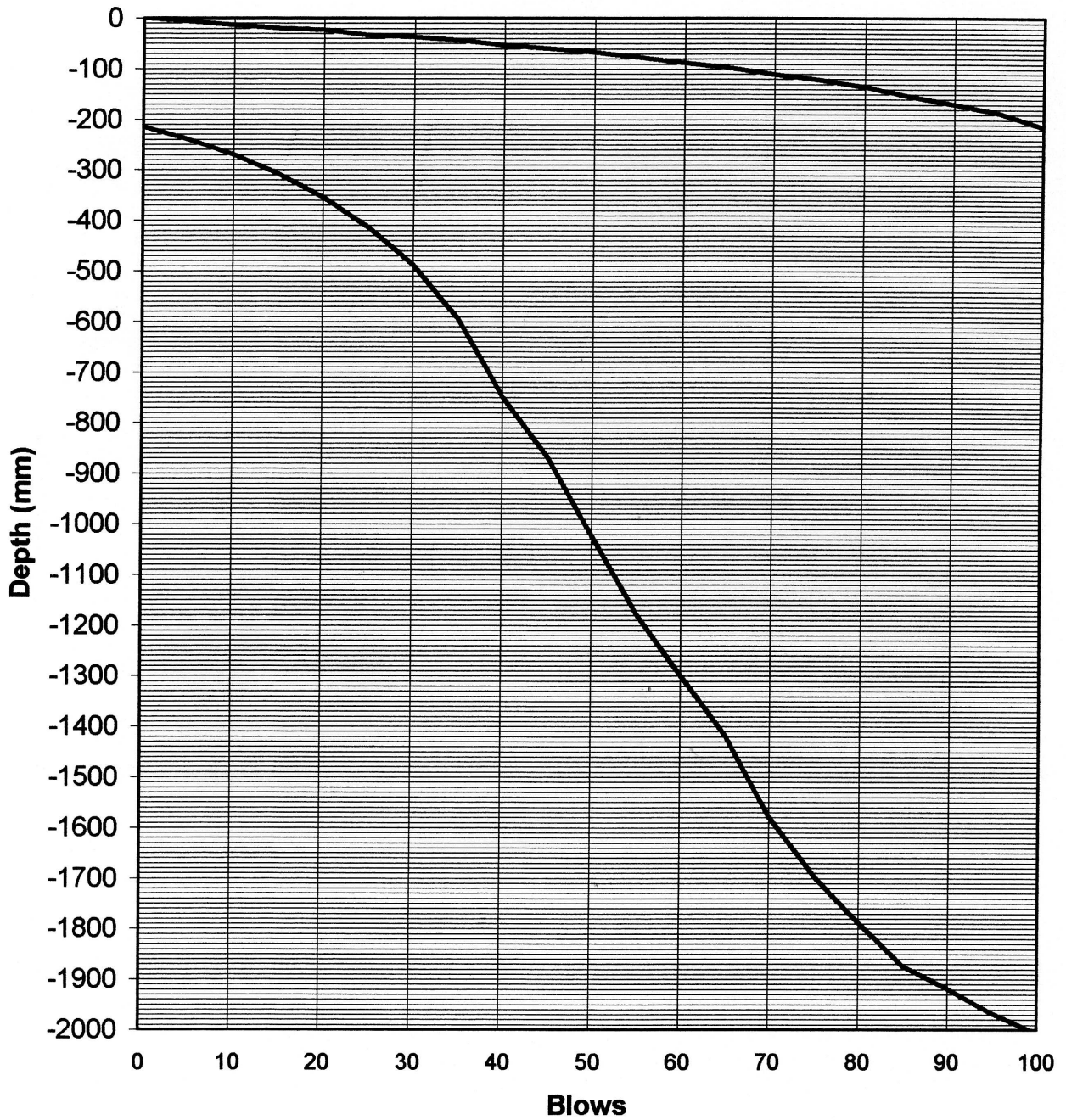
DKP/790-16



COUNTRY VIEW ESTATE Testpit (TP 4)	
DEPTH TO mm	ENGINEERING GEOLOGICAL PROFILE DESCRIPTION
0-500	Slightly moist, brownish-yellow, open textured silty sand-Fine colluvium DCP derived SPT value > 20 Troxler Nuclear Density Measurements 0-300mm
500-1400	Slightly moist light yellow to reddish, loose open textured silty sand DCP derived SPT value 10 Estimated bearing capacity 75kPa Two undisturbed samples taken at 1.4m for collapse potential and double consolidation tests
1400 -1700	Slightly moist, yellow mottled red and black loose nodular ferricrete in loose open-textured sandy matrix DCP derived SPT value 10-12 Estimated bearing capacity 75 kPa to 90 kPa Troxler Nuclear Density Measurements bottom of testpit from 1.7 to 2.0m (300mm)
NOTES Excavated to 1.70m only no refusal See DCP graph 4B Strength of DCP profile from 700 to 3300 SPT value 10 Estimated bearing capacity for this horizon 2 600mm is 75 kPa. DCP encountered more competent material below 3.6m with SPT value >20 No groundwater intersected	
Profiled: September/2004 by P.L. Roux	



GEOPRO DCP 4



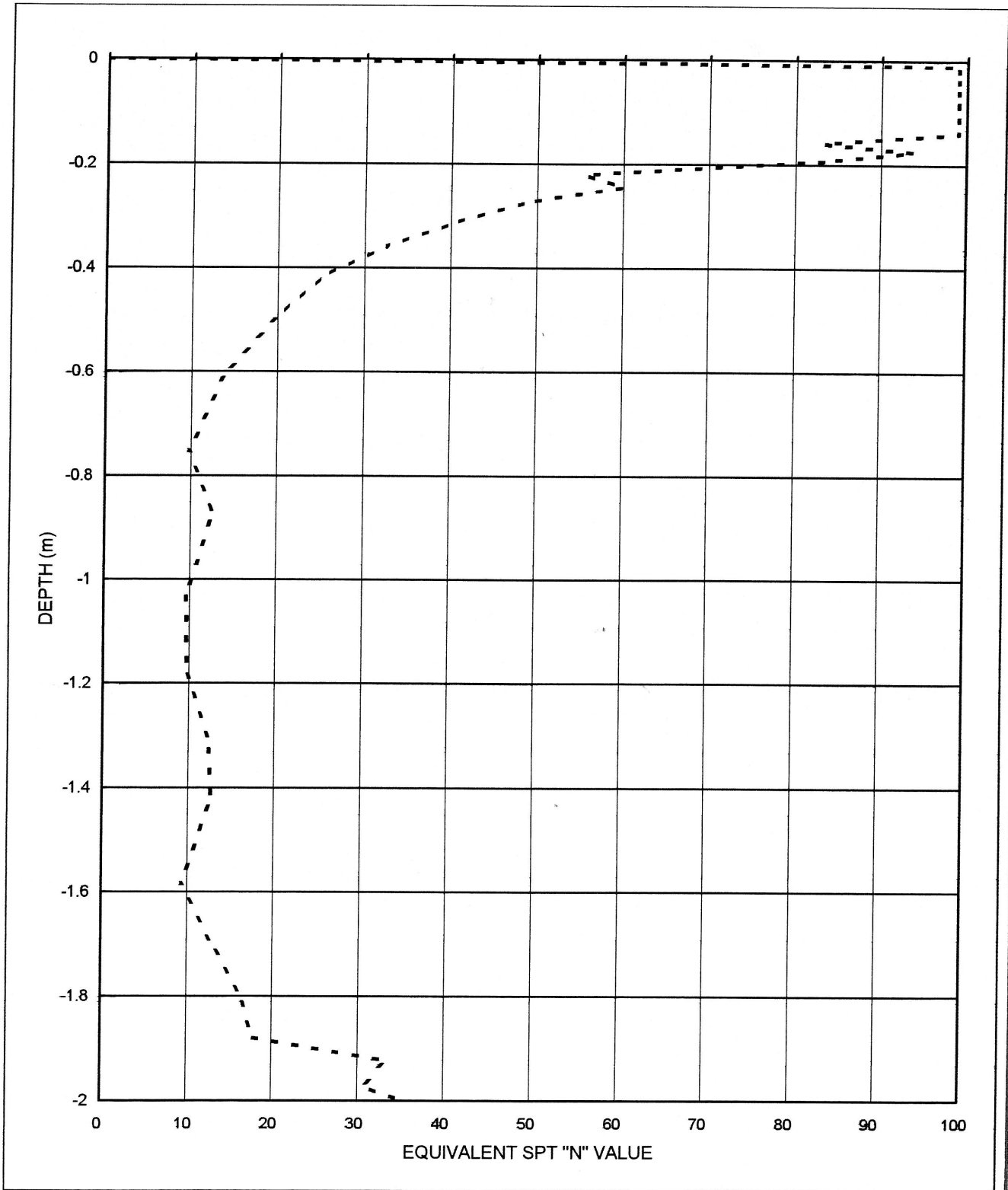
NOTE :

DKP/790-07



UNIVERSITEIT VAN PRETORIA
UNIVERSITY OF PRETORIA
YUNIBESITHI YA PRETORIA

CLIENT:
PROJECT COUNTRYVIEW GARDENS
PROJECT NO.: S04-790
DATE: 30/05/2004
POSITION: DCP 4



DKP/790.17

SOILLAB

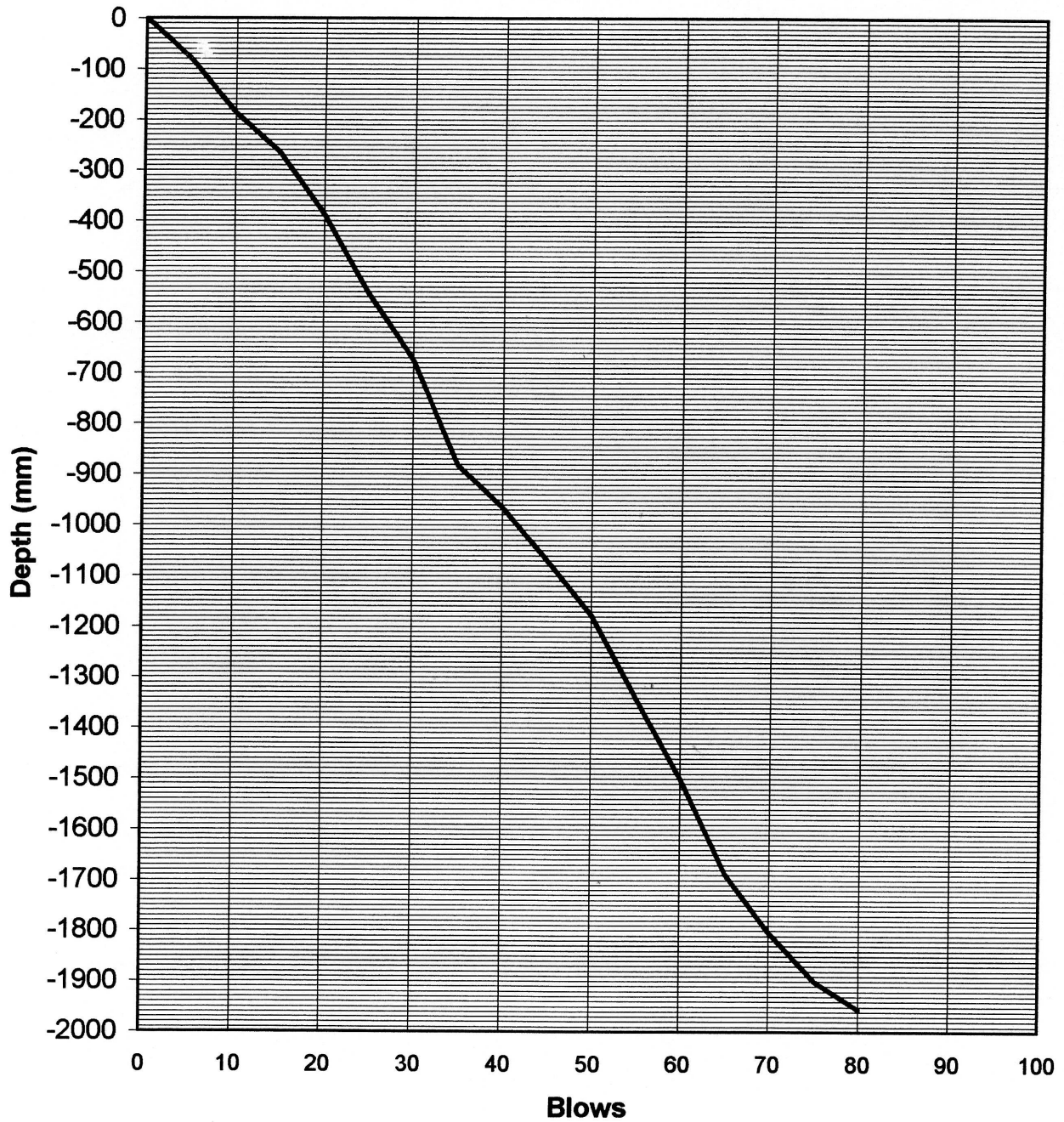
(PTY) LTD
Reg No 1971/00112/07

230 Albertus Street
La Montagne
Tel (012) 481-3999

P O Box 72928
Lynnwood Ridge 0040
Fax (012) 481-3812



GEOPRO DCP 4 (B)

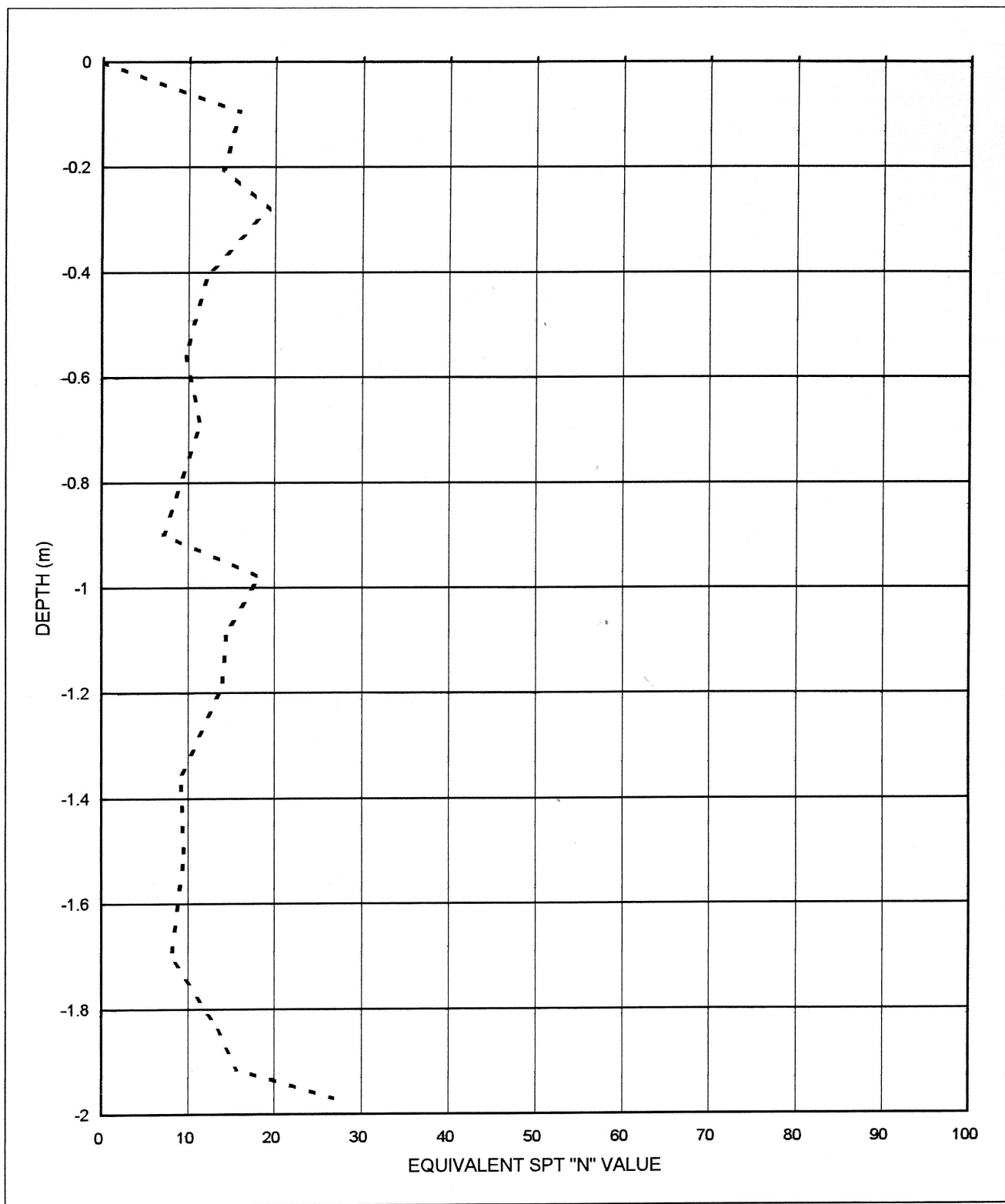


NOTE : DCP STARTED IN BOTTOM OF TP (- 1.7m)

DKP/790-08



CLIENT: GEOFORS
PROJECT: COUNTRYVIEW GARDENS
PROJECT NO.: S04-790
DATE: 30/05/2004
POSITION: DCP 4 (B)



DKP/790-18

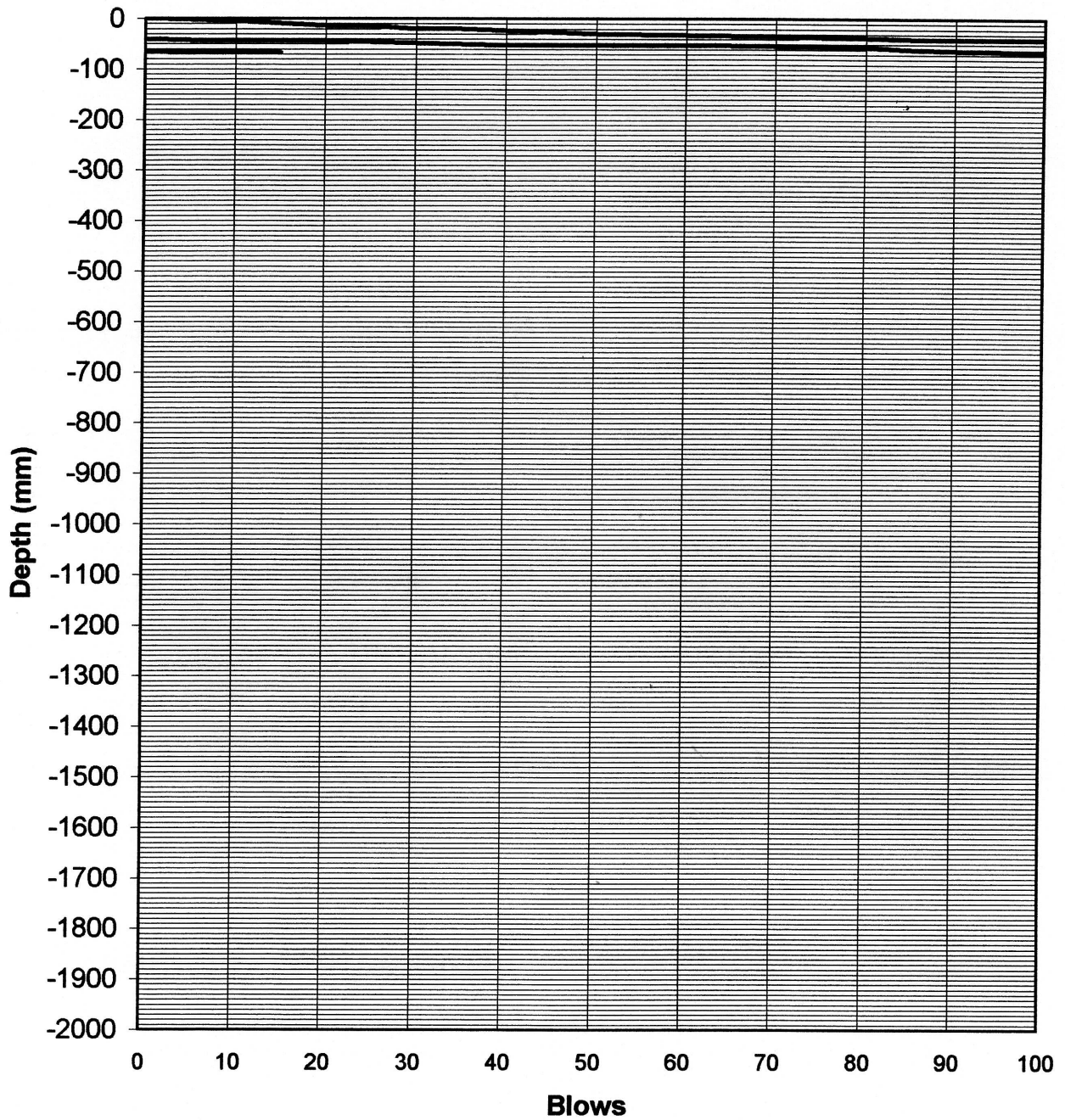


COUNTRY VIEW ESTATE Testpit (TP 5)	
DEPTH TO mm	ENGINEERING GEOLOGICAL PROFILE DESCRIPTION
0-500	Dry, yellow brown, very dense, open textured silty sand-Fine colluvium DCP derived SPT value > 80+ DCP refusal at 0.1m, top of TP1 Troxler Nuclear Density Measurements 0-300mm
500-700	Dry, yellowish loose open textured silty sand -Fine colluvium Scattered quartz and iron oxide nodules in sandy matrix (nodular ferricrete)
700 - 1400	Slightly moist, yellow and red highly weathered granite- very soft rock with mostly soil characteristics with a loose to very loose consistency. (Estimated bearing capacity of 50 kPa to 75 kPa) Troxler Nuclear Density Measurements bottom of testpit from 1.4 to 1.7m (300mm)
	NOTES Excavated to 1.40m only no refusal See DCP graph 5B DCP derived SPT values generally between 5 and 15 (1.4 to 2.8m) Encountered more competent material with SPT values of between 20 to 80 (2.8 to 3.4m) No groundwater intersected
Profiled: September/2004 by P.L. Roux	



GEOPRO

DCP 5

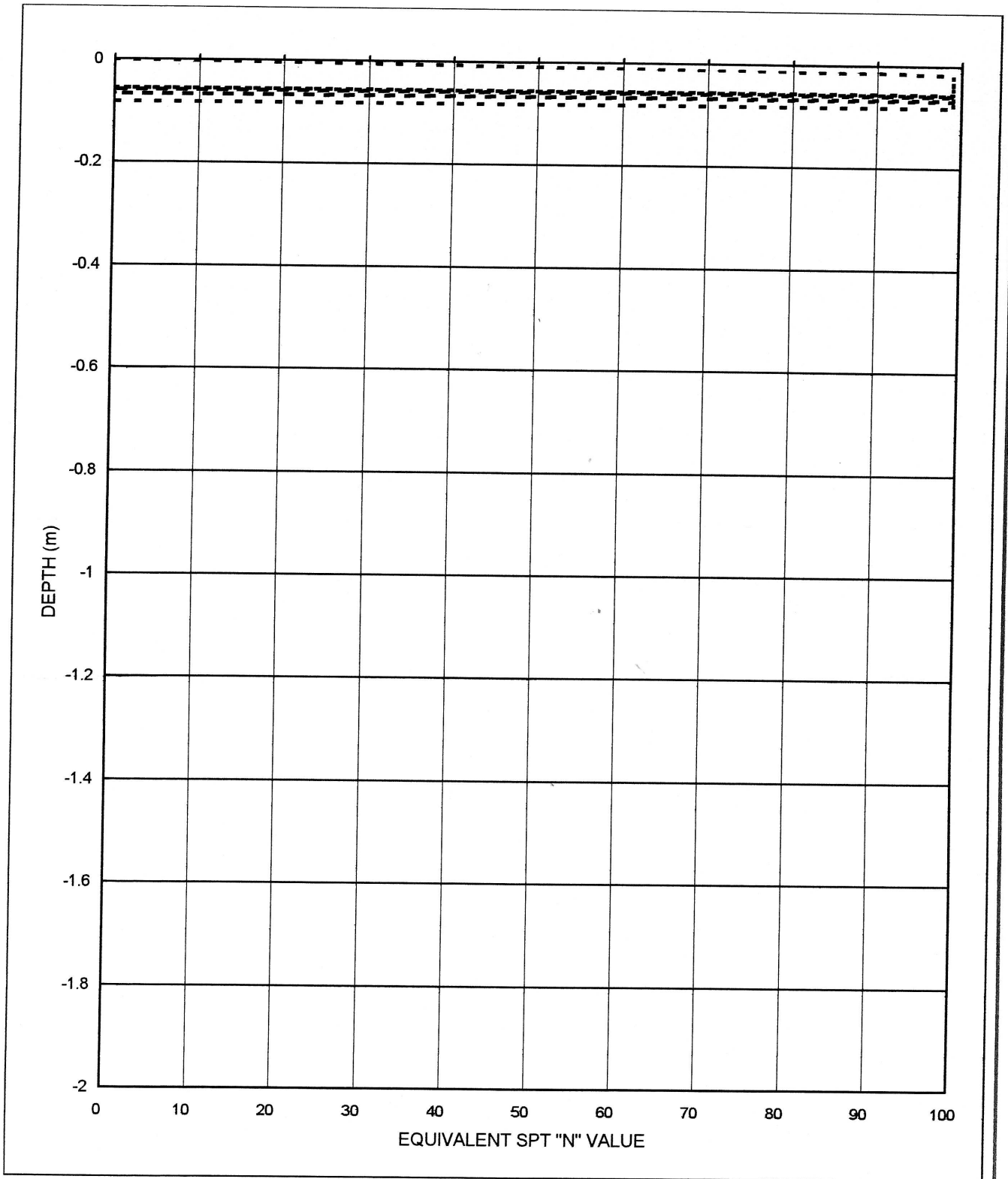


NOTE : DCP REFUSED AT 82mm

DKP/790-09

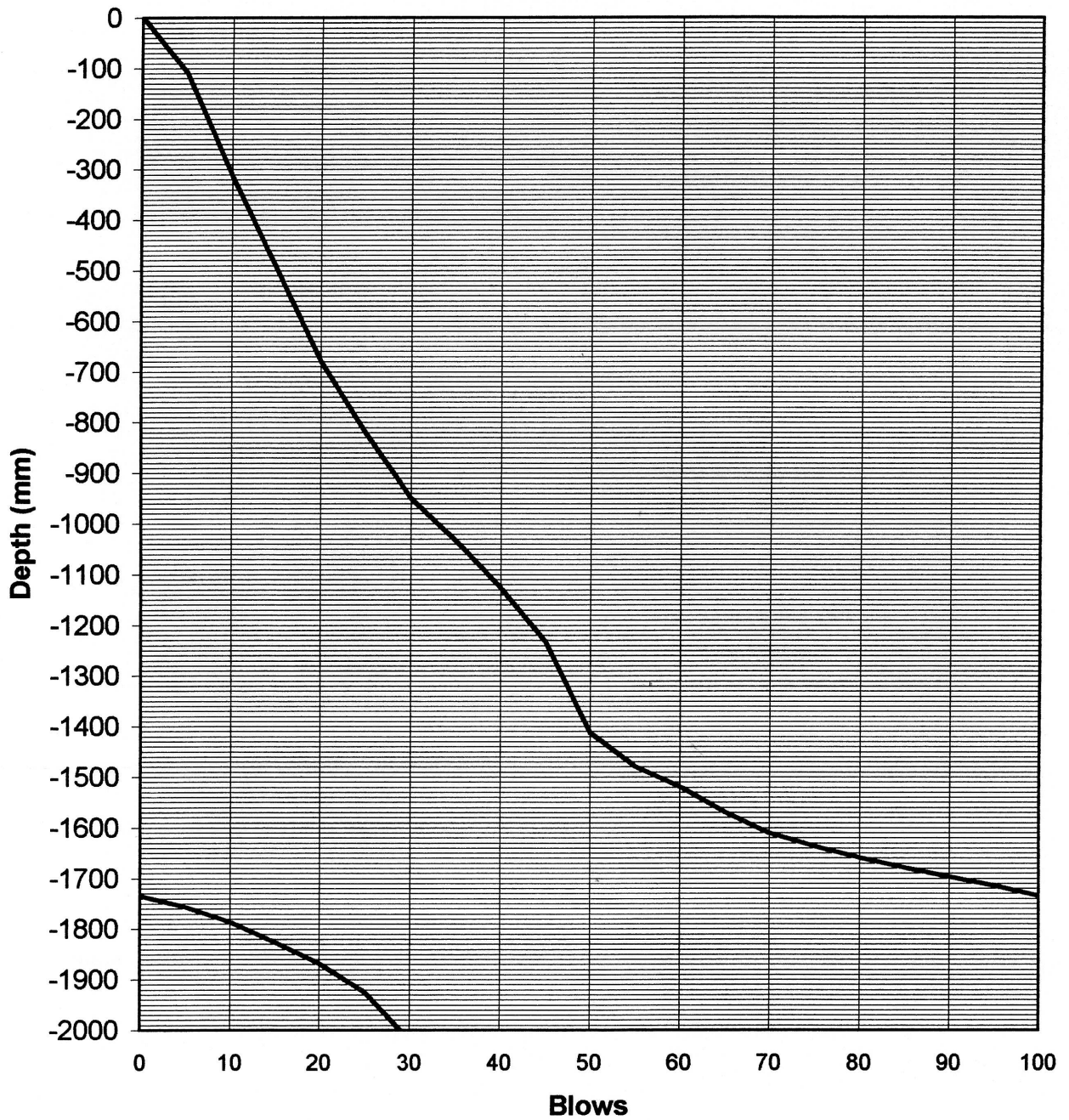


CLIENT: [REDACTED]
PROJECT COUNTRYVIEW GARDENS
PROJECT NO.: S04-790
DATE: 30/05/2004
POSITION: DCP 5





GEOPRO DCP 5 (B)

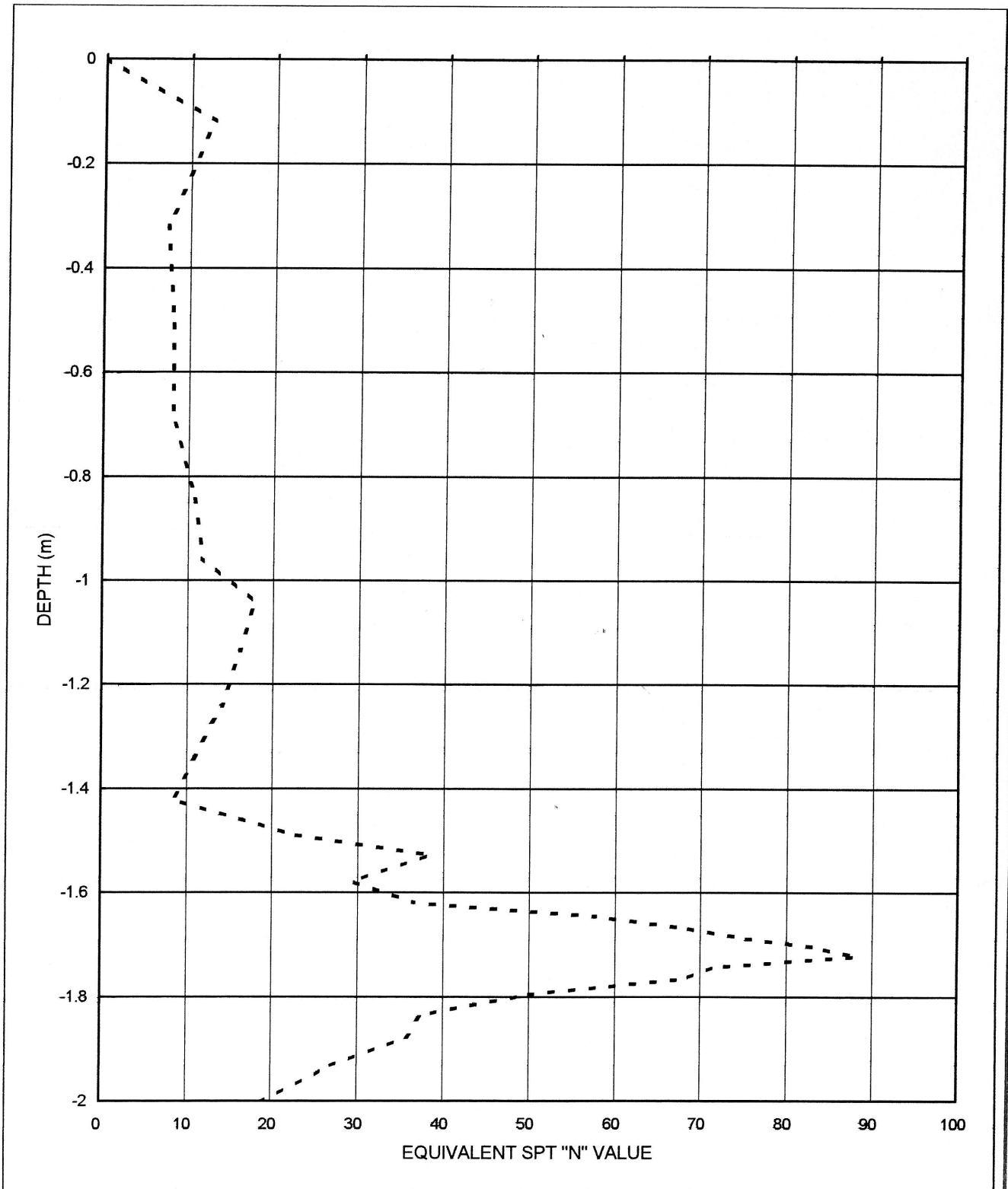


NOTE : DCP STARTED IN BOTTOM OF TP (- 1.4m)

DKP/790-10



CLIENT:
PROJECT COUNTRYVIEW GARDENS
PROJECT NO.: S04-790
DATE: 30/05/2004
POSITION: DCP 5 (B)

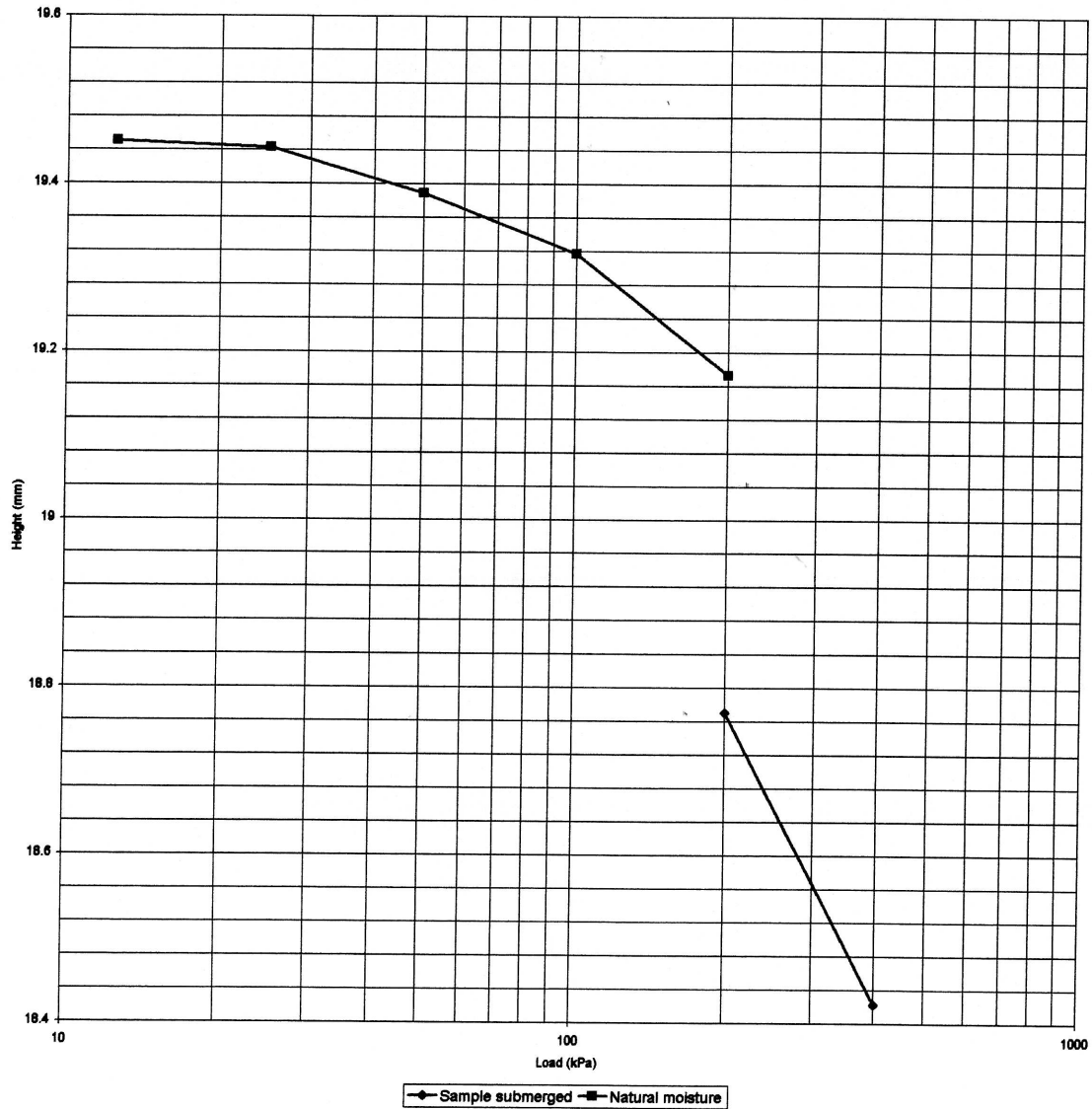


DKP/790-20



PROJECT:	COUNTRYVIEW GARDENS	INITIAL DRY DENSITY (kg/m ³)	1659
SAMPLE NR.	TP 4 (2)	INITIAL MOISTURE (%)	6.2
DEPTH (m):	1.4	MOISTURE AFTER TEST (%)	17.0
INITIAL HEIGHT OF SAMPLE (mm)	19.5	RELATIVE DENSITY	2.684
SAMPLE CONDITION	UNDISTURBED	INITIAL VOID RATIO	0.618
		VOID RATIO AFTER SOAKING	0.557
		% COLLAPSE	2.06

LOAD (kPa)	0	12.5	25	50	100	200	W	400
HEIGHT (mm)	19.500	19.450	19.442	19.388	19.316	19.172	18.770	18.422
VOID RATIO	0.618	0.614	0.613	0.609	0.603	0.591	0.557	0.529

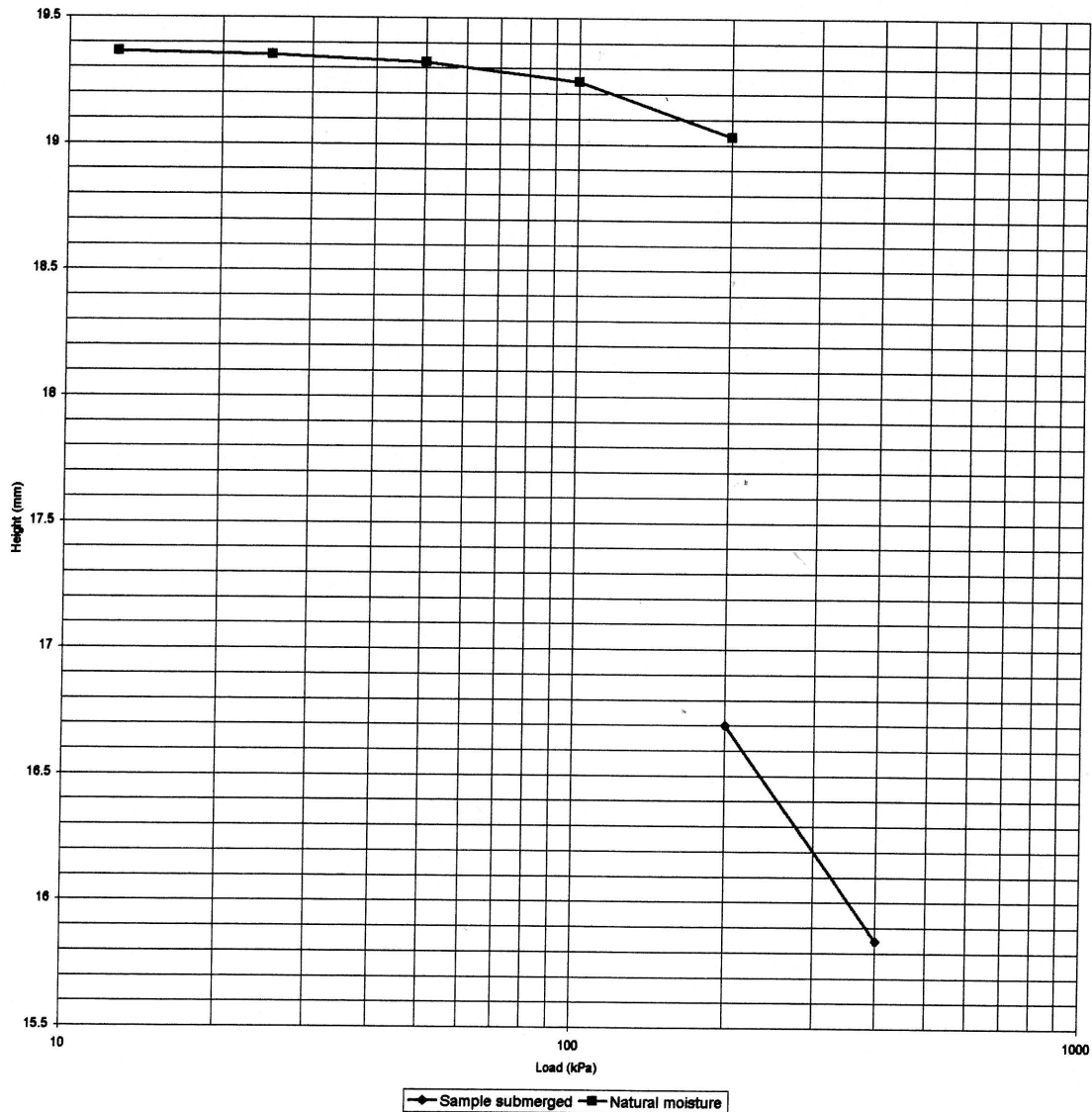


KONS/SWGPOTENTIAL/790-02



PROJECT:	COUNTRYVIEW GARDENS	INITIAL DRY DENSITY (kg/m ³)	1296
SAMPLE NR.	TP 4 (1)	INITIAL MOISTURE (%)	10.7
DEPTH (m):	1.4	MOISTURE AFTER TEST (%)	24.8
INITIAL HEIGHT OF SAMPLE (mm)	19.4	RELATIVE DENSITY	2.698
SAMPLE CONDITION	UNDISTURBED	INITIAL VOID RATIO	1.081
		VOID RATIO AFTER SOAKING	0.791
		% COLLAPSE	12.02

LOAD (kPa)	0	12.5	25	50	100	200	W	400
HEIGHT (mm)	19.400	19.362	19.350	19.322	19.246	19.030	16.698	15.844
VOID RATIO	1.081	1.077	1.076	1.073	1.065	1.041	0.791	0.700



KONS/SWKG/POTENTIAL/790-01



PROJECT: COUNTRYVIEW GARDENS INITIAL DRY DENSITY (kg/m³): 1296

SAMPLE NO: TP 4 INITIAL MOISTURE CONTENT (%):

SAMPLE SOAKED	NATURAL MOISTURE
10.4	9.8

DEPTH (m): 1.4 MOISTURE CONTENT AFTER TEST (%):

20.8	8.1
------	-----

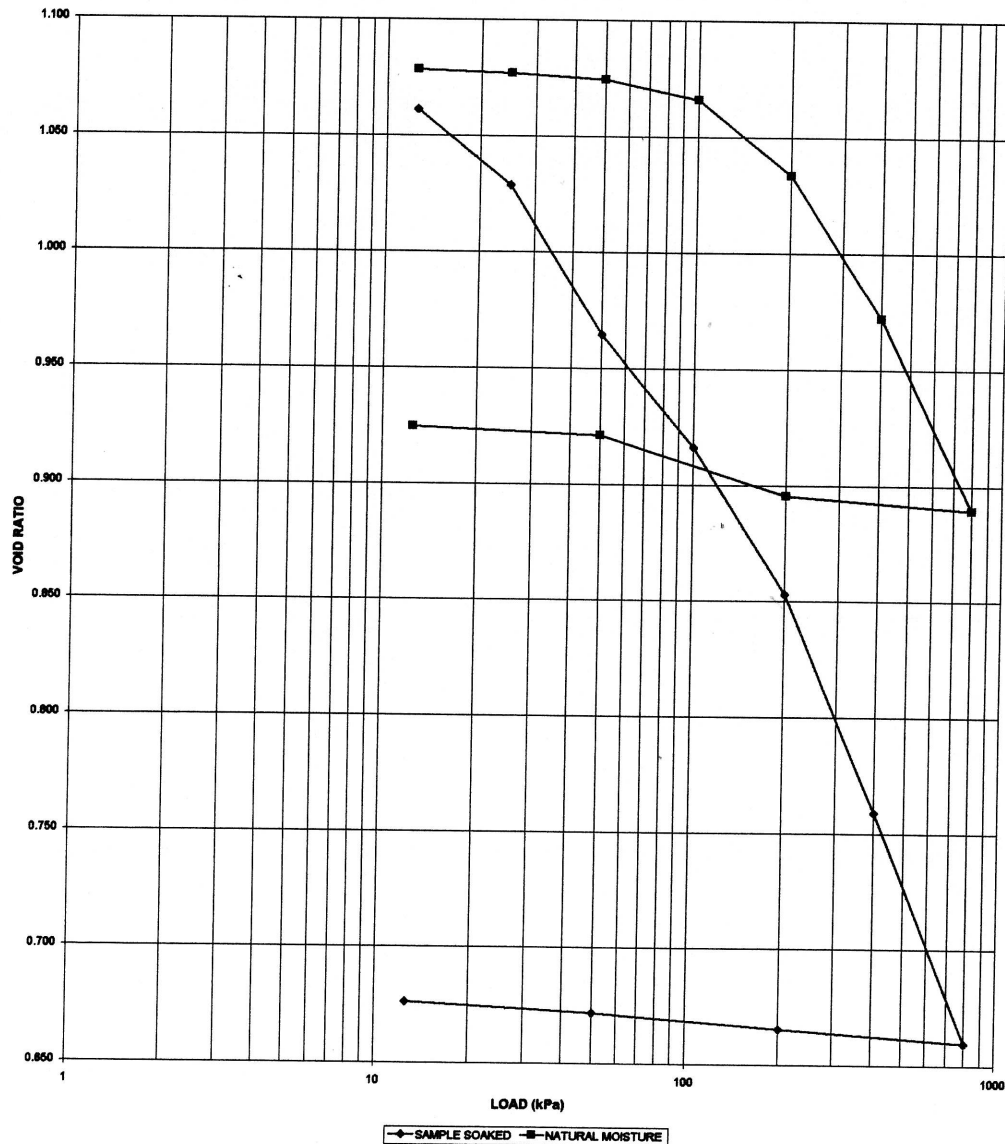
INITIAL HEIGHT OF SAMPLE (mm): 19.4 RELATIVE DENSITY: 2.698

SAMPLE STATE: UNDISTURBED INITIAL VOID RATIO: 1.082

VOID RATIO AFTER SOAKING: 1.091

LOAD (kPa):	0	W	12.5	25	50	100	200	400	600	200	50	12.5
HEIGHT (mm):	19.40	19.48	19.20	18.90	18.30	17.85	17.28	16.39	15.46	15.52	15.57	15.62
VOID RATIO	1.082	1.091	1.061	1.029	0.964	0.916	0.853	0.759	0.659	0.665	0.672	0.676

LOAD (kPa):	0	12.5	25	50	100	200	400	800	200	50	12.5
HEIGHT (mm):	19.30	19.26	19.25	19.23	19.15	18.85	18.28	17.51	17.57	17.81	17.84
VOID RATIO	1.082	1.078	1.077	1.074	1.066	1.033	0.972	0.889	0.895	0.921	0.924



KONS/KONSOLIDASIE-DUBBEL/790-02



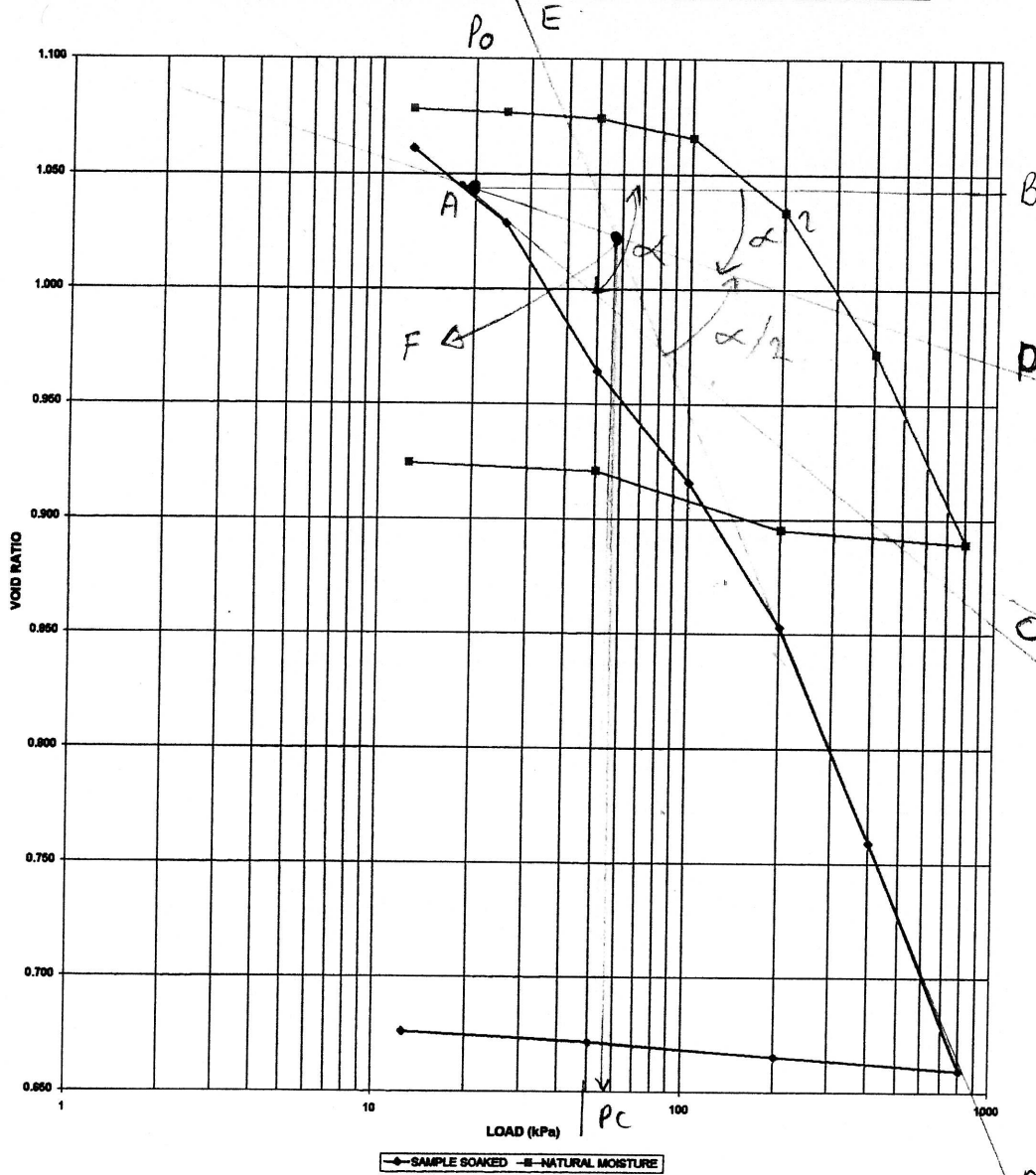
PROJECT: COUNTRYVIEW GARDENS INITIAL DRY DENSITY (kg/m³): 1296
 SAMPLE NO: TP 4 INITIAL MOISTURE CONTENT (%):

SAMPLE SOAKED	NATURAL MOISTURE
10.4	9.8

 DEPTH (m): 1.4 MOISTURE CONTENT AFTER TEST (%): 20.8 8.1
 INITIAL HEIGHT OF SAMPLE (mm): 19.4 RELATIVE DENSITY: 2.688
 SAMPLE STATE: UNDISTURBED INITIAL VOID RATIO: 1.082
 VOID RATIO AFTER SOAKING: 1.091

LOAD (kPa):	0	12.5	25	50	100	200	400	800	200	50	12.5	
HEIGHT (mm):	19.40	19.48	19.20	18.90	18.30	17.85	17.26	16.39	15.46	15.52	15.57	15.82
VOID RATIO	1.082	1.091	1.081	1.029	0.984	0.918	0.853	0.759	0.659	0.665	0.672	0.676

LOAD (kPa):	0	12.5	25	50	100	200	400	800	200	50	12.5
HEIGHT (mm):	19.30	19.26	19.25	19.23	19.15	18.85	18.28	17.51	17.57	17.81	17.84
VOID RATIO	1.082	1.078	1.077	1.074	1.066	1.033	0.972	0.889	0.895	0.921	0.924



$P_c = 58 \text{ kPa}$

KONS/KONSOLIDASIE-DUBBEL/790-02



PROJECT: COUNTRYVIEW GARDENS INITIAL DRY DENSITY (kg/m³): 1296

SAMPLE NO: TP 4 INITIAL MOISTURE CONTENT (%):

SAMPLE SOAKED	NATURAL MOISTURE
10.4	9.8

DEPTH (m): 1.4 MOISTURE CONTENT AFTER TEST (%): 20.8 8.1

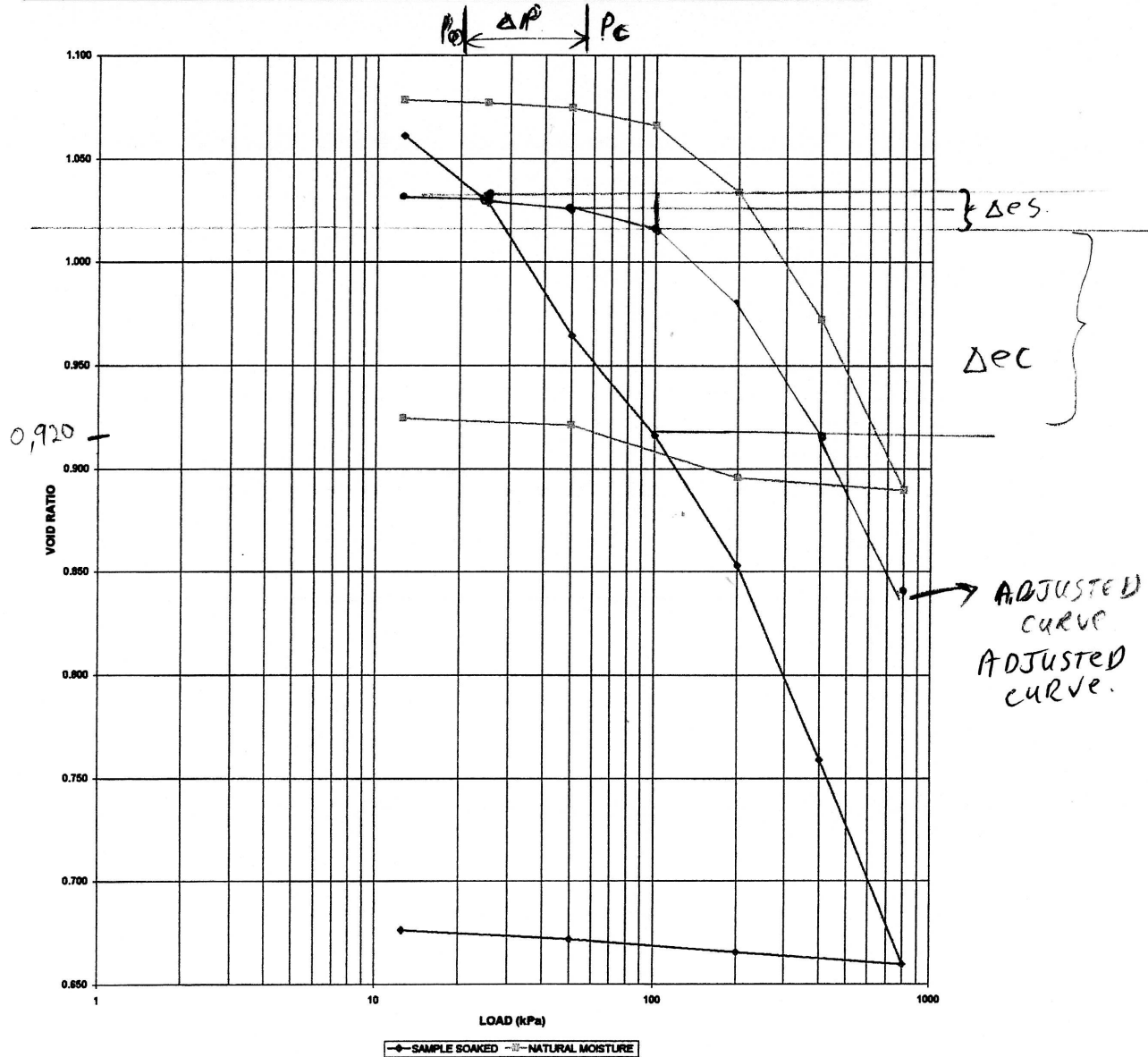
INITIAL HEIGHT OF SAMPLE (mm): 19.4 RELATIVE DENSITY: 2.698

SAMPLE STATE: UNDISTURBED INITIAL VOID RATIO: 1.082

VOID RATIO AFTER SOAKING: 1.091

LOAD (kPa):	0	W	12.5	25	50	100	200	400	800	200	50	12.5
HEIGHT (mm):	19.40	19.48	19.20	18.90	18.30	17.85	17.26	16.39	15.46	15.52	15.57	15.82
VOID RATIO	1.082	1.091	1.061	1.029	0.964	0.916	0.853	0.759	0.659	0.665	0.672	0.676

LOAD (kPa):	0	12.5	25	50	100	200	400	800	200	50	12.5
HEIGHT (mm):	19.30	19.26	19.25	19.23	19.15	18.85	18.28	17.51	17.57	17.81	17.84
VOID RATIO	1.082	1.078	1.077	1.074	1.066	1.033	0.972	0.889	0.895	0.921	0.924



KONS/KONSOLIDASIE-DUBBEL/790-02



PROJECT: COUNTRYVIEW GARDENS INITIAL DRY DENSITY (kg/m³): 1705

SAMPLE NO: TP 4 (2) INITIAL MOISTURE CONTENT (%):

SAMPLE SOAKED	NATURAL MOISTURE
5.8	5.3

DEPTH (m): 1.4 MOISTURE CONTENT AFTER TEST (%): 18.9 4.1

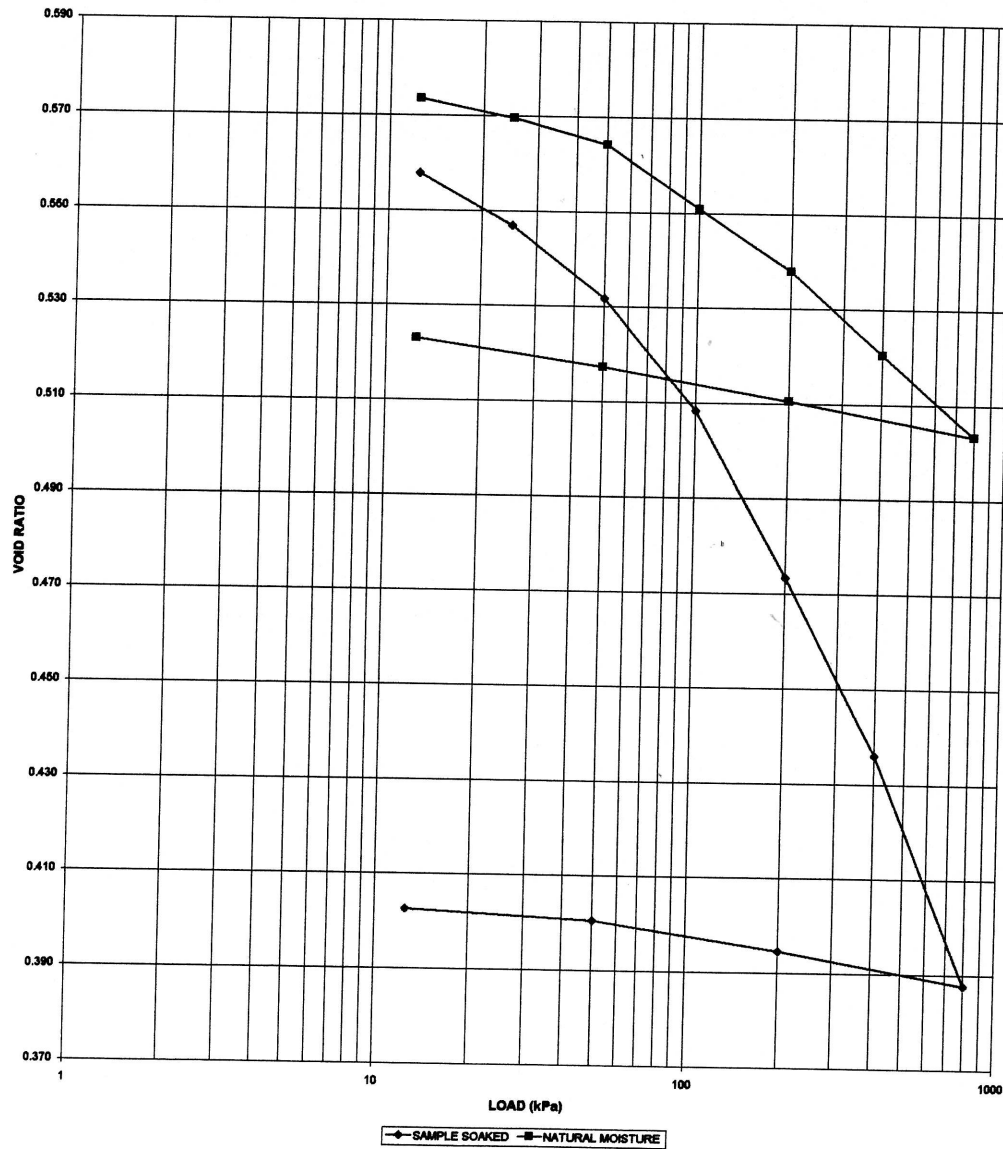
INITIAL HEIGHT OF SAMPLE (mm): 19.4 RELATIVE DENSITY: 2.684

SAMPLE STATE: UNDISTURBED INITIAL VOID RATIO: 0.575

VOID RATIO AFTER SOAKING: 0.576

LOAD (kPa):	0	W	12.5	25	50	100	200	400	800	200	50	12.5
HEIGHT (mm):	19.40	19.41	19.19	19.06	18.87	18.58	18.15	17.69	17.10	17.18	17.25	17.28
VOID RATIO	0.575	0.576	0.558	0.547	0.532	0.508	0.473	0.438	0.388	0.394	0.400	0.402

LOAD (kPa):	0	12.5	25	50	100	200	400	800	200	50	12.5
HEIGHT (mm):	19.30	19.28	19.24	19.17	19.01	18.85	18.63	18.43	18.51	18.60	18.67
VOID RATIO	0.575	0.573	0.569	0.564	0.551	0.538	0.520	0.503	0.511	0.517	0.523



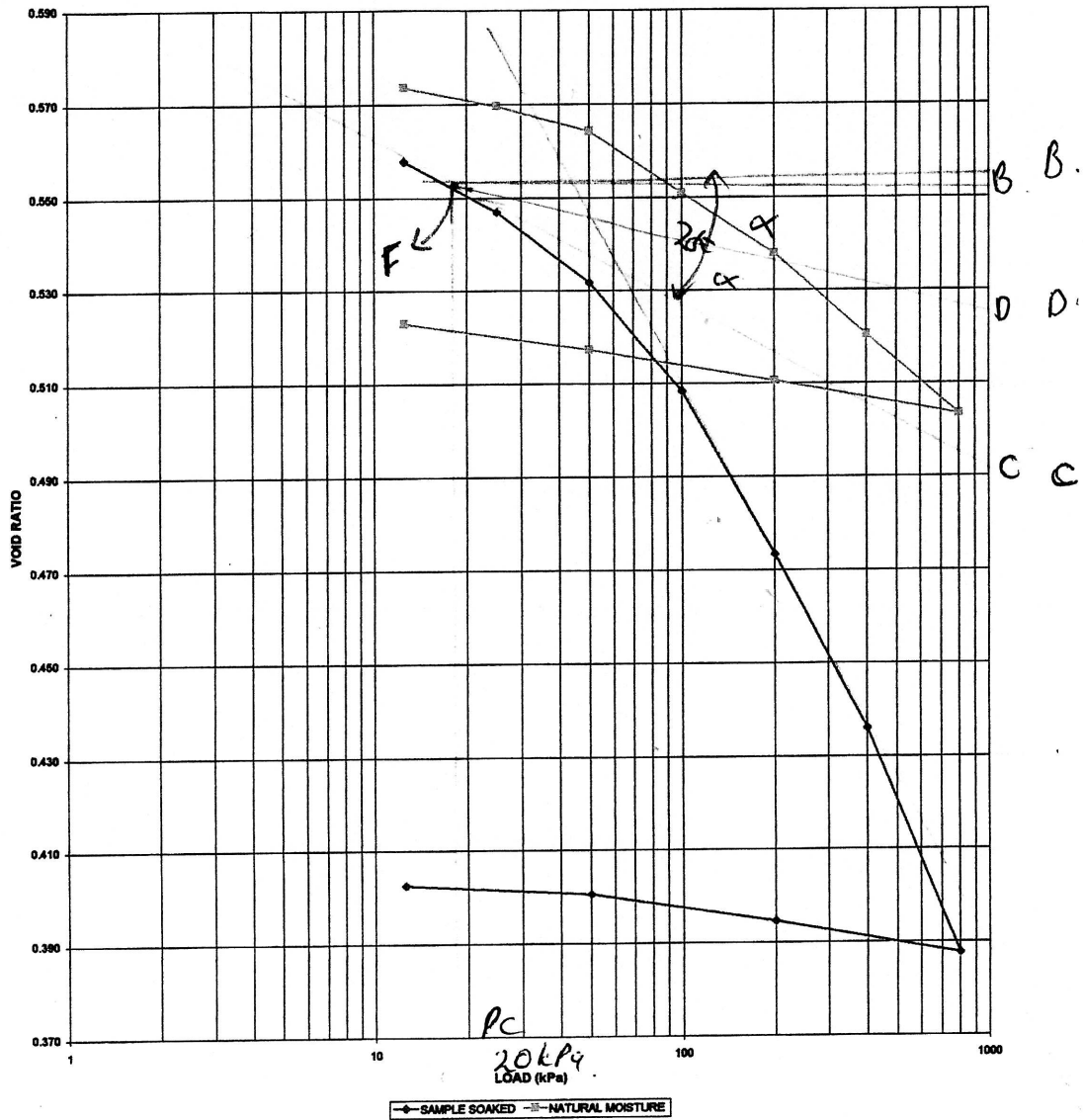
KONS/KONSOLIDASIE-DUBBEL/790-01



PROJECT:	COUNTRYVIEW GARDENS	INITIAL DRY DENSITY (kg/m ³):	1705				
SAMPLE NO:	TP 4 (2)	INITIAL MOISTURE CONTENT (%):	<table border="1"><tr><td>SAMPLE SOAKED</td><td>NATURAL MOISTURE</td></tr><tr><td>5.8</td><td>5.3</td></tr></table>	SAMPLE SOAKED	NATURAL MOISTURE	5.8	5.3
SAMPLE SOAKED	NATURAL MOISTURE						
5.8	5.3						
DEPTH (m):	1.4	MOISTURE CONTENT AFTER TEST (%):	<table border="1"><tr><td>16.9</td><td>4.1</td></tr></table>	16.9	4.1		
16.9	4.1						
INITIAL HEIGHT OF SAMPLE (mm):	19.4	RELATIVE DENSITY:	2.684				
SAMPLE STATE:	UNDISTURBED	INITIAL VOID RATIO:	0.575				
		VOID RATIO AFTER SOAKING:	0.576				

LOAD (kPa):	0	W	12.5	25	50	100	200	400	800	200	50	12.5
HEIGHT (mm):	19.40	19.41	19.19	19.08	18.87	18.58	18.15	17.89	17.10	17.18	17.25	17.28
VOID RATIO	0.575	0.576	0.558	0.547	0.532	0.508	0.473	0.436	0.388	0.394	0.400	0.402

LOAD (kPa):	0	12.5	25	50	100	200	400	800	200	50	12.5
HEIGHT (mm):	19.30	19.28	19.24	19.17	19.01	18.85	18.63	18.43	18.51	18.60	18.67
VOID RATIO	0.575	0.573	0.569	0.564	0.551	0.538	0.520	0.503	0.511	0.517	0.523



KONS/KONSOLIDASIE-DUBBEL/790-01



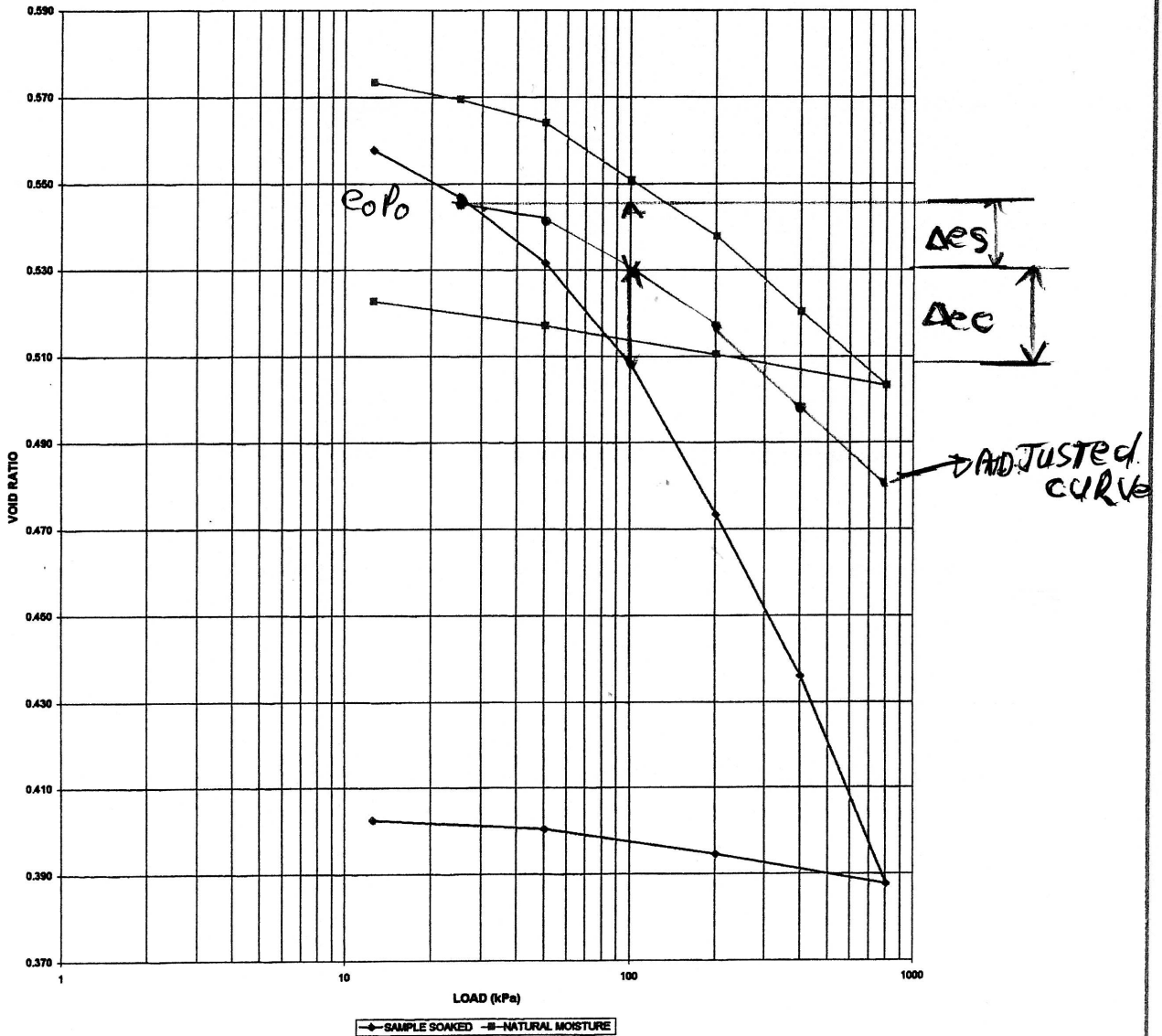
PROJECT: COUNTRYVIEW GARDENS INITIAL DRY DENSITY (kg/m³): 1705
 SAMPLE NO: TP 4 (2) INITIAL MOISTURE CONTENT (%):

SAMPLE SOAKED	NATURAL MOISTURE
5.8	5.3

 DEPTH (m): 1.4 MOISTURE CONTENT AFTER TEST (%): 16.9 4.1
 INITIAL HEIGHT OF SAMPLE (mm): 19.4 RELATIVE DENSITY: 2.884
 SAMPLE STATE: UNDISTURBED INITIAL VOID RATIO: 0.575
 VOID RATIO AFTER SOAKING: 0.576

LOAD (kPa):	0	W	12.5	25	50	100	200	400	800	200	50	12.5
HEIGHT (mm):	19.40	19.41	19.19	19.06	18.87	18.58	18.15	17.69	17.10	17.18	17.25	17.28
VOID RATIO	0.575	0.578	0.558	0.547	0.532	0.508	0.473	0.436	0.388	0.394	0.400	0.402

LOAD (kPa):	0	12.5	25	50	100	200	400	800	200	50	12.5
HEIGHT (mm):	19.30	19.28	19.24	19.17	19.01	18.85	18.63	18.43	18.51	18.60	18.67
VOID RATIO	0.575	0.573	0.568	0.564	0.551	0.538	0.520	0.503	0.511	0.517	0.523



KONS/KONSOLIDASIE-DUBBEL/780-01



SOIL ANALYSIS BY : SOILLAB (Pty)
Lab reference No. : S04-790

Page : 1
Date Printed : 2004-09-29

Customer : GEOPRO
Job Description : COUNTRYVIEW GARDENS
Road Number :

Job Number : S04-790
Contract Number :
Date : 2004-08-27

SAMPLE DESCRIPTION						
Sample Number	13188					
Sample Position	TP @ DCP2					
Sample Depth (mm)	700-1600					
Material Description	DARK Y/O W/ GRANITE SANDY CLAY					
Max size of boulder (mm)	-					
SCREEN ANALYSIS (% PASS)						
75,00 mm	100					
63,00 mm	100					
53,00 mm	100					
37,50 mm	100					
26,50 mm	100					
19,00 mm	100					
13,20 mm	100					
4,750 mm	100					
2,000 mm	91					
0,425 mm	62					
0,075 mm	41					
SOIL MORTAR						
Coarse Sand 2,000-0,425	31					
Coarse Fine Sd 0,425-0,250	6					
Medium Fine Sd 0,250-0,150	8					
Fine Fine Sand 0,150-0,075	10					
Material <0,075	45					
CONSTANTS						
Grading Modulus	1.06					
Liquid Limit	37					
Plasticity Index	16					
Linear Shrinkage (%)	8.0					
Sand Equivalent						
Classification - TRB	A-6 (3)					
Classification - TRH14	G8					
CBR / UCS VALUES		CBR				
MOD. AASHTO						
Max Dry Density (kg/m ³)	1930					
Optimum Moisture Cont (%) .	11.3					
Moulding Moisture Cont (%) .	11.4					
Dry Density (kg/m ³)	1930					
% of Max Dry Density	100.0					
100% Mod CBR/UCS	63					
% Swell	0.1					
NRB						
Dry Density (kg/m ³)	1820					
% of Max Dry Density	94.3					
100% NRB CBR/UCS	25					
% Swell	0.5					
PROCTOR						
Dry Density (kg/m ³)	1688					
% of Max Dry Density	87.5					
100% Proc CBR/UCS	9					
% Swell	0.3					
CBR / UCS VALUES						
100% Mod AASHTO	63					
98% Mod AASHTO	46					
97% Mod AASHTO	39					
95% Mod AASHTO	28					
93% Mod AASHTO	21					
90% Mod AASHTO	13					



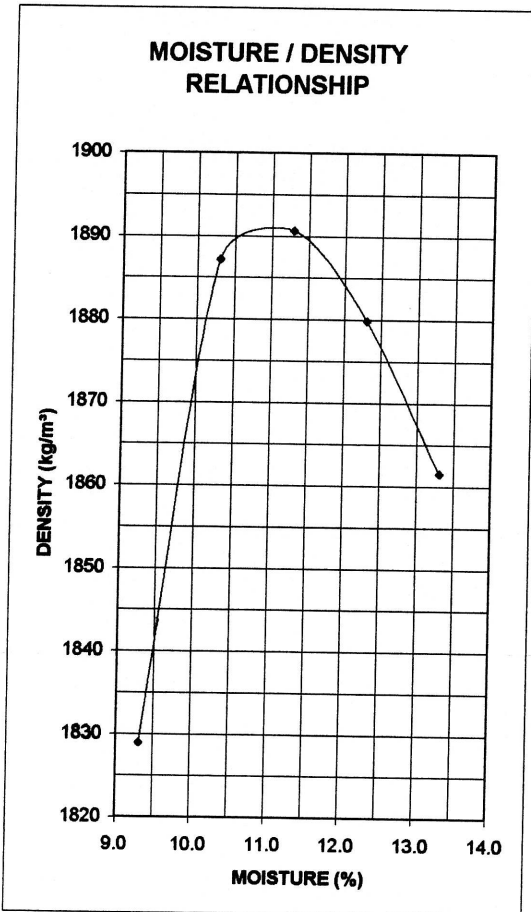
PROJECT : COUNTRYVIEW GARDENS

DATE : 2004-09-02

Position	TP 2	TP 2	TP 4	TP 4	TP 5	TP 5		
Layer	SURFACE	BOTTOM	SURFACE	BOTTOM	SURFACE	BOTTOM		
Peg distance/Test No.		OF TP		OF TP		OF TP		
Depth (mm)	0-300	0-300	0-300	0-300	0-300	0-300		

Field Moisture Content	5.1	10.2	8.9	3.9	3.3	9.0		
Field Dry Density (kg/m ³)	1661	1623	1711	1697	1891	1646		
Optimum Moisture Content (%)		11.0		11.0		11.0		
Max./Appar. Density (kg/m ³)		1891		1891		1891		

Percentage Compaction (%)		85.8		89.7		87.0		
---------------------------	--	------	--	------	--	------	--	--



Sketch Plan



REMARKS:

DENSITY/790-01